Skeletal muscle oxygen delivery in heart failure and breast cancer: mechanisms and therapeutic insights

by

Ramona Elaine Weber

B.S., Kansas State University, 2019
M.S., Kansas State University, 2020

AN ABSTRACT OF A DISSERTATION

submitted in partial fulfillment of the requirements for the degree

DOCTOR OF PHILOSOPHY

Department of Kinesiology
College of Health and Human Sciences

KANSAS STATE UNIVERSITY
Manhattan, Kansas

2025

Abstract

The onset of exercise requires precise cardiovascular adjustments to ensure adequate skeletal muscle oxygen delivery ($\dot{Q}O_2$) to meet the metabolic demands ($\dot{V}O_2$) of contractions. A hallmark of exercise intolerance is reduced nitric oxide (NO) bioavailability (e.g. endothelial dysfunction) and $\dot{Q}O_2$-to-$\dot{V}O_2$ mismatch that effectively reduces the partial pressure gradient for O_2 diffusion across the interstitial space ($PO_2$is) and disrupts the intracellular milieu. This presents significant quandaries for individuals diagnosed with heart failure (HF) and breast cancer (BC), both of which are malignancies associated with O_2 transport dysfunction and are compounded with limited therapeutic options available to support exercise tolerance. With this, Chapter 2 examines the effects of targeting downstream of NO dysfunction (via soluble guanylyl cyclase (sGC) stimulator) to improve vascular NO-sensitivity, exercise tolerance and $PO_2$is during contractions in HF rats. Evidence suggests that there is a bi-directional relationship between HF and BC, with each condition predisposing individuals to the other. While in HF, central O_2 transport dysfunction largely precedes and promotes O_2 transport limitations, BC, as an isolated condition, does not directly impact cardiac function. Therefore, in Chapter 3 we investigated the impact of tumor-bearing alone on maximal O_2 uptake during exercise ($\dot{V}O_2$max) in BC rats. Despite no change in $\dot{V}O_2$max before and after tumor growth, tumor-bearing BC rats had a reduced exercise economy, suggesting that peripheral O_2 transport limitations likely have a role in limiting sustained exercise performance. In Chapter 4, we measured the resting and contracting $PO_2$is in BC rats and to what extent NO-signaling has in control over $PO_2$is kinetics. We found that BC rats displayed decreased endothelium-independent vasodilation coupled with an increased reliance on basal NO production in comparison to healthy controls. Collectively, these findings highlight the critical role that NO has in regulating $\dot{Q}O_2$-to-$\dot{V}O_2$ matching in both HF and BC.

Skeletal muscle oxygen delivery in heart failure and breast cancer: mechanisms and therapeutic insights

by

Ramona Elaine Weber

B.S., Kansas State University, 2019
M.S., Kansas State University, 2020

A DISSERTATION

submitted in partial fulfillment of the requirements for the degree

DOCTOR OF PHILOSOPHY

Department of Kinesiology
College of Health and Human Sciences

KANSAS STATE UNIVERSITY
Manhattan, Kansas

2025

Approved by:

Co-Major Professor
Dr. Timothy I. Musch

Approved by:

Co-Major Professor
Dr. David C. Poole

Copyright

Abstract

The onset of exercise requires precise cardiovascular adjustments to ensure adequate skeletal muscle oxygen delivery ($\dot{Q}O_2$) to meet the metabolic demands ($\dot{V}O_2$) of contractions. A hallmark of exercise intolerance is reduced nitric oxide (NO) bioavailability (e.g. endothelial dysfunction) and $\dot{Q}O_2$-to-$\dot{V}O_2$ mismatch that effectively reduces the partial pressure gradient for O_2 diffusion across the interstitial space ($PO_2$is) and disrupts the intracellular milieu. This presents significant quandaries for individuals diagnosed with heart failure (HF) and breast cancer (BC), both of which are malignancies associated with O_2 transport dysfunction and are compounded with limited therapeutic options available to support exercise tolerance. With this, Chapter 2 examines the effects of targeting downstream of NO dysfunction (via soluble guanylyl cyclase (sGC) stimulator) to improve vascular NO-sensitivity, exercise tolerance and $PO_2$is during contractions in HF rats. Evidence suggests that there is a bi-directional relationship between HF and BC, with each condition predisposing individuals to the other. While in HF, central O_2 transport dysfunction largely precedes and promotes O_2 transport limitations, BC, as an isolated condition, does not directly impact cardiac function. Therefore, in Chapter 3 we investigated the impact of tumor-bearing alone on maximal O_2 uptake during exercise ($\dot{V}O_2$max) in BC rats. Despite no change in $\dot{V}O_2$max before and after tumor growth, tumor-bearing BC rats had a reduced exercise economy, suggesting that peripheral O_2 transport limitations likely have a role in limiting sustained exercise performance. In Chapter 4, we measured the resting and contracting $PO_2$is in BC rats and to what extent NO-signaling has in control over $PO_2$is kinetics. We found that BC rats displayed decreased endothelium-independent vasodilation coupled with an increased reliance on basal NO production in comparison to healthy controls. Collectively, these findings highlight the critical role that NO has in regulating $\dot{Q}O_2$-to-$\dot{V}O_2$ matching in both HF and BC.

Table of Contents

List of Figures

List of Tables

Acknowledgements

I am incredibly grateful to have had the support from the apogee of exercise physiologists over the past 5 years. To my committee members, Drs. David C. Poole, Timothy I. Musch, Brad J. Behnke, Stephanie E. Hall, and Carl J. Ade: your consistent inspiration and unwavering support has impacted my growth insurmountably. You've made my passage in science challenging, rewarding, and most important of all, fun.

My appreciation also goes to the faculty, staff, and graduate students in the Department of Kinesiology at Kansas State University for their camaraderie and the stimulating discussions that inspired me throughout my academic journey. Their collective wisdom and encouragement have been a cornerstone of my research experience. I'd especially like to acknowledge the members of RatLab#100 that I have shared innumerable days alongside: Sue, thank you for providing a shoulder, a hand, and encouragement when I needed it the most; Trenton, I am lucky to have received my initial training by a patient, thorough, wise and punny individual; Nathan, thank you for always providing comedic relief and toxic coffee; and lastly, to my sidekick, Kiana Schulze, I am incredibly thankful to have shared an office, a lab space, and a friendship with you. I look forward to our continued shenanigans and like a petrified banana, I am always pleased to hang.

To my family, friends and pets, thank you for providing me with support throughout this journey. Specifically, Jonah, who picked up countless days on Nigel-duty; Joanna, who reminded me to slow down; Auni, who reminded me to stay resilient; Casey, who never failed to encourage me both gently and violently; Kyla, who understood me always; Darbi, for protecting my sanity; my Grandma Brigette, for instilling the hard work ethic I carry; and my Grandma Betty, for not letting me go a single day un-blessed. I love each of you to the moon and back.

Dedication

This dissertation is dedicated to my dad, Marty Weber (1962-2023), of whom I am sure was just dying to read this. I miss you each and every day.

Preface

Chapter 2 & 3 of this dissertation represents an original research article that are currently in peer-review process or have been published. Citations are listed below and these articles are reproduced here with permission from the publisher.

Weber RE, Schulze KM, Horn AG, McCoach TE, White ZJ, Hageman KS, Hall SE, Sandner P, Behnke BJ, Musch TI, Poole DC. Effects of soluble guanylyl cyclase stimulator on skeletal muscle oxygenation and exercise capacity in heart failure with mildly reduced ejection fraction. *Experimental Phys*. *In review*, 2025.

Weber RE, Schulze KM, Kenney NJ, Scheuermann BC, Kunkel ON, Ade CJ, Musch TI, Behnke BJ, Poole DC. Tumor bearing in untreated breast cancer decreases exercise tolerance without lowering maximal oxygen uptake in rats. *Am J Cancer Res*. 2025 Feb 15;15(2):487-500.

Chapter 1 - Introduction

Fluctuations in atmospheric and molecular oxygen (O_2) have been a driving force in the evolution of life, particularly during the Cambrian explosion (~540 million years ago), when extreme O_2 oscillations coincided with a rapid diversification of animal phyla (He et al., 2019). This evolutionary pressure has shaped the physiology of organisms, particularly the ability to regulate O_2 supply and demand. In mammals, the coordinated capacity of the cardiopulmonary and muscular systems to rapidly transport O_2 (~100x above resting rate (Klausen et al., 1982; Richardson et al., 1993)) to muscle during exercise exemplifies this adaptability. The integration and efficiency of these systems, quantified by maximal O_2 uptake during exercise ($\dot{V}O_2max$), serves as a strong predictor of quality of life.

Skeletal muscle oxygen delivery

Adenosine triphosphate (ATP) is the primary energy source for all living mammals. Immediate elevations in O_2 flux, and thus ATP demand, across the rest to contraction transient (Behnke et al., 2001) are achieved through limited stores of intracellular ATP and phosphagen systems. Concurrently, there is a rapid response from the cardiovascular system (Krogh & Lindhard, 1913) to supply blood flow to muscle which exceeds the immediate demand (Grassi et al., 1996). As contractions continue, increased vascular conductance, local metabolic biproducts, and neuromuscular feedback (Delp & Laughlin, 1998) provide balanced O_2 delivery-to-O_2 demand which is integral to maintain the intracellular pressure of O_2 (Hogan et al., 1992). As described by Fick's law of diffusion, O_2 flux ($\dot{V}O_2$) from the muscle capillary bed to fuel mitochondria is determined by both the available surface area for exchange (DO_2) and the O_2 partial pressure gradient:

$$\dot{V}O_2 = DO_2 \times (PO_2mv - PO_2ic).$$

The gradient between microvascular PO_2 (PO_2mv, ~30-40 mmHg) (Behnke et al., 2001) and intracellular PO_2 (PO_2ic, ~10 mmHg) (Honig & Gayeski, 1993) establishes the driving force for O_2 diffusion across significant resistance within the carrier free region, i.e., the interstitial space (Colburn et al., 2020). Thus, the kinetics profile of skeletal muscle interstitial PO_2 ($PO_2$is) during transitions in metabolic demand provides information on the sensitive regulation between both upstream O_2 delivery ($\dot{Q}O_2$) and intracellular $\dot{V}O_2$. Accordingly, alterations in skeletal muscle $PO_2$is have a direct impact on muscular metabolic and contractile function (Hogan et al., 1992; Kindig et al., 2005), such that lowering $PO_2$is, and thus, PO_2ic, directly impacts the production of ATP by the mitochondria via:

$$3ADP + 3Pi + \frac{1}{2}O_2 + NADH + H^+ \rightarrow 3\,ATP + NAD + H_2O$$

A decreased or increased PO_2ic serves as a regulator and, respectively, elevates or reduces the degree of intracellular perturbations ([NADH], [ADP], [H^+], and [Pi]) (Wilson et al., 1977). With respect to interpreting the relative roles of altered $\dot{Q}O_2$ and DO_2 conductances at a given $\dot{V}O_2$, the Wagner diagram (Figure 1.2) conflates Fick's law of diffusion (*see above*) with the Fick Principle:

$$\dot{V}O_2 = \dot{Q}O_2 \times (CaO_2 - CvO_2)$$

where CaO_2 and CvO_2 are the arterial and venous O_2 content, respectively. These relationships provide a template to evaluate the impact of altered blood flow on skeletal muscle $\dot{Q}O_2$ and DO_2 in healthy and disease states. One of the key mediators involved in regulating PO_2 in health, and especially when faced with O_2 transport limitations associated with disease, is the ubiquitous gaseous molecule nitric oxide (NO).

Nitric oxide-mediated skeletal muscle oxygen delivery

Since its biochemical pathway was discovered in the early 1980's (Furchgott & Zawadzki, 1980; Ignarro et al., 1987) NO has gained extensive attention among exercise physiologists in its ability to regulate both $\dot{Q}O_2$ and $\dot{V}O_2$ (Stamler & Meissner, 2001). During exercise mechanical force against the endothelium (shear stress) promotes NO production from endothelial NO synthase (eNOS), thereafter, NO diffuses into smooth muscle cells to activate the primary intracellular receptor, soluble guanylyl cyclase (sGC) (Arnold et al., 1977; Katsuki et al., 1977), which catalyzes cyclic GMP (cGMP) synthesis, leading to reduced intracellular calcium levels, and vascular smooth muscle cell vasodilation (Figure 1.1). Early studies demonstrate that NO is an important molecule involved in supplying O_2 delivery during exercise. Specifically, Hester et al. presented evidence that NO is important in the initial hyperemic response (Hester et al., 1993) and in addition, Hirai et al. reported that inhibition of NO formation in rats attenuated hindlimb blood flow during moderate intensity treadmill running (Hirai et al., 1994). NO is also a potent, rapid and reversible inhibitor of cytochrome C oxidase (Cleeter et al., 1994) which may serve to control reactive O_2 species (ROS), regulate muscle PO_2 (Thomas et al., 2001), and improve mitochondrial efficiency (increased P:O ratio) (Larsen et al., 2011)—all of which act to reduce the O_2 cost of exercise. Notably, the production of NO varies significantly between sexes, with important implications for disease development and progression.

Sexual dimorphism in nitric oxide signaling

Females exhibit a superior capacity for NO production compared to males, attributable to estrogen-mediated activation of endothelial nitric oxide synthase (eNOS) (Rubanyi et al., 1997). This enhanced capacity for NO synthesis in females not only contributes to improved cardiovascular protection but also significantly reduces the risk of cardiovascular events (Taddei et al., 1996). Despite lower blood pressure in females than males (Reckelhoff, 2001), evidence

that this relates to heterogenous blood flow patterns to skeletal muscle during exercise remains equivocal (Kellawan et al., 2015; Thompson et al., 2007). Notably, Craig et al. utilized phosphorescence quenching techniques to measure resting and contracting skeletal muscle $PO_2$is in rats, revealing that healthy female rats exhibit a greater responsiveness to alterations in NO bioavailability exemplified by greater reductions in $PO_2$is with eNOS blockade compared to male rats (Craig et al., 2018). This heightened sensitivity to NO likely also has a role in the more attenuated $PO_2$is values reached during contractions in female rats with heart failure versus male heart failure rats (Craig et al., 2019). A reduction in estrogen receptors in vascular endothelial cells after menopause is associated with reduced eNOS-mediated dilation (Gavin et al., 2009), an increased cardiovascular disease risk (Leening et al., 2014), which promotes a greater likelihood of breast cancer diagnosis (Angelov et al., 2025). Understanding the interplay between NO signaling, skeletal muscle $PO_2$is, and exercise tolerance can illuminate potential therapeutic avenues for optimizing cardiovascular health, particularly in light of the differential manifestations of diseases in males and females.

Nitric oxide-mediated skeletal muscle dysfunction

NO-sGC signaling is highly sensitive to oxidative stress such that the reduced ferrous (Fe^{2+}) state of the heme moiety within sGC is essential for NO responsiveness; oxidation to the ferric (Fe^{3+}) state or heme loss, often due to elevated ROS, renders sGC insensitive to NO (Figure 1.1, right) (Stuehr et al., 2021). Additionally, eNOS can become uncoupled, reacting with ROS to form peroxynitrite, which further attenuates NO bioavailability and sGC function (Gerassimou et al., 2007). Diseases states involved with increased oxidative stress disrupt NO-production and lessen $\dot{Q}O_2$ which culminates in inefficient removal of metabolic biproducts,

augmented reliance upon glycolysis and finite energy stores, and, ultimately, exercise intolerance.

Exercise intolerance is a hallmark of both heart failure (HF) and breast cancer (BC), the leading causes of death in women worldwide (Savarese et al., 2023; Sung et al., 2021). Interestingly, epidemiological data indicate that HF patients have a higher incidence of cancer (Del Buono et al., 2019; Piña et al., 2003) and the presence of HF increases future cancer risk (Banke et al., 2016; Hasin et al., 2013; Koelwyn et al., 2020). These connections may arise from shared underlying mechanisms, particularly vascular and metabolic dysfunction, predisposing patients to both conditions (Zeng et al., 2022). In summary, the interaction between estrogen, NO signaling, and vascular function not only underscores gender differences in cardiovascular fitness but also highlights the importance of considering these factors in the context of HF and BC in women. Accordingly, improving NO-mediated function through pharmaceutical agonists or exercise training may attenuate vascular dysfunction and improve exercise capacity.

Skeletal muscle oxygen delivery in heart failure

Heart failure (HF) is the leading cause of mortality and morbidity globally (Del Buono et al., 2019). Following a myocardial infarction reduced cardiac output leads to profound limitations on the O_2 transport cascade through marked by perturbations in peripheral vascular (Katz et al., 1993) and metabolic (Drexler et al., 1992) dysregulation which contribute to compromised $PO_2$is control (Craig et al., 2019) and exercise intolerance (Poole et al., 2012). Despite this, limited pharmaceutical avenues are available for HF patients that go beyond treating symptom burden and instead promote peripheral adaptations to improve exercise tolerance, highlighting the need for alternative therapeutic strategies. Importantly, upstream dysfunction within the NO-sGC cascade may limit the effects of NO-donors, such that milder

disease states could demonstrate better efficacy in terms of modulating heme-intact sGC signaling. With this in mind, we used a novel approach in Chapter 2 to investigate how increasing sGC sensitivity to NO, via sGC stimulators, effects skeletal muscle $PO_2$is and exercise tolerance in heart failure (HF) with mildly reduced ejection fraction (HFmrEF).

Skeletal muscle oxygen delivery in breast cancer

Approximately one in eight women in the United states will be diagnosed with breast cancer (BC) in their lifetime (Giaquinto et al., 2024). BC patients are at a heightened risk for cardiovascular disease (CVD) mortality (Bradshaw et al., 2016) due, in part, to sedentary deconditioning associated with cancer-related skeletal muscle fatigue (Peel et al., 2014; Wilson et al., 2020). Historically, there have been two main areas of focus regarding exercise intolerance in oncology: 1) the negative impacts of anticancer therapy on cardiac and skeletal muscle function, and 2) cancer cachexia (i.e., significant muscle wasting associated with a decline in physical function) with the former receiving scant attention in BC patients. Specifically, individuals with BC exhibit a unique phenotype in that prior to anti-cancer treatment they display reduced exercise capacity, despite relatively normal cardiac function (Beaudry et al., 2019; Koivula et al., 2024), and cancer-related deficits in muscle function in the absence of muscle atrophy (Baracos et al., 2018; Klassen et al., 2014). In Chapter 3, we measured $\dot{V}O_2$max in therapy-naïve BC rats to establish whether or not tumor-bearing effects whole body O_2 transport during maximal exercise. Despite no changes in $\dot{V}O_2$max, BC rats displayed a reduced exercise economy. This aligns with previous findings which suggest that alterations in calcium handling (Wilson et al., 2019), contractile dysfunction (Mader et al., 2022), and mitochondrial ATP production (Wilson et al., 2020b) are promoting early-onset fatigue in BC. Given the intricate relationship between skeletal muscle $PO_2$is and muscular energetics, it is likely that dysfunction

within the O_2 transport cascade has a role in limiting exercise tolerance early in the breast cancer continuum. Therefore, in Chapter 4 we sought to determine how BC, as an isolated condition, impacts skeletal muscle $PO_2$is and to what degree NO signaling dysfunction may impair the dynamic matching between $\dot{Q}O_2$ and $\dot{V}O_2$ during contractions.

Summary

Exercise intolerance has profound implications for health-related quality of life and is associated with increased morbidity and mortality across cardiovascular and oncological populations (Del Buono et al., 2019; Jones et al., 2012). Understanding the pathophysiology of exercise intolerance, particularly regarding the interplay of NO in both HF and BC, is crucial for developing better therapeutic strategies aimed at improving functional capacity and, subsequently, overall health outcomes. The effective management of exercise intolerance could offer significant benefits, potentially enhancing quality of life and reducing healthcare burdens associated with the dual challenges of heart failure and cancer. Thus, targeted therapies that aim to restore or enhance NO signaling, improve O_2 delivery and/or extraction during exercise may address an important therapeutic gap in treating patients suffering from these conditions.

References

Arnold, W. P., Mittal, C. K., Katsuki, S., & Murad, F. (1977). Nitric oxide activates guanylate cyclase and increases guanosine 3':5'-cyclic monophosphate levels in various tissue preparations. *Proceedings of the National Academy of Sciences of the United States of America*, *74*(8), 3203–3207.

Banke, A., Schou, M., Videbaek, L., Møller, J. E., Torp-Pedersen, C., Gustafsson, F., Dahl, J. S., Køber, L., Hildebrandt, P. R., & Gislason, G. H. (2016). Incidence of cancer in patients with chronic heart failure: A long-term follow-up study. *European Journal of Heart Failure*, *18*(3), 260–266.

Baracos, V. E., Martin, L., Korc, M., Guttridge, D. C., & Fearon, K. C. H. (2018). Cancer-associated cachexia. *Nature Reviews. Disease Primers*, *4*, 17105.

Beaudry, R. I., Howden, E. J., Foulkes, S., Bigaran, A., Claus, P., Haykowsky, M. J., & Gerche, A. L. (2019). Determinants of exercise intolerance in breast cancer patients prior to anthracycline chemotherapy. *Physiological Reports*, *7*(1), e13971.

Behnke, B. J., Kindig, C. A., Musch, T. I., Koga, S., & Poole, D. C. (2001). Dynamics of microvascular oxygen pressure across the rest-exercise transition in rat skeletal muscle. *Respiration Physiology*, *126*(1), 53–63.

Bozkurt, B., Coats, A. J. S., Tsutsui, H., Abdelhamid, C. M., Adamopoulos, S., Albert, N., Anker, S. D., Atherton, J., Böhm, M., Butler, J., Drazner, M. H., Michael Felker, G., Filippatos, G., Fiuzat, M., Fonarow, G. C., Gomez-Mesa, J.-E., Heidenreich, P., Imamura, T., Jankowska, E. A., … Zieroth, S. (2021). Universal definition and classification of heart failure: A report of the Heart Failure Society of America, Heart Failure Association of the European Society of Cardiology, Japanese Heart Failure Society and Writing Committee of the Universal Definition of Heart Failure: Endorsed by the Canadian Heart Failure Society, Heart Failure Association of India, Cardiac Society of Australia and New Zealand, and Chinese Heart Failure Association. *European Journal of Heart Failure*, *23*(3), 352–380.

Bradshaw, P. T., Stevens, J., Khankari, N., Teitelbaum, S. L., Neugut, A. I., & Gammon, M. D. (2016). Cardiovascular Disease Mortality Among Breast Cancer Survivors. *Epidemiology (Cambridge, Mass.)*, *27*(1), 6–13.

Cleeter, M. W., Cooper, J. M., Darley-Usmar, V. M., Moncada, S., & Schapira, A. H. (1994). Reversible inhibition of cytochrome c oxidase, the terminal enzyme of the mitochondrial respiratory chain, by nitric oxide. Implications for neurodegenerative diseases. *FEBS Letters*, *345*(1), 50–54.

Colburn, T. D., Hirai, D. M., Craig, J. C., Ferguson, S. K., Weber, R. E., Schulze, K. M., Behnke, B. J., Musch, T. I., & Poole, D. C. (2020). Transcapillary PO2 gradients in contracting muscles across the fibre type and oxidative continuum. *The Journal of Physiology*, *598*(15), 3187–3202.

Craig, J. C., Colburn, T. D., Hirai, D. M., Musch, T. I., & Poole, D. C. (2019). Sexual dimorphism in the control of skeletal muscle interstitial Po2 of heart failure rats: Effects of dietary nitrate supplementation. *Journal of Applied Physiology (Bethesda, Md.: 1985)*, *126*(5), 1184–1192.

Craig, J. C., Colburn, T. D., Hirai, D. M., Schettler, M. J., Musch, T. I., & Poole, D. C. (2018). Sex and nitric oxide bioavailability interact to modulate interstitial Po2 in healthy rat skeletal muscle. *Journal of Applied Physiology (Bethesda, Md.: 1985)*, *124*(6), 1558–1566.

Del Buono, M. G., Arena, R., Borlaug, B. A., Carbone, S., Canada, J. M., Kirkman, D. L., Garten, R., Rodriguez-Miguelez, P., Guazzi, M., Lavie, C. J., & Abbate, A. (2019). Exercise Intolerance in Patients With Heart Failure: JACC State-of-the-Art Review. *Journal of the American College of Cardiology*, *73*(17), 2209–2225.

Delp, M. D., & Laughlin, M. H. (1998). Regulation of skeletal muscle perfusion during exercise. *Acta Physiologica Scandinavica*, *162*(3), 411–419.

Federspiel, W. J., & Popel, A. S. (1986). A theoretical analysis of the effect of the particulate nature of blood on oxygen release in capillaries. *Microvascular Research*, *32*(2), 164–189.

Furchgott, R. F., & Zawadzki, J. V. (1980). The obligatory role of endothelial cells in the relaxation of arterial smooth muscle by acetylcholine. *Nature*, *288*(5789), 373–376.

Gavin, K. M., Seals, D. R., Silver, A. E., & Moreau, K. L. (2009). Vascular endothelial estrogen receptor alpha is modulated by estrogen status and related to endothelial function and endothelial nitric oxide synthase in healthy women. *The Journal of Clinical Endocrinology and Metabolism*, *94*(9), 3513–3520.

Gerassimou, C., Kotanidou, A., Zhou, Z., Simoes, D. C. M., Roussos, C., & Papapetropoulos, A. (2007). Regulation of the expression of soluble guanylyl cyclase by reactive oxygen species. *British Journal of Pharmacology*, *150*(8), 1084–1091.

Giaquinto, A. N., Sung, H., Newman, L. A., Freedman, R. A., Smith, R. A., Star, J., Jemal, A., & Siegel, R. L. (2024). Breast cancer statistics 2024. *CA: A Cancer Journal for Clinicians*, *74*(6), 477–495.

Grassi, B., Gladden, L. B., Stary, C. M., Wagner, P. D., & Hogan, M. C. (1998). Peripheral O2 diffusion does not affect V(O2)on-kinetics in isolated insitu canine muscle. *Journal of Applied Physiology (Bethesda, Md.: 1985)*, *85*(4), 1404–1412.

Grassi, B., Poole, D. C., Richardson, R. S., Knight, D. R., Erickson, B. K., & Wagner, P. D. (1996). Muscle O2 uptake kinetics in humans: Implications for metabolic control. *Journal of Applied Physiology (Bethesda, Md.: 1985)*, *80*(3), 988–998.

Hasin, T., Gerber, Y., McNallan, S. M., Weston, S. A., Kushwaha, S. S., Nelson, T. J., Cerhan, J. R., & Roger, V. L. (2013). Patients with heart failure have an increased risk of incident cancer. *Journal of the American College of Cardiology*, *62*(10), 881–886.

He, T., Zhu, M., Mills, B. J. W., Wynn, P. M., Zhuravlev, A. Y., Tostevin, R., Pogge von Strandmann, P. A. E., Yang, A., Poulton, S. W., & Shields, G. A. (2019). Possible links between extreme oxygen perturbations and the Cambrian radiation of animals. *Nature Geoscience*, *12*(6), 468–474.

Hester, R. L., Eraslan, A., & Saito, Y. (1993). Differences in EDNO contribution to arteriolar diameters at rest and during functional dilation in striated muscle. *The American Journal of Physiology*, *265*(1 Pt 2), H146-151.

Hirai, T., Visneski, M. D., Kearns, K. J., Zelis, R., & Musch, T. I. (1994). Effects of NO synthase inhibition on the muscular blood flow response to treadmill exercise in rats. *Journal of Applied Physiology (Bethesda, Md.: 1985)*, *77*(3), 1288–1293.

Hogan, M. C., Arthur, P. G., Bebout, D. E., Hochachka, P. W., & Wagner, P. D. (1992). Role of O2 in regulating tissue respiration in dog muscle working in situ. *Journal of Applied Physiology (Bethesda, Md.: 1985)*, *73*(2), 728–736.

Honig, C. R., & Gayeski, T. E. (1993). Resistance to O2 diffusion in anemic red muscle: Roles of flux density and cell PO2. *The American Journal of Physiology*, *265*(3 Pt 2), H868-875.

Ignarro, L. J., Buga, G. M., Wood, K. S., Byrns, R. E., & Chaudhuri, G. (1987). Endothelium-derived relaxing factor produced and released from artery and vein is nitric oxide. *Proceedings of the National Academy of Sciences of the United States of America*, *84*(24), 9265–9269.

Jones, L. W., Courneya, K. S., Mackey, J. R., Muss, H. B., Pituskin, E. N., Scott, J. M., Hornsby, W. E., Coan, A. D., Herndon, J. E., Douglas, P. S., & Haykowsky, M. (2012). Cardiopulmonary function and age-related decline across the breast cancer survivorship continuum. *Journal of Clinical Oncology: Official Journal of the American Society of Clinical Oncology*, *30*(20), 2530–2537.

Katsuki, S., Arnold, W., Mittal, C., & Murad, F. (1977). Stimulation of guanylate cyclase by sodium nitroprusside, nitroglycerin and nitric oxide in various tissue preparations and comparison to the effects of sodium azide and hydroxylamine. *Journal of Cyclic Nucleotide Research*, *3*(1), 23–35.

Kellawan, J. M., Johansson, R. E., Harrell, J. W., Sebranek, J. J., Walker, B. J., Eldridge, M. W., & Schrage, W. G. (2015). Exercise vasodilation is greater in women: Contributions of nitric oxide synthase and cyclooxygenase. *European Journal of Applied Physiology*, *115*(8), 1735–1746.

Kindig, C. A., Musch, T. I., Basaraba, R. J., & Poole, D. C. (1999). Impaired capillary hemodynamics in skeletal muscle of rats in chronic heart failure. *Journal of Applied Physiology (Bethesda, Md.: 1985)*, *87*(2), 652–660.

Kindig, C. A., Walsh, B., Howlett, R. A., Stary, C. M., & Hogan, M. C. (2005). Relationship between intracellular PO2 recovery kinetics and fatigability in isolated single frog myocytes. *Journal of Applied Physiology (Bethesda, Md.: 1985)*, *98*(6), 2316–2319.

Klassen, O., Schmidt, M. E., Scharhag-Rosenberger, F., Sorkin, M., Ulrich, C. M., Schneeweiss, A., Potthoff, K., Steindorf, K., & Wiskemann, J. (2014). Cardiorespiratory fitness in breast cancer patients undergoing adjuvant therapy. *Acta Oncologica (Stockholm, Sweden)*, *53*(10), 1356–1365.

Klausen, K., Secher, N. H., Clausen, J. P., Hartling, O., & Trap-Jensen, J. (1982). Central and regional circulatory adaptations to one-leg training. *Journal of Applied Physiology: Respiratory, Environmental and Exercise Physiology*, *52*(4), 976–983.

Koelwyn, G. J., Newman, A. A. C., Afonso, M. S., van Solingen, C., Corr, E. M., Brown, E. J., Albers, K. B., Yamaguchi, N., Narke, D., Schlegel, M., Sharma, M., Shanley, L. C., Barrett, T. J., Rahman, K., Mezzano, V., Fisher, E. A., Park, D. S., Newman, J. D., Quail, D. F., … Moore, K. J. (2020). Myocardial infarction accelerates breast cancer via innate immune reprogramming. *Nature Medicine*, *26*(9), 1452–1458.

Koivula, T., Uurasmaa, T.-M., Han, C., Maaniitty, T., Latifi, S., Lempiäinen, S., Kalliokoski, K., Sundberg, C. J., Rundqvist, H., Anttila, K., Minn, H., Knuuti, J., & Heinonen, I. (2024). Myocardial blood flow in newly diagnosed breast cancer patients at rest and during exercise. *iScience*, *27*(11), 111081.

Krogh, A., & Lindhard, J. (1913). The regulation of respiration and circulation during the initial stages of muscular work. *The Journal of Physiology*, *47*(1–2), 112–136.

Larsen, F. J., Schiffer, T. A., Borniquel, S., Sahlin, K., Ekblom, B., Lundberg, J. O., & Weitzberg, E. (2011). Dietary inorganic nitrate improves mitochondrial efficiency in humans. *Cell Metabolism*, *13*(2), 149–159.

Leening, M. J. G., Ferket, B. S., Steyerberg, E. W., Kavousi, M., Deckers, J. W., Nieboer, D., Heeringa, J., Portegies, M. L. P., Hofman, A., Ikram, M. A., Hunink, M. G. M., Franco, O. H., Stricker, B. H., Witteman, J. C. M., & Roos-Hesselink, J. W. (2014). Sex differences in lifetime risk and first manifestation of cardiovascular disease: Prospective population based cohort study. *BMJ (Clinical Research Ed.)*, *349*, g5992.

Mader, T., Chaillou, T., Alves, E. S., Jude, B., Cheng, A. J., Kenne, E., Mijwel, S., Kurzejamska, E., Vincent, C. T., Rundqvist, H., & Lanner, J. T. (2022). Exercise reduces intramuscular stress and counteracts muscle weakness in mice with breast cancer. *Journal of Cachexia, Sarcopenia and Muscle*, *13*(2), 1151–1163.

Peel, A. B., Thomas, S. M., Dittus, K., Jones, L. W., & Lakoski, S. G. (2014). Cardiorespiratory fitness in breast cancer patients: A call for normative values. *Journal of the American Heart Association*, *3*(1), e000432.

Piña, I. L., Apstein, C. S., Balady, G. J., Belardinelli, R., Chaitman, B. R., Duscha, B. D., Fletcher, B. J., Fleg, J. L., Myers, J. N., Sullivan, M. J., & American Heart Association Committee on exercise, rehabilitation, and prevention. (2003). Exercise and heart failure: A statement from the American Heart Association Committee on exercise, rehabilitation, and prevention. *Circulation*, *107*(8), 1210–1225.

Poole, D. C., & Musch, T. I. (2023). Capillary-Mitochondrial Oxygen Transport in Muscle: Paradigm Shifts. *Function (Oxford, England)*, *4*(3), zqad013.

Reckelhoff, J. F. (2001). Gender differences in the regulation of blood pressure. *Hypertension (Dallas, Tex.: 1979)*, *37*(5), 1199–1208.

Richardson, R. S., Poole, D. C., Knight, D. R., Kurdak, S. S., Hogan, M. C., Grassi, B., Johnson, E. C., Kendrick, K. F., Erickson, B. K., & Wagner, P. D. (1993). High muscle blood flow in man: Is maximal O2 extraction compromised? *Journal of Applied Physiology (Bethesda, Md.: 1985)*, *75*(4), 1911–1916.

Richardson, T. E., Kindig, C. A., Musch, T. I., & Poole, D. C. (2003). Effects of chronic heart failure on skeletal muscle capillary hemodynamics at rest and during contractions. *Journal of Applied Physiology (Bethesda, Md.: 1985)*, *95*(3), 1055–1062.

Roca, J., Agusti, A. G., Alonso, A., Poole, D. C., Viegas, C., Barbera, J. A., Rodriguez-Roisin, R., Ferrer, A., & Wagner, P. D. (1992). Effects of training on muscle O2 transport at VO2max. *Journal of Applied Physiology (Bethesda, Md.: 1985)*, *73*(3), 1067–1076.

Rubanyi, G. M., Freay, A. D., Kauser, K., Sukovich, D., Burton, G., Lubahn, D. B., Couse, J. F., Curtis, S. W., & Korach, K. S. (1997). Vascular estrogen receptors and endothelium-derived nitric oxide production in the mouse aorta. Gender difference and effect of estrogen receptor gene disruption. *The Journal of Clinical Investigation*, *99*(10), 2429–2437.

Sandner, P., Vakalopoulos, A., Hahn, M. G., Stasch, J.-P., & Follmann, M. (2021). Soluble guanylate cyclase stimulators and their potential use: A patent review. *Expert Opinion on Therapeutic Patents*, *31*(3), 203–222.

Savarese, G., Becher, P. M., Lund, L. H., Seferovic, P., Rosano, G. M. C., & Coats, A. J. S. (2023). Global burden of heart failure: A comprehensive and updated review of epidemiology. *Cardiovascular Research*, *118*(17), 3272–3287.

Stamler, J. S., & Meissner, G. (2001). Physiology of nitric oxide in skeletal muscle. *Physiological Reviews*, *81*(1), 209–237.

Stuehr, D. J., Misra, S., Dai, Y., & Ghosh, A. (2021). Maturation, inactivation, and recovery mechanisms of soluble guanylyl cyclase. *The Journal of Biological Chemistry*, *296*, 100336.

Sung, H., Ferlay, J., Siegel, R. L., Laversanne, M., Soerjomataram, I., Jemal, A., & Bray, F. (2021). Global Cancer Statistics 2020: GLOBOCAN Estimates of Incidence and Mortality Worldwide for 36 Cancers in 185 Countries. *CA: A Cancer Journal for Clinicians*, *71*(3), 209–249.

Taddei, S., Virdis, A., Ghiadoni, L., Mattei, P., Sudano, I., Bernini, G., Pinto, S., & Salvetti, A. (1996). Menopause is associated with endothelial dysfunction in women. *Hypertension (Dallas, Tex.: 1979)*, *28*(4), 576–582.

Thomas, D. D., Liu, X., Kantrow, S. P., & Lancaster, J. R. (2001). The biological lifetime of nitric oxide: Implications for the perivascular dynamics of NO and O2. *Proceedings of the National Academy of Sciences of the United States of America*, *98*(1), 355–360.

Thompson, B. C., Fadia, T., Pincivero, D. M., & Scheuermann, B. W. (2007). Forearm blood flow responses to fatiguing isometric contractions in women and men. *American Journal of Physiology. Heart and Circulatory Physiology*, *293*(1), H805-812.

Wagner, P. D. (1996). Determinants of maximal oxygen transport and utilization. *Annual Review of Physiology*, *58*, 21–50.

Wagner, P. D. (2000). Diffusive resistance to O2 transport in muscle. *Acta Physiologica Scandinavica*, *168*(4), 609–614.

Wilson, D. F., Owen, C. S., & Erecińska, M. (1977). Regulation of mitochondrial respiration in intact tissues: A mathematical model. *Advances in Experimental Medicine and Biology*, *94*, 279–287.

Wilson, H. E., Rhodes, K. K., Rodriguez, D., Chahal, I., Stanton, D. A., Bohlen, J., Davis, M., Infante, A. M., Hazard-Jenkins, H., Klinke, D. J., Pugacheva, E. N., & Pistilli, E. E. (2019). Human Breast Cancer Xenograft Model Implicates Peroxisome Proliferator-activated Receptor Signaling as Driver of Cancer-induced Muscle Fatigue. *Clinical Cancer Research: An Official Journal of the American Association for Cancer Research*, *25*(7), 2336–2347.

Wilson, H. E., Stanton, D. A., Montgomery, C., Infante, A. M., Taylor, M., Hazard-Jenkins, H., Pugacheva, E. N., & Pistilli, E. E. (2020a). Skeletal muscle reprogramming by breast cancer regardless of treatment history or tumor molecular subtype. *NPJ Breast Cancer*, *6*, 18.

Wilson, H. E., Stanton, D. A., Montgomery, C., Infante, A. M., Taylor, M., Hazard-Jenkins, H., Pugacheva, E. N., & Pistilli, E. E. (2020b). Skeletal muscle reprogramming by breast cancer regardless of treatment history or tumor molecular subtype. *NPJ Breast Cancer*, *6*, 18.

Zeng, X., Jiang, S., Ruan, S., Zhu, L., Lian, H., Liu, M., Guo, Z., Guo, J., Ye, C., Cheng, Y., & Dong, J. (2022). Cardiovascular risk factors and breast cancer incidence in a large middle-aged cohort study. *BMC Cancer*, *22*(1), 534.

Figure 1.1. *Schematic of the nitric oxide-soluble guanylyl cyclase signaling pathway.*

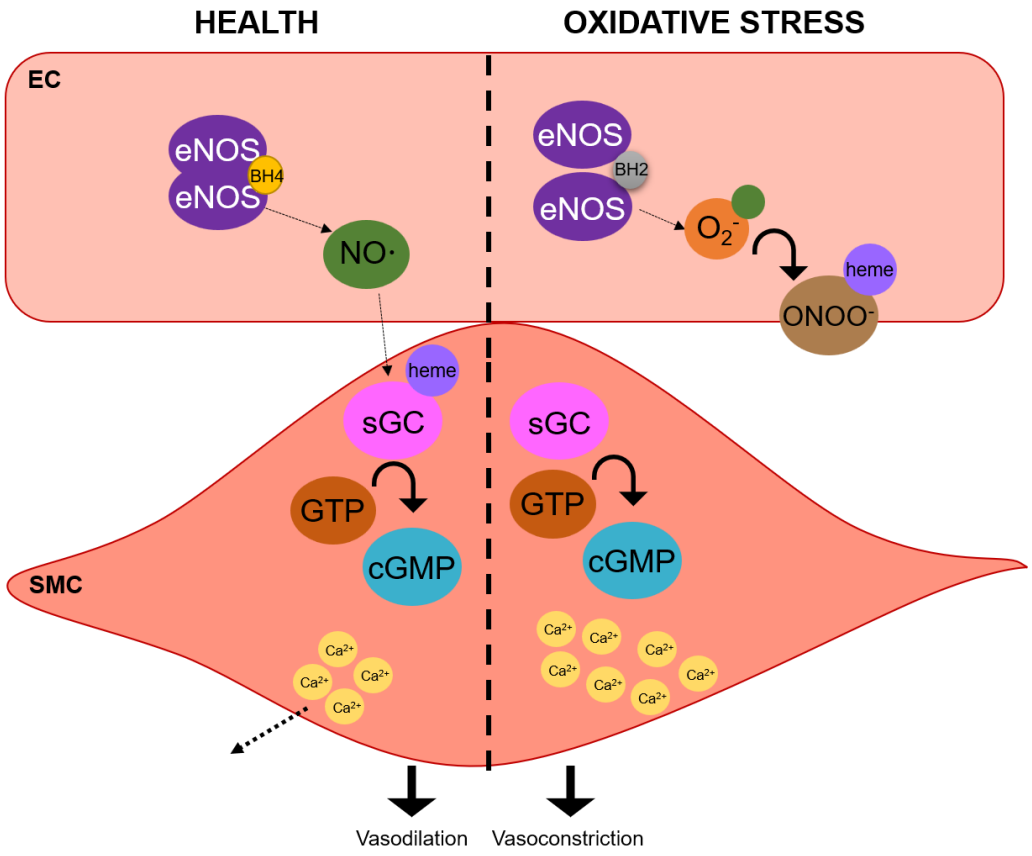

eNOS, endothelial nitric oxide synthase; BH4, tetrahydrobiopterin; NO, nitric oxide; sGC, soluble guanylyl cyclase; GTP, guanosine monophosphate; cGMP, cyclin guanosine monophosphate; O_2^-; superoxide; $ONOO^-$; peroxynitrite; Ca^{2+}, calcium. *Left*: in healthy conditions heme-intact sGC promotes the conversion of GTP to cGMP to induce smooth muscle cell vasodilation. *Right*: in oxidative stress conditions elevated free radicals (O_2^-, $ONOO^-$) scavenge NO and the sGC heme moiety, which increases intracellular Ca^{2+} and reduces smooth muscle cell relaxation.

Figure 1.2. *Wagner diagram: Perfusive and diffusive components of O_2 transport.*

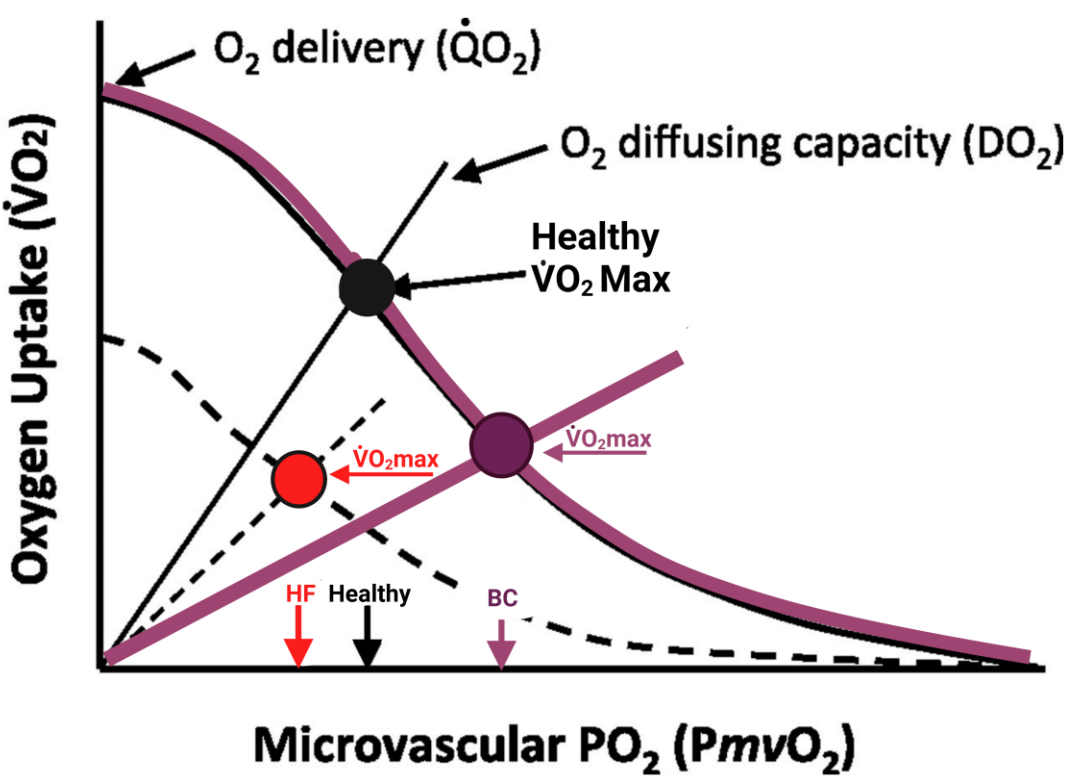

Adapted from Poole et al., 2012. Facets of the perfusive (curved line, Fick's principle) and the diffusive (straight line from origin, Fick's law of diffusion) components of O_2 transport conflate to yield maximal O_2 uptake ($\dot{V}O_2$max) in health vs. heart failure (HF, dashed lines/red) and breast cancer (BC, pink lines). In HF, $\dot{V}O_2$ is reduced by both impaired perfusive and diffusive O_2 transport such that microvascular PO_2 ($PmvO_2$) may be either the same or lower than in health while in BC, $PmvO_2$ may be higher secondary to reduced O_2 despite higher or normal blood flow and impaired O_2 extraction.

Chapter 2 - Effect of soluble guanylyl cyclase stimulator on skeletal muscle oxygenation in HFmrEF

Abstract

Heart failure (HF) with a mildly reduced ejection fraction (HFmrEF; 40-49%) is present in up to 25% of HF patients. Therapeutic treatment options for HFmrEF-associated exercise intolerance are limited. Nitric oxide (NO)-independent stimulation of soluble guanylyl cyclase (sGC) to improve vascular function offers a novel approach to enhance skeletal muscle oxygenation (interstitial pressure of O_2, $PO_2$is) and exercise capacity. We tested the hypotheses that the sGC stimulator BAY 41-2272 (BAY41) would increase exercise tolerance, skeletal muscle $PO_2$is during contractions, and nitric oxide (NO)-sensitivity in HFmrEF rats. Healthy (*n*=20) and HFmrEF (*n*=25) Sprague-Dawley rats (3-4 months) were used for this investigation. HFmrEF was confirmed via echocardiography and rats were randomized and treated with either 1.0 mg kg^{-1} of BAY41 or vehicle for 2 weeks followed by exercise testing and spinotrapezius muscle phosphorescence quenching measurements during 1Hz contractions. HFmrEF rats had a lower exercise capacity vs. Healthy rats during treadmill exercise (834±169 vs. 1138±214 s; P<0.001). BAY41 increased exercise capacity (1158 ± 223s; P<0.01) and muscle oxygenation index (1461±427 vs 1108±239 mmHg·s; P=0.049) during 1Hz contractions versus HFmrEF control rats. Sodium nitroprusside superfusion elicited a faster response time in BAY41-treated HFmrEF rats versus controls (150±18 vs. 220±50; P<0.05). Following SNP superfusion, BAY41-treated HFmrEF rats had a significantly elevated muscle oxygenation index during contractions versus controls (3104±703 vs 2365±682 mmHg·s; P=0.027). These data suggest that sGC stimulator BAY41-2272 can improve skeletal muscle oxygenation and increase the exercise capacity in HFmrEF rats potentially via enhanced NO-sensitivity in the vascular smooth muscle.

Introduction

Heart failure (HF) imposes an extensive healthcare burden afflicting ~64 million people worldwide and is classified into three subtypes based on left ventricular (LV) ejection fraction (EF): HF with preserved EF (HFpEF), reduced EF (HFrEF), and HF with mildly reduced ejection fraction EF (HFmrEF) (Bozkurt et al., 2021; Savarese et al., 2023). It is estimated that HFmrEF makes up ~25% of the clinical HF population (Hsu et al., 2017). These individuals have a significantly reduced peak oxygen uptake during exercise ($\dot{V}O_2$peak) of ~17 mL kg^{-1} min^{-1} (range: ~12-21 mL kg^{-1} min^{-1}) (Pugliese et al., 2019). $\dot{V}O_2$ peak stratifies risk for cardiac transplant, clinical trial inclusion criteria, and innovative pharmacotherapy for all degrees of HF(Parikh et al., 2009); however, HFmrEF (EF: 40%-49%) is frequently excluded from clinical trials that instead focus on severe HF (Savarese et al., 2022). This poses a significant challenge for individuals with HFmrEF, because timely initiation of guideline-directed medical therapy is crucial. One promising target is the nitric oxide (NO)-soluble guanylyl cyclase (sGC)-cyclic guanosine monophosphate (cGMP) signaling pathway, which could potentially be leveraged to improve skeletal muscle O_2 transport and impede disease progression in HFmrEF.

In HF, reduced NO bioavailability and impaired NO-mediated vasodilation (Katz et al., 1996; Kiowski et al., 1998; Kubo et al., 1991) underlie, in part, the microvascular O_2 supply ($\dot{Q}O_2$) response which is inadequate to match metabolic demand ($\dot{V}O_2$) in skeletal muscle at the onset of exercise (Poole et al., 2012). Consequently, the partial pressure of O_2 within the interstitial space ($PO_2$is), which is directly reflective of $\dot{Q}O_2$-to-$\dot{V}O_2$ matching, decreases with worsening HF (slower $\dot{V}O_2$ kinetics, increased O_2 delivery dependence) (Craig et al., 2019). Targeting the downstream NO-receptor sGC has been shown to increase exercise tolerance in

humans and animal models of cardiovascular disease (Ghofrani et al., 2013; Hu et al., 2023); however, the effects on peripheral O_2 transport are not known.

The NO-sGC system plays an important role in the regulation of vascular tone by increasing cGMP to promote tissue relaxation (Derbyshire & Marletta, 2012). The spectrum of oxidative stress across HF severity reduces sGC sensitivity to upstream NO (Derbyshire & Marletta, 2012) and/or renders sGC inactive via oxidation (Stasch & Hobbs, 2009) thereby disrupting NO-cGMP signaling. Therefore, the discovery of NO-independent sGC stimulators was a landmark in targeting and enhancing cGMP signaling (Sandner et al., 2021). These compounds, like Vericiguat, stimulate sGC in the absence of NO, increase sGC sensitivity, and have a synergistic effect with endogenous NO (Breitenstein et al., 2017; Sandner et al., 2021). Unfortunately, sGC stimulation in patients with worsening HFrEF did not improve exercise capacity (Armstrong et al., 2020). A secondary analysis revealed that sGC stimulators were more effective at reducing all-cause mortality in stable HF, which suggests that targeting sGC in HFmrEF may be efficacious (Butler et al., 2022).Therefore, the aim of the present study was to investigate the effects sGC stimulation on skeletal muscle oxygenation ($PO_2$is) and exercise tolerance in rats with HFmrEF. We tested the hypotheses that compared to vehicle treated rats, HFmrEF rats treated with the sGC stimulator BAY 41-2272 (BAY41) would 1) have enhanced $PO_2$is kinetics during contractions (i.e., slower $PO_2$is fall from rest to contractions), 2) increased sensitivity to exogenous NO (i.e., accelerated rise in $PO_2$is) and 3) an improved exercise capacity.

Methods

Ethical Approval

All procedures were approved by the Institutional Animal Care and Use Committee of Kansas State University (Protocol #4719), conformed to the Guide for the Care and Use of Laboratory Animals published by the US National Institutes of Health (NIH Publication No. 85-23, revised 1985), and conducted according to the National Research Council Guide for the Care and Use of Laboratory Animals. Experiments were performed on male Sprague-Dawley rats (*n* = 45; 3-4 months old, Charles River Laboratories, Wilmington, MA). Upon arrival, animals were maintained in accredited (Association for the Assessment and Accreditation of Laboratory and Animal Care) animal facilities under a 12:12 h light: dark cycle with food and water provided *ad libitum*. The experimental design for both the non-invasive and invasive measurements is presented in Figure 2.1.

Myocardial infarction procedure

Rats were randomized to either Healthy (*n*=20) or HFmrEF (*n* = 25) groups. HFmrEF was induced via surgical ligation of the left main coronary artery (i.e., myocardial infarction, MI). Immediately prior to surgery, HFmrEF rats were administered Amiodarone (110 mg kg^{-1} i.p.) to reduce the development of ventricular arrythmias during the procedure. Rats were anesthetized with a 2.5% isoflurane-O_2 mixture and intubated for mechanical ventilation with a rodent respirator (model 680, Harvard Apparatus, Holliston, MA) for the duration of the surgical procedure. The heart was then exposed via a thoracotomy at the fifth intercostal space and the left main coronary artery was ligated with 6–0 silk suture ∼1-2 mm distal to the edge of the left atrium. The incision was closed and rats were administered ampicillin (50 mg kg^{-1} i.m.) to reduce susceptibility to infection, and analgesic agents (bupivacaine (1.5 mg kg^{-1} s.c.),

buprenorphine (0.01-0.05 mg kg^{-1} i.m.)). Rats were monitored for ~4 h post-surgery for arrhythmias and signs of stress. An intensive 14-day post-operative plan ensured daily assessment (reduced appetite, weight loss, changes in gait/posture, etc.).

Echocardiography

Five weeks following the MI procedure, LV function was assessed via transthoracic echocardiography (*see Figure 2.1*) using a commercially available system (Logiq S8; GE Health Care, Milwaukee, WI) with an 18 MHz linear transducer (L8-18i) as previously described (Craig et al., 2019). Rats were initially anesthetized with a 5% isoflurane-O_2 mixture and maintained on <2.5% isoflurane-O_2 (Butler Health Supply, Doblin, OH) while positioned on a heating pad to keep core temperature at ~37°C (measured via rectal thermometer). Standard 2-dimensional and M-mode images from the mid-papillary level were obtained with frame rates of >50 frames/s. Ventricular dimensions and wall thicknesses were obtained from M-mode measurements over 4 consecutive cardiac cycles. Measurements presented are an average of the 4 cardiac cycles. LV internal dimensions (ID, cm) and posterior wall (PW, cm) thicknesses were measured at end systole (LVIDs, cm; PWs, cm) and end diastole (LVIDd, cm; PWd, cm). Fractional shortening (FS, %) was calculated from the measurements of LV chamber diameters: FS = [(LVIDd – LVIDs)/LVIDd] × 100. LV end-systolic (LVESv, ml) and end-diastolic (LVEDv, ml) volumes were calculated using the Teicholz formula: LV volume = (7.0/2.4 + LV dimension) × LV dimension^3. Stroke volume was calculated as: SV = LVEDv- LVESv. Ejection fraction (EF, %) was calculated as: EF = [(LVEDv- LVESv)/LVEDv] × 100. Eight rats had EF% outside the window of interest (40-49%), and were therefore excluded from this study.

Treadmill acclimatization and time to exhaustion

Following the initial echocardiogram, all rats were familiarized with running on a motor-driven treadmill for 5 min day^{-1} for 5 days at 25 m min^{-1} up a 5% grade. Following treadmill familiarization, rats performed a time to exhaustion test to assess exercise capacity (Copp et al., 2009; Poole et al., 2020). All exercise tests were performed between 8 AM and 4 PM to diminish diurnal variation in the results (Clark & Conlee, 1979). Throughout the exercise protocols, the room temperature was maintained at ~21-22ºC. The time to exhaustion protocol consisted of a progressive exercise test where rats began at a speed of 25 m min^{-1} up a 5% grade for 15 min. Thereafter, the speed increased 5 m min^{-1} every 15 min until the rat was unable or unwilling to maintain pace with the treadmill belt despite encouragement by manual bursts of high-pressure air aimed at the hindlimbs. Fatigue was preceded by a lowering of the hindquarters and a raised snout, which results in a significantly altered gait. Time from the start to the cessation of exercise was measured and recorded to the nearest second. Exhaustion was confirmed by placing the rat in a supine position and observing absence or the delay of the righting reflex (Poole et al., 2020). This protocol typically induces exhaustion within 1500 s, concomitant with running constituting severe intensity exercise (i.e., above critical speed) (Copp et al., 2009). Rats were weighed upon completion of the test and the results reflect the rat's end exercise weight. Distance run was calculated by multiplying the time by the speed of the treadmill belt at each increment.

Drug dosing

Following initial time to exhaustion protocols, Healthy and HFmrEF rats were randomly assigned to sGC stimulator (Healthy + BAY41, *n*=10; HFmrEF+ BAY41, *n*=10) or vehicle (Healthy, *n*=10; HFmrEF, *n*=7) treatment groups. The sGC stimulator BAY 41-2272 (5-Cyclopropyl-2-[1-(2-fluorobenzyl)-1H-pyrazolo[3,4-b]pyridin-3-yl]-pyrimidin-4-ylamine, Bayer Pharmaceuticals, Wuppertal, Germany) was weighed and mixed with a vehicle which consisted

of 10% Transcutol (diethylene glycol monoethyl ether, Sigma Aldrich, St. Louis, MO), 20% Cremophor EL (Sigma Aldrich, St. Louis, MO), and 70% water to obtain a dose of 1.0 mg kg^{-1} BAY41 in 1 ml of vehicle. This dose accounts for the ~6-7-fold greater resting metabolic rate in rats compared to humans (Poole et al., 2020). BAY41 or vehicle was administered via oral gavage, detailed previously (Weber et al., 2022), b.i.d. for 14 days. The day following the final dose we performed the same protocol detailed above (*see Echocardiography and Time to exhaustion*).

Surgical preparations and phosphorescence quenching

24 hours following the final time to exhaustion measurements, rats were anesthetized with a 5% isoflurane-O_2 mixture and maintained with 2.5% isoflurane-O_2 while core temperature was kept at ~37°C (measured via rectal thermometer). The left carotid artery was isolated, cannulated and a 2-French catheter-tip pressure transducer (Millar Instruments, Houston, TX, USA) was advanced into the LV to measure LV end diastolic pressure (LVEDP) and changes in LV pressure over time (LV dP/dT). After the Millar measurements, the transducer was removed and the carotid artery was cannulated with PE-10 connected to PE-50 (Intra-Medic polyethylene tubing; Clay Adams Brand, Benton, Dickson and Company, Sparks, MD) to measure mean arterial pressure and heart rate (Digi-Med BPA; Model 400). A second catheter was placed in the caudal artery for administration of pentobarbital sodium anesthesia (50 mg ml^{-1}) and arterial blood sampling. Rats were then transitioned to pentobarbital sodium anesthesia (20 mg kg^{-1} body weight i.a.) while the concentration of isoflurane decreased and subsequently discontinued. The depth of anesthesia was regularly monitored via toe pinch and palpebral reflex with pentobarbital anesthesia supplemented (3.5-7.0 mg kg^{-1}) as necessary during experimentation.

To exteriorize the spinotrapezius muscle, the overlying skin and fascia were carefully removed from the mid-dorsal-caudal region and the spinotrapezius muscle was exposed. Importantly, this exteriorization does not damage vascular supply or neural innervation to the muscle (Bailey et al., 2000; Gray, 1973; Kindig et al., 1999). This muscle was chosen for its similar fiber-type composition and oxidative capacity to the untrained human quadriceps muscle (Delp & Duan, 1996). Silver wire electrodes were sutured (6-0 silk) to the rostral (cathode) and caudal (anode) regions of the muscle to induce twitch contractions. The muscle was continuously superfused with Krebs-Henseleit bicarbonate-buffered solution (4.7 mM KCl, 2.0 mM $CaCl_2$, 2.4 mM $MgSO_4$, 131 mM NaCl, and 22 mM $NaHCO_3$; pH = 7.40; equilibrated with 5% CO_2-95% N_2 at 38°C) and the adjacent tissue was covered with Saran wrap (S.C. Johnson & Son, Racine, WI) to minimize dehydration.

Figure 2.1B describes the experimental protocol described herein. All the following measurements were completed in a dark room to minimize interference with phosphorescence signal. Oxyphor G4 (Pd-meso-tetra-(3,5-dicarboxyphenyl)-tetrabenzo-porphyrin), a phosphorescent probe that permits the dynamic visualization of tissue PO_2 (Esipova et al., 2011), was injected locally into the muscle (3-4 injections 10 μL at 10 μM concentration) using a 29 G needle. Care was taken to avoid damaging any visible vasculature. Following G4 injections, the spinotrapezius muscle was covered with Saran wrap (S.C. Johnson & Son, Racine, WI) to minimize dehydration during a 15 min period that allows for diffusion of Oxyphor G4 throughout the muscle and into the interstitial space. A bifurcated light guide was positioned ~3-4 mm above the surface of the exposed muscle in a field absent of large vessels.

Thereafter, a frequency domain phosphorimeter (PMOD 500; Oxygen Enterprises, Philadelphia, PA) was used as previously described (Craig et al., 2018), to determine resting and

contracting $PO_2$is during two separate control (CON) and sodium nitroprusside superfusion (SNP, 300 μM) conditions. Twitch contractions were electrically evoked (1Hz, 6 V, 2 ms pulse duration) with a Grass S88 Stimulator (Quincy, MA) for 180 s and $PO_2$is was measured and recorded at 2 s intervals throughout the duration of the protocol. This stimulation protocol elicits ~4-5-fold increase in $\dot{Q}O_2$ and a ~7-fold increase in $\dot{V}O_2$ that is consistent with moderate intensity exercise (Behnke et al., 2001; Hirai et al., 2013). Immediately following control $PO_2$is measurements, 0.3 ml of blood was sampled from the caudal artery catheter for the analysis of arterial blood gases. After 30 min of recovery, $PO_2$is was measured briefly (~30 s) to verify a return to baseline values. Thereafter, the spinotrapezius was superfused with SNP for 180 s and $PO_2$is was continuously recorded. Once a stable $PO_2$is was confirmed (additional 180 s), the same stimulation protocol above was repeated in the presence of SNP. Following the last contraction protocol, rats were euthanized via pentobarbital sodium (>100 mg kg^{-1}) overdose and cardiac excision. MI size (% infarct) was determined by planimetry as previously described (Craig et al., 2019; Pfeffer et al., 1979).

Analysis of interstitial PO_2 kinetics

The kinetics analyses of the $PO_2$is response was measured utilizing the Stern-Volmer relationship. Direct measurement of phosphorescence lifetime yielded $PO_2$is via the following equation:

$$\mathrm{PO_2} = \left(\frac{\tau^{\circ}}{\tau - 1}\right) \Big/ (\mathrm{k_Q} \times \tau^{\circ})$$

where k_Q is the quenching constant and τ and τ° are the phosphorescence lifetimes at the ambient O_2 concentration and in the absence of O_2, respectively. In tissues at 32.3°C (muscle surface temperature ~32°C) the parameters for G4 were as follows: k_Q of 258 mmHg s^{-1} and τ^0 of 226

μs. Muscle temperature does not change appreciably during the contraction protocol herein, therefore the phosphorescence lifetime is affected exclusively by the PO_2. The kinetics analyses of the $PO_2$is response during contractions was modeled with $PO_2$is measurements collected during 30 s of rest and 180 s of contractions and with either a one- or two-component model:

One-component:

$$\mathrm{PO_2(t)} = \mathrm{PO_{2(BL)}} - \Delta_1 PO_2\left[1 - e^{(-t-TD_1/\tau_1)}\right]$$

Two-component:

$$\mathrm{PO_2(t)} = \mathrm{PO_{2(BL)}} - \Delta_1 \mathrm{PO_2}\left[1 - e^{(-t-TD_1/\tau_1)}\right] + \Delta_2 \mathrm{PO_2}\left[1 - e^{(-t-TD_1/\tau_1)}\right]$$

The SNP superfusion response was fit with $PO_2$is at rest (30 s) and during 180 s of SNP superfusion:

$$\mathrm{PO_2(t)} = \mathrm{PO_{2(BL)}} + \Delta_1 \mathrm{PO_2}\left[1 - e^{(-t-TD_1/\tau_1)}\right]$$

where PO_2(t) represents the $PO_2$is at any given timepoint, $PO_{2(BL)}$ corresponds to the 30 s of resting $PO_2$is before contractions, Δ_1PO_2 and Δ_2PO_2 are the amplitude for the first and second components, respectively, TD_1 and TD_2 are the time delays for the first and second component, respectively, and τ_1 and τ_2 are the time constants (i.e., the time required to reach 63% of the amplitude) for each component. Appropriate fits were determined by: 1) the coefficient of determination, 2) sum of the squared residuals, and 3) visual inspection and analysis of the model fit to the data and residuals. Mean response time (MRT) is the overall kinetics of the primary and secondary responses during contractions or SNP superfusion (Macdonald et al., 1997):

One-component:

$$\mathrm{MRT} = \mathrm{TD_1} + \tau_1$$

Two-component:

$$\mathrm{MRT} = (\Delta_1/\Delta_{\mathrm{total}})(\mathrm{TD_1} + \tau_1) + (\Delta_2/\Delta_{\mathrm{total}})(\mathrm{TD_2} + \tau_2)$$

where TD_1 and TD_2, Δ_1 and Δ_2, and τ_1 and τ_2 are defined above, and Δ_{total} corresponds to the total change in PO_2 (i.e., $\Delta_1 + \Delta_2$) when two-component modeling was necessary. When a secondary component was present the primary amplitude was constrained to not exceed the nadir value to maximize the accuracy of the primary response kinetics. Since the second amplitude (Δ_2PO_2, undershoot of the $PO_2$is) was often mono-exponential in nature, it was manually calculated by subtracting the difference between the $PO_2$is at the end of contractions minus the nadir value of $PO_2$is during contractions. The time taken to reach 63% of the response was determined independent of modeling procedures (T_{63}). Area under the curve (AUC, mmHg·s) was integrated by summing each 2 s value across the 180 s contraction or during superfusion protocols to provide an index of overall spinotrapezius muscle interstitial oxygenation.

Western immunoblotting

In a subset of animals (Healthy, *n*=4; Healthy + BAY41, *n*=4; HFmrEF, *n*=6; HFmrEF + BAY41, *n*=7), 20 mg portions of spinotrapezius muscle samples were homogenized in radio-immune precipitation assay (RIPA) buffer (Sigma-Aldrich) containing a protease and phosphatase inhibitor (Pierce Protease and Phosphatase Inhibitor Mini Tablet, ThermoFisher Scientific) prepared according to manufacturer guidelines. Lysate protein concentrations were determined using the Qubit 4 Fluorometer with Protein Broad Range Assay kit (ThermoFisher Scientific). Protein quantification in medial costal diaphragm lysates was completed with Jess Simple Western (ProteinSimple) automated western blot analysis with primary antibodies for soluble guanylyl cyclase subunit beta 1 (sGCβ1; NBP1-89784, Novus Biologicals, 1:10 dilution) and superoxide dismutase 1 (SOD1; NBP1-90186, Novus Biologicals, 1:100 dilution). Lysate protein concentrations were equalized (1 mg/ml) before protein quantification and each target protein was assessed in a single trial to ensure equivalent primary antibody exposure across

spinotrapezius lysates, thus, removing the need for a housekeeping protein. Protein expression was quantified with Compass for Simple Western software.

Statistical analysis

Statistical analyses and curve fitting were performed using a commercially available software package (SigmaPlot 12.5, Systat Software, San Jose, CA). Two-way ANOVA tests were performed to determine differences in time to exhaustion, morphological characteristics, echocardiographic and Millar LV pressures, protein expression, and to detect differences present in $PO_2$is kinetics parameters. A two-way repeated measures ANOVA was used to evaluate temporal interactions (Group x Time) during $PO_2$is measurements. Normality was assessed using the Shapiro-Wilk test. If either the normality or equal variance assumptions were violated, a Mann-Whitney rank-sum test was used to compare the above variables. Tukey post hoc tests were used for multiple comparisons when significant differences were detected. If datasets were missing values, statistical analysis was done using a two-way mixed ANOVA test, followed by post-hoc pairwise comparisons using Fisher's Least Significant Difference test. Data are presented as the group mean ± SD. Significance was accepted at $P < 0.05$ unless otherwise stated.

Results

Echocardiographic and morphometric data

At 5 weeks, all Healthy rats (*n*=20) displayed normal LV function (LVEF ~80%), whereas 17/25 MI rats displayed HFmrEF (LVEF between 40-49%). No differences in LV function were present within groups prior to randomization into vehicle or BAY41 groups (5 weeks). 37 rats (Healthy, *n*=10; Healthy + BAY41, *n*=10; HFmrEF, *n*=7; HFmrEF + BAY41, *n*=10) were analyzed for hemodynamic and morphometric data. No differences were present in body weight (Healthy, 503 ± 76; Healthy + BAY41, 468 ± 83; HFmrEF, 513 ± 48; HFmrEF + BAY41, 486 ± 30 g; P > 0.05), LV mass (Healthy, 1.02 ± 0.07; Healthy + BAY41, 1.05 ± 0.07, HFmrEF, 1.03 ± 0.07; HFmrEF + BAY41, 1.05 ± 0.20 g, P > 0.05), or lung weight (Healthy, 1.61 ± 0.16; Healthy + BAY41, 1.75 ± 0.20; HFmrEF, 1.74 ± 0.10; HFmrEF + BAY41, 1.79 ± 0.29 g; P > 0.05). LV echocardiographic measurements following the dosing regimen (at 7 weeks post-MI) are presented in Table 2.1. The ~2-2.5-fold increase in LVEDv was compensated for by a reduction in FS and EF, such that SV was unchanged in HFmrEF rats. Despite significantly higher LVEDP (16 ± 3 vs. 13 ± 2 mmHg; P=0.005) and lower LV d*P*/d*T* (6300 ± 1142 vs. 7359 ± 1034 mmHg s^{-1}; P = 0.021) in HFmrEF vs. Healthy rats, respectively, no statistical differences in Millar catheter measurements were detected within treated and untreated conditions for HFmrEF (LVEDP, P=0.218; LVdP/dT, P=0.341) or Healthy (LVEDP, P=0.115; LV d*P*/d*T*, P=0.846). These data and the index of myocardial damage (~30%) indicate moderate HF within HFmrEF groups.

Time to exhaustion

29 rats (Healthy, *n*=6; Healthy + BAY41, *n*=7; HFmrEF, *n*=7; HFmrEF + BAY41, *n*=9) who ran below 1500 s were analyzed for time to exhaustion protocols. There were no differences

in time to exhaustion prior to drug/vehicle randomization within Healthy (1349 ± 128 vs. 1395 ± 312 s, P = 0.781) or HFmrEF (1016 ± 286 vs. 1073 ± 242 s, P = 0.708) groups. Time to exhaustion was greater HFmrEF + BAY41 (1158 ± 223 s) in comparison to HFrEF rats (834 ± 169 s; P=0.006) such that there were no differences between Healthy, Healthy + BAY41, and HFmrEF + BAY41 rats time to exhaustion (P > 0.05).

Arterial blood gases and hemodynamics

No differences in heart rate (HR) or mean arterial pressure (MAP) between Healthy and Healthy + BAY41 or HFmrEF and HFmrEF + BAY41 rats were present during CON and SNP protocols (P > 0.05). PaO_2 was reduced in HFmrEF + BAY41 rats compared to HFmrEF rats (86.1 ± 8.2 vs. 95.6 ± 10.9, mmHg, P=0.044), whereas [O_2] saturation was not significantly different (P > 0.05). No statistical differences in pH, CO_2, O_2 saturation, hematocrit, or lactate were present among groups (P=0.189).

Control interstitial PO_2 kinetics

33 rats (Healthy, *n*=8; Healthy + BAY41, *n*=8; HFmrEF, *n*=7; HFmrEF + BAY41, *n*=10) were analyzed for CON PO_2*is* kinetics. Four Healthy rats were excluded from the data set due to hemodynamic complications during/following catheterization. Four Healthy rats, 7 Healthy + BAY41, 4 HFmrEF, and 9 HFmrEF + BAY41 exhibited $PO_2$is profiles that transiently fell below the contracting steady state (i.e., undershoot, Δ_2PO_2) necessitating a two-component model fit. $PO_2$is kinetics and nadir between HFmrEF and HFmrEF + BAY41 rats (Table 2.2) were not different, however HFmrEF + BAY41 rats had a higher baseline $PO_2$is (P=0.046). HFmrEF BAY41 rats had a significantly increased $PO_2$is during steady-state contractions as compared to HFmrEF rats (Figure 2.3A, gray inset; 140-180 s; P < 0.05). The differences between the $PO_2$is profiles during the rest-contraction transient in HFmrEF groups were such that a substantially

higher overall muscle oxygenation (AUC) was observed within the spinotrapezius muscle of HFmrEF + BAY41 vs HFmrEF rats (P=0.027).

Sodium nitroprusside (SNP) interstitial PO_2 kinetics

31 rats (Healthy, *n*=8; Healthy + BAY41, *n*=6; HFmrEF, *n*=7; HFmrEF + BAY41, *n*=10) were analyzed for SNP PO_2*is* kinetics. Two Healthy + BAY41 rats were excluded from the data set due to hemodynamic complications during SNP superfusion (MAP < 70 mmHg) (Behnke et al., 2006). Mean SNP superfusion $PO_2$is kinetics parameters are presented in Table 2.3. HFmrEF + BAY41 rats had a greater sensitivity to SNP compared with HFmrEF rats as evidenced by the reduced T_{63} (P=0.011) and MRT (P=0.016). During SNP superfusion and incubation there was a greater increase in $PO_2$is in HFmrEF + BAY41 in comparison to HFmrEF rats (Figure 2.4A; 78-262 s; $P < 0.05$) and, as a result, substantially higher overall muscle interstitial oxygenation (i.e., AUC) (P=0.027). Mean spinotrapezius muscle $PO_2$is responses after SNP superfusion and during contractions are shown in Figure 2.5 and the kinetics parameters derived from model fits are presented in Table 2.4. SNP elevated $PO_2$is in HFmrEF + BAY41 vs HFmrEF rats during the steady state contractions (46-180 s; Figure 2.5A, $P < 0.05$). To better visualize the different temporal profiles among groups, Figure 2.6 illustrates the relative (% change from PO_2 at baseline) kinetics during the CON and SNP protocols. Note the greater time constant (slower rate of decline) in all groups following SNP which occurred to a greater degree in BAY41-treated rats (Healthy and HFmrEF).

sGCβ1 and SOD1 expression

21 samples of spinotrapezius muscle (Healthy, *n*=4; Healthy + BAY41, *n*=4; HFmrEF, *n*=6; HFmrEF + BAY41, *n*=7) were used to measure sGCβ1 and SOD1 expression via western immunoblotting (Figure 2.7). There was a significant increase in spinotrapezius muscle sGCβ1

expression in HFmrEF + BAY41 versus HFmrEF controls ($P = 0.045$), while no such differences were detected between Healthy groups ($P = 0.733$). SOD1 protein expression was not different between groups or within conditions ($P > 0.05$).

Discussion

This is the first investigation, to our knowledge, to demonstrate that a sGC stimulator (BAY 41-2272) can increase exercise tolerance potentially by altering the dynamic matching between skeletal muscle $\dot{Q}O_2$ and $\dot{V}O_2$ in HFmrEF rats. Specifically, compared with HFmrEF control rats, BAY41-treated HFmrEF rats had an elevated $PO_2$is during steady-state contractions coupled with an increased responsiveness to SNP superfusion (reduced time constant, increased overall muscle oxygenation). Further, the increased $PO_2$is and NO-sensitivity in HFmrEF + BAY41 rats was associated with an improved exercise tolerance not seen in Healthy rats.

This investigation used the MI model of HF (Pfeffer et al., 1979) to demonstrate characteristics consistent with human pathology. Notably, the HFmrEF condition established herein evidenced a dilated cardiomyopathy (**Table 2.1**) with no explicit hypertrophy (unchanged LVPWd, LVPWs, or LV mass vs. Healthy rats); which aligns closely with intermediate features of cardiovascular disease represented in the clinical population (Hsu et al., 2017).

Exercise capacity in HFmrEF

Individuals with HFmrEF display an exercise intolerance which is believed to be primarily due to impaired O_2 extraction similar to HFpEF (Pugliese et al., 2019). However, HFmrEF patients share a phenotype akin to HFrEF (male sex, increased prevalence of ischemic heart disease, and greater benefit from β-blockers) (Savarese et al., 2022). Despite no reduction in peak cardiac output (Pugliese et al., 2019), an MI-induced redistribution of $\dot{Q}O_2$ in HFmrEF (Musch & Terrell, 1992) would significantly affect spatial and temporal O_2 matching (Kindig et al., 1999) within and among skeletal muscles and reduce exercise tolerance preceding cardiac manifestations. We investigated MI rats with an EF of 40-49% to provide insight into the mechanisms underpinning exercise intolerance in HFmrEF and observed that sGC stimulator

treatment in HFmrEF rats resulted in a substantially greater (~40% longer) time to exhaustion in comparison to the HFmrEF controls (Figure 2.2). One explanation for this finding is that the sGC stimulator could increase the sensitivity of sGC to the NO-cGMP cascade within fast twitch fibers, which are recruited more heavily during exercise in HF than in health (Poole et al., 2012). Altogether more sensitive NO-sGC signaling would be expected to play a superior role in speeding $\dot{V}O_2$ kinetics during exercise when mechanically-induced endothelial NO synthase activation greatly increases endogenous NO production (Jones et al., 2021).

sGC signaling plays a vital role in skeletal muscle fatigability (Moon et al., 2017) and mitochondrial O_2 consumption (Hoffmann et al., 2015). Hu et al. demonstrated, in doxorubicin-treated mice, that 2 weeks of sGC stimulator administration increased skeletal muscle cGMP content to control levels which was associated with an increased running time and distance (Hu et al., 2023) (as seen herein). We found greater sGCβ1 expression in the skeletal muscle of HFmrEF + BAY41 rats (Figure 2.7). This, coupled with no change in SOD1 expression, the main antioxidant responsible for superoxide ($O_2^{\cdot -}$) scavenging (Guzik et al., 2002), suggests reduced $O_2^{\cdot -}$ production in HFmrEF + BAY41 rats. In rats with arterial hypertension, Reutten et al. suggested that early hypertension-induced changes in sGC signaling can be functionally compensated by sGC agonists, whereas greater disease severity and increased $O_2^{\cdot -}$ formation render the NO-sGC pathway inert (Ruetten et al., 1999).

Effect of sGC stimulator on interstitial PO_2 in HFmrEF

Both small (<30%) and large (>30%) MI results in the attenuation and/or redistribution of cardiac output during exercise, which is consistent with peripheral vascular dysfunction and reduced NO bioavailability (Ferreira et al., 2006). sGC stimulators have a dual mode of action in that they target sGC directly (downstream of endothelial dysfunction, NO scavenging) and

increase the sensitivity of sGC to low circulating NO (Sandner et al., 2021). NO-sGC signaling affects skeletal muscle contractile function, through both modulation of $\dot{Q}O_2$ and partial inhibition of cellular respiration ($\dot{V}O_2$) (Jones et al., 2021), which makes sGC a prime candidate to help coordinate skeletal muscle $\dot{Q}O_2$-to-$\dot{V}O_2$ matching (Poole et al., 2012). Such an effect would promote a faster rate of transcapillary O_2 flux whilst simultaneously lowering the $\dot{V}O_2$ requirements.

HFmrEF + BAY41 rats had a higher $PO_2$is during steady-state contractions versus the HFmrEF control rats (Figure 2.3; 140-180 s). There was also an increased overall index of muscle oxygenation within the spinotrapezius muscle of HFmrEF + BAY41 rats during the transition from rest to contractions (0-60 s) and throughout the entire contractile response. When mitochondrial O_2 consumption increases during contractions, a higher $PO_2$is is integral to preserve the transmural pressure head necessary for O_2 diffusion (DO_2) (Poole et al., 2012). Further, muscular metabolic recovery and phosphocreatine replenishment are dependent on O_2 availability, therefore, a greater $PO_2$is at the end of contractions is also expected to also reduce fatigue-accumulating metabolites and increase exercise tolerance (Kindig et al., 2005; Paganini et al., 1997).

Acute exposure of smooth muscle cells to sGC stimulators elicits concentration-dependent relaxation (via increased cGMP production) (Mülsch et al., 1997) that is further increased by exogenous NO (Sandner et al., 2021; Stasch & Hobbs, 2009). Our results are consistent with these findings, given the robust vasodilatory response in BAY41-treated rats during SNP superfusion (Figure 2.4). The reduced MRT in HFmrEF + BAY41 with SNP superfusion (Table 2.4) suggests that BAY41 restores vascular smooth muscle NO responsiveness; which would be expected to compensate for low circulating NO or desensitized

sGC in HFmrEF. These findings highlight the mechanistic potential of sGC stimulation to target vascular dysfunction in NO-deficient states. The SNP contraction response in HFmrEF + BAY41 rats elicited a $PO_2$is that was ~2-fold higher and ~3-fold longer (Figure 2.5A) than that seen during the control contractions (Figure 2.3A), which could be due, in part, to increased skeletal muscle $\dot{Q}O_2$ and shear-stress-mediated NO production (Katz et al., 1996) that complements the synergistic action of sGC stimulators (Sandner et al., 2021). The blunted $PO_2$is kinetics response post-SNP (emphasized in Figure 2.6) is advantageous to support sustained exercise bouts by preserving the driving pressure that facilitates temporal O_2 delivery. Earlier reports found that using a sGC activator in moderate HF resulted in a significant increase in the $PO_2$is during the onset of contractions, without impacting the steady-state contracting $PO_2$is (Weber et al., 2022), which contrasts with the sGC stimulator data herein. A higher $PO_2$is at the onset of contractions is expected to speed $\dot{V}O_2$ kinetics, reduce the reliance upon phosphagen systems, anaerobic ATP replenishment, and intracellular metabolic perturbations that contribute to exhaustion (Poole et al., 2012). Therefore, it is conceivable that, the combination of sGC activators and sGC stimulators could effectively target all populations of sGC (heme-oxidized/heme-free and wildtype, native heme) and potentially alter the overall $PO_2$is kinetics response.

Clinical implications

Even in optimally treated HF patients sustain the risk of adverse outcomes (Greene et al., 2021) which draws attention to investigating the value of novel HF pharmacotherapies across the spectrum of disease severity, especially in the early disease phases (Sato et al., 2017). Exercise training is one of the few interventions that improves exercise capacity and $\dot{V}O_2$peak across HF subtypes (O'Connor et al., 2009), reinforcing the importance of skeletal muscle and vascular function in HF pathophysiology. However, long-term adherence and accessibility to structured

exercise programs remains as a barrier to widespread implementation. A medication that directly enhances skeletal muscle oxygen utilization, vascular function, and metabolic efficiency could bridge this gap, offering a much-needed strategy to improve exercise tolerance and quality of life in HF patients while complementing existing therapies.

Experimental considerations

The MI model of HF in rats permits investigation of physiological mechanisms specific to HFmrEF in the absence of comorbidities and/or multiple pharmaceutical interventions present in human patients. Such factors confound data interpretation and limit physiological insights into experimental treatments. However, it must be emphasized that chronic vascular diseases and risk factors that promote the etiology of HFmrEF do complicate the translation of these findings to the clinical human population. Secondly, in consideration of the LV measurements presented, it has been recognized that global longitudinal strain may be a more reliable parameter of LV dysfunction in HF (Kalam et al., 2014) and that EF can change appreciably over time. Herein, we used echocardiographic techniques to assess ventricular function as established previously for this MI model (Weber et al., 2022) and made repeated measures to best simulate HFmrEF etiology. We did not see any improvements in cardiac function with the sGC stimulator in HFmrEF rats, however, it is important to note that recovery of LV function is no guarantee of freedom from future cardiac events (Merlo et al., 2015), whereas measurements like flow-mediated dilation and $\dot{V}O_2$peak represent strong predictors of adverse outcomes independent of EF (Meyer et al., 2005; Pugliese et al., 2019).

Conclusions

The data herein demonstrate that the sGC stimulator BAY 41-2272 can increase exercise capacity by enhancing skeletal muscle oxygenation in HFmrEF. This effect of pharmacological sGC stimulation on O_2 transport may be due to improvements in vascular function and NO sensitivity in the skeletal muscle vasculature. Investigating sGC stimulators in combination with exogenous NO-donors or sGC activators to treat HFmrEF-related skeletal muscle dysfunction constitutes an exciting avenue for future research.

References

Armstrong, P. W., Pieske, B., Anstrom, K. J., Ezekowitz, J., Hernandez, A. F., Butler, J., Lam, C. S. P., Ponikowski, P., Voors, A. A., Jia, G., McNulty, S. E., Patel, M. J., Roessig, L., Koglin, J., O'Connor, C. M., & VICTORIA Study Group. (2020). Vericiguat in Patients with Heart Failure and Reduced Ejection Fraction. *The New England Journal of Medicine*, *382*(20), 1883–1893.

Bailey, J. K., Kindig, C. A., Behnke, B. J., Musch, T. I., Schmid-Schoenbein, G. W., & Poole, D. C. (2000). Spinotrapezius muscle microcirculatory function: Effects of surgical exteriorization. *American Journal of Physiology. Heart and Circulatory Physiology*, *279*(6), H3131-3137.

Behnke, B. J., Kindig, C. A., Musch, T. I., Koga, S., & Poole, D. C. (2001). Dynamics of microvascular oxygen pressure across the rest-exercise transition in rat skeletal muscle. *Respiration Physiology*, *126*(1), 53–63.

Behnke, B. J., Padilla, D. J., Ferreira, L. F., Delp, M. D., Musch, T. I., & Poole, D. C. (2006). Effects of arterial hypotension on microvascular oxygen exchange in contracting skeletal muscle. *Journal of Applied Physiology (Bethesda, Md.: 1985)*, *100*(3), 1019–1026.

Bozkurt, B., Coats, A. J. S., Tsutsui, H., Abdelhamid, C. M., Adamopoulos, S., Albert, N., Anker, S. D., Atherton, J., Böhm, M., Butler, J., Drazner, M. H., Michael Felker, G., Filippatos, G., Fiuzat, M., Fonarow, G. C., Gomez-Mesa, J.-E., Heidenreich, P., Imamura, T., Jankowska, E. A., … Zieroth, S. (2021). Universal definition and classification of heart failure: A report of the Heart Failure Society of America, Heart Failure Association of the European Society of Cardiology, Japanese Heart Failure Society and Writing Committee of the Universal Definition of Heart Failure: Endorsed by the Canadian Heart Failure Society, Heart Failure Association of India, Cardiac Society of Australia and New Zealand, and Chinese Heart Failure Association. *European Journal of Heart Failure*, *23*(3), 352–380.

Breitenstein, S., Roessig, L., Sandner, P., & Lewis, K. S. (2017). Novel sGC Stimulators and sGC Activators for the Treatment of Heart Failure. *Handbook of Experimental Pharmacology*, *243*, 225–247.

Butler, J., Stebbins, A., Melenovský, V., Sweitzer, N. K., Cowie, M. R., Stehlik, J., Khan, M. S., Blaustein, R. O., Ezekowitz, J. A., Hernandez, A. F., Lam, C. S. P., Nkulikiyinka, R., O'Connor, C. M., Pieske, B. M., Ponikowski, P., Spertus, J. A., Voors, A. A., Anstrom, K. J., Armstrong, P. W., & VICTORIA Study Group. (2022). Vericiguat and Health-Related Quality of Life in Patients With Heart Failure With Reduced Ejection Fraction: Insights From the VICTORIA Trial. *Circulation. Heart Failure*, *15*(6), e009337.

Clark, J. H., & Conlee, R. K. (1979). Muscle and liver glycogen content: Diurnal variation and endurance. *Journal of Applied Physiology: Respiratory, Environmental and Exercise Physiology*, *47*(2), 425–428.

Copp, S. W., Davis, R. T., Poole, D. C., & Musch, T. I. (2009). Reproducibility of endurance capacity and VO2peak in male Sprague-Dawley rats. *Journal of Applied Physiology (Bethesda, Md.: 1985)*, *106*(4), 1072–1078.

Craig, J. C., Colburn, T. D., Caldwell, J. T., Hirai, D. M., Tabuchi, A., Baumfalk, D. R., Behnke, B. J., Ade, C. J., Musch, T. I., & Poole, D. C. (2019). Central and peripheral factors mechanistically linked to exercise intolerance in heart failure with reduced ejection fraction. *American Journal of Physiology. Heart and Circulatory Physiology*, *317*(2), H434–H444.

Craig, J. C., Colburn, T. D., Hirai, D. M., Schettler, M. J., Musch, T. I., & Poole, D. C. (2018). Sex and nitric oxide bioavailability interact to modulate interstitial Po2 in healthy rat skeletal muscle. *Journal of Applied Physiology (Bethesda, Md.: 1985)*, *124*(6), 1558–1566.

Delp, M. D., & Duan, C. (1996). Composition and size of type I, IIA, IID/X, and IIB fibers and citrate synthase activity of rat muscle. *Journal of Applied Physiology (Bethesda, Md.: 1985)*, *80*(1), 261–270.

Derbyshire, E. R., & Marletta, M. A. (2012). Structure and regulation of soluble guanylate cyclase. *Annual Review of Biochemistry*, *81*, 533–559.

Esipova, T. V., Karagodov, A., Miller, J., Wilson, D. F., Busch, T. M., & Vinogradov, S. A. (2011). Two new "protected" oxyphors for biological oximetry: Properties and application in tumor imaging. *Analytical Chemistry*, *83*(22), 8756–8765.

Ferreira, L. F., Hageman, K. S., Hahn, S. A., Williams, J., Padilla, D. J., Poole, D. C., & Musch, T. I. (2006). Muscle microvascular oxygenation in chronic heart failure: Role of nitric oxide availability. *Acta Physiologica (Oxford, England)*, *188*(1), 3–13.

Ghofrani, H.-A., D'Armini, A. M., Grimminger, F., Hoeper, M. M., Jansa, P., Kim, N. H., Mayer, E., Simonneau, G., Wilkins, M. R., Fritsch, A., Neuser, D., Weimann, G., Wang, C., & CHEST-1 Study Group. (2013). Riociguat for the treatment of chronic thromboembolic pulmonary hypertension. *The New England Journal of Medicine*, *369*(4), 319–329.

Gray, S. D. (1973). Rat spinotrapezius muscle preparation for microscopic observation of the terminal vascular bed. *Microvascular Research*, *5*(3), 395–400.

Greene, S. J., Butler, J., & Fonarow, G. C. (2021). Contextualizing Risk Among Patients With Heart Failure. *JAMA*, *326*(22), 2261–2262.

Guzik, T. J., Mussa, S., Gastaldi, D., Sadowski, J., Ratnatunga, C., Pillai, R., & Channon, K. M. (2002). Mechanisms of increased vascular superoxide production in human diabetes mellitus: Role of NAD(P)H oxidase and endothelial nitric oxide synthase. *Circulation*, *105*(14), 1656–1662.

Hirai, D. M., Copp, S. W., Ferguson, S. K., Holdsworth, C. T., Musch, T. I., & Poole, D. C. (2013). The NO donor sodium nitroprusside: Evaluation of skeletal muscle vascular and metabolic dysfunction. *Microvascular Research*, *85*, 104–111.

Hoffmann, L. S., Etzrodt, J., Willkomm, L., Sanyal, A., Scheja, L., Fischer, A. W. C., Stasch, J.-P., Bloch, W., Friebe, A., Heeren, J., & Pfeifer, A. (2015). Stimulation of soluble guanylyl cyclase protects against obesity by recruiting brown adipose tissue. *Nature Communications*, *6*, 7235.

Hsu, J. J., Ziaeian, B., & Fonarow, G. C. (2017). Heart Failure With Mid-Range (Borderline) Ejection Fraction: Clinical Implications and Future Directions. *JACC. Heart Failure*, *5*(11), 763–771.

Hu, B.-A., Li, Y.-L., Han, H.-T., Lu, B., Jia, X., Han, L., Ma, W.-X., Zhu, P., Wang, Z.-H., Zhang, W., Zhong, M., & Zhang, L. (2023). Stimulation of soluble guanylate cyclase by vericiguat reduces skeletal muscle atrophy of mice following chemotherapy. *Frontiers in Pharmacology*, *14*, 1112123.

Jones, A. M., Vanhatalo, A., Seals, D. R., Rossman, M. J., Piknova, B., & Jonvik, K. L. (2021). Dietary Nitrate and Nitric Oxide Metabolism: Mouth, Circulation, Skeletal Muscle, and Exercise Performance. *Medicine and Science in Sports and Exercise*, *53*(2), 280–294.

Kalam, K., Otahal, P., & Marwick, T. H. (2014). Prognostic implications of global LV dysfunction: A systematic review and meta-analysis of global longitudinal strain and ejection fraction. *Heart (British Cardiac Society)*, *100*(21), 1673–1680.

Katz, S. D., Krum, H., Khan, T., & Knecht, M. (1996). Exercise-induced vasodilation in forearm circulation of normal subjects and patients with congestive heart failure: Role of endothelium-derived nitric oxide. *Journal of the American College of Cardiology*, *28*(3), 585–590.

Kindig, C. A., Musch, T. I., Basaraba, R. J., & Poole, D. C. (1999). Impaired capillary hemodynamics in skeletal muscle of rats in chronic heart failure. *Journal of Applied Physiology (Bethesda, Md.: 1985)*, *87*(2), 652–660.

Kindig, C. A., Walsh, B., Howlett, R. A., Stary, C. M., & Hogan, M. C. (2005). Relationship between intracellular PO2 recovery kinetics and fatigability in isolated single frog myocytes. *Journal of Applied Physiology (Bethesda, Md.: 1985)*, *98*(6), 2316–2319.

Kiowski, W., Sütsch, G., Schalcher, C., Brunner, H. P., & Oechslin, E. (1998). Endothelial control of vascular tone in chronic heart failure. *Journal of Cardiovascular Pharmacology*, *32 Suppl 3*, S67-73.

Kubo, S. H., Rector, T. S., Bank, A. J., Williams, R. E., & Heifetz, S. M. (1991). Endothelium-dependent vasodilation is attenuated in patients with heart failure. *Circulation*, *84*(4), 1589–1596.

Macdonald, M., Pedersen, P. K., & Hughson, R. L. (1997). Acceleration of VO2 kinetics in heavy submaximal exercise by hyperoxia and prior high-intensity exercise. *Journal of Applied Physiology (Bethesda, Md.: 1985)*, *83*(4), 1318–1325.

Merlo, M., Stolfo, D., Anzini, M., Negri, F., Pinamonti, B., Barbati, G., Ramani, F., Lenarda, A. D., & Sinagra, G. (2015). Persistent recovery of normal left ventricular function and dimension in idiopathic dilated cardiomyopathy during long-term follow-up: Does real healing exist? *Journal of the American Heart Association*, *4*(1), e001504.

Meyer, B., Mörtl, D., Strecker, K., Hülsmann, M., Kulemann, V., Neunteufl, T., Pacher, R., & Berger, R. (2005). Flow-mediated vasodilation predicts outcome in patients with chronic heart failure: Comparison with B-type natriuretic peptide. *Journal of the American College of Cardiology*, *46*(6), 1011–1018.

Moon, Y., Balke, J. E., Madorma, D., Siegel, M. P., Knowels, G., Brouckaert, P., Buys, E. S., Marcinek, D. J., & Percival, J. M. (2017). Nitric Oxide Regulates Skeletal Muscle Fatigue, Fiber Type, Microtubule Organization, and Mitochondrial ATP Synthesis Efficiency Through cGMP-Dependent Mechanisms. *Antioxidants & Redox Signaling*, *26*(17), 966–985.

Mülsch, A., Bauersachs, J., Schäfer, A., Stasch, J. P., Kast, R., & Busse, R. (1997). Effect of YC-1, an NO-independent, superoxide-sensitive stimulator of soluble guanylyl cyclase, on smooth muscle responsiveness to nitrovasodilators. *British Journal of Pharmacology*, *120*(4), 681–689.

Musch, T. I., & Terrell, J. A. (1992). Skeletal muscle blood flow abnormalities in rats with a chronic myocardial infarction: Rest and exercise. *The American Journal of Physiology*, *262*(2 Pt 2), H411-419.

O'Connor, C. M., Whellan, D. J., Lee, K. L., Keteyian, S. J., Cooper, L. S., Ellis, S. J., Leifer, E. S., Kraus, W. E., Kitzman, D. W., Blumenthal, J. A., Rendall, D. S., Miller, N. H., Fleg, J. L., Schulman, K. A., McKelvie, R. S., Zannad, F., Piña, I. L., & HF-ACTION Investigators. (2009). Efficacy and safety of exercise training in patients with chronic heart failure: HF-ACTION randomized controlled trial. *JAMA*, *301*(14), 1439–1450.

Paganini, A. T., Foley, J. M., & Meyer, R. A. (1997). Linear dependence of muscle phosphocreatine kinetics on oxidative capacity. *The American Journal of Physiology*, *272*(2 Pt 1), C501-510.

Parikh, M. N., Lund, L. H., Goda, A., & Mancini, D. (2009). Usefulness of peak exercise oxygen consumption and the heart failure survival score to predict survival in patients >65 years of age with heart failure. *The American Journal of Cardiology*, *103*(7), 998–1002.

Pfeffer, M. A., Pfeffer, J. M., Fishbein, M. C., Fletcher, P. J., Spadaro, J., Kloner, R. A., & Braunwald, E. (1979). Myocardial infarct size and ventricular function in rats. *Circulation Research*, *44*(4), 503–512.

Poole, D. C., Copp, S. W., Colburn, T. D., Craig, J. C., Allen, D. L., Sturek, M., O'Leary, D. S., Zucker, I. H., & Musch, T. I. (2020). Guidelines for animal exercise and training protocols for cardiovascular studies. *American Journal of Physiology. Heart and Circulatory Physiology*, *318*(5), H1100–H1138.

Poole, D. C., Hirai, D. M., Copp, S. W., & Musch, T. I. (2012). Muscle oxygen transport and utilization in heart failure: Implications for exercise (in)tolerance. *American Journal of Physiology. Heart and Circulatory Physiology*, *302*(5), H1050-1063.

Pugliese, N. R., Fabiani, I., Santini, C., Rovai, I., Pedrinelli, R., Natali, A., & Dini, F. L. (2019). Value of combined cardiopulmonary and echocardiography stress test to characterize the haemodynamic and metabolic responses of patients with heart failure and mid-range ejection fraction. *European Heart Journal. Cardiovascular Imaging*, *20*(7), 828–836.

Ruetten, H., Zabel, U., Linz, W., & Schmidt, H. H. (1999). Downregulation of soluble guanylyl cyclase in young and aging spontaneously hypertensive rats. *Circulation Research*, *85*(6), 534–541.

Sandner, P., Vakalopoulos, A., Hahn, M. G., Stasch, J.-P., & Follmann, M. (2021). Soluble guanylate cyclase stimulators and their potential use: A patent review. *Expert Opinion on Therapeutic Patents*, *31*(3), 203–222.

Sato, T., Yoshihisa, A., Kanno, Y., Suzuki, S., Yamaki, T., Sugimoto, K., Kunii, H., Nakazato, K., Suzuki, H., Saitoh, S.-I., Ishida, T., & Takeishi, Y. (2017). Cardiopulmonary exercise testing as prognostic indicators: Comparisons among heart failure patients with reduced, mid-range and preserved ejection fraction. *European Journal of Preventive Cardiology*, *24*(18), 1979–1987.

Savarese, G., Becher, P. M., Lund, L. H., Seferovic, P., Rosano, G. M. C., & Coats, A. J. S. (2023). Global burden of heart failure: A comprehensive and updated review of epidemiology. *Cardiovascular Research*, *118*(17), 3272–3287.

Savarese, G., Stolfo, D., Sinagra, G., & Lund, L. H. (2022). Heart failure with mid-range or mildly reduced ejection fraction. *Nature Reviews. Cardiology*, *19*(2), 100–116.

Stasch, J.-P., & Hobbs, A. J. (2009). NO-independent, haem-dependent soluble guanylate cyclase stimulators. *Handbook of Experimental Pharmacology*, *191*, 277–308.

Weber, R. E., Schulze, K. M., Colburn, T. D., Horn, A. G., Hageman, K. S., Ade, C. J., Hall, S. E., Sandner, P., Musch, T. I., & Poole, D. C. (2022). Capillary hemodynamics and contracting skeletal muscle oxygen pressures in male rats with heart failure: Impact of soluble guanylyl cyclase activator. *Nitric Oxide: Biology and Chemistry*, *119*, 1–8.

Table 2.1. *Echocardiography of left ventricular function and pressure measurements.*

	Healthy (*n*=10)	Healthy + BAY41 (*n*=10)	HFmrEF (*n*=7)	HFmrEF + BAY41 (*n*=10)
LVIDd, cm	0.66 ± 0.06	0.66 ± 0.12	0.92 ± 0.15*****	0.91 ± 0.12*****
LVIDs, cm	0.31 ± 0.05	0.35 ± 0.11	0.74 ± 0.12*****	0.73 ± 0.09*****
LVPWd, cm	0.25 ± 0.05	0.28 ± 0.11	0.24 ± 0.06	0.25 ± 0.07
LVPWs, cm	0.36 ± 0.06	0.39 ± 0.07	0.31 ± 0.06	0.36 ± 0.10
FS, %	52 ± 5	48 ± 9	19 ± 4 *****	20 ± 5 *****
LVEDV, ml	0.67 ± 0.16	0.70 ± 0.37	1.73 ± 0.69*****	1.60 ± 0.41*****
LVESV, ml	0.09 ± 0.04	0.14 ± 0.12	0.97 ± 0.37*****	0.86 ± 0.23*****
SV, ml	0.58 ± 0.13	0.57 ± 0.26	0.76 ± 0.33	0.74 ± 0.22
EF, %	87 ± 4	83 ± 9	43 ± 3 *****	42 ± 5 *****
MI Size (%)	---	---	30 ± 5	30 ± 8
LVEDP, mmHg	12 ± 2	11 ± 3	15 ± 2	17 ± 2
LV d*P*/d*T,* mmHg/s	7250 ± 544	7416 ± 1559	6581 ± 1234	6018 ± 1044

Data are means ± SD. *n*, number of rats; LV, left ventricular, LVIDd, LV internal diameter in diastole; LVIDs, LV internal diameter in systole; LVPWd, LV posterior wall in diastole; LVPWs, LV posterior wall in systole; FS, fractional shortening; LVEDV, LV end diastolic volume; LVESV, LV end systolic volume; SV, stroke volume; EF, ejection fraction; MI, myocardial infarction; LVEDP, LV end diastolic pressure; LV d*P*/d*T*, LV change in pressure over change in time. * $P < 0.05$ vs Healthy. Analyzed via two-way ANOVA.

Table 2.2. *Interstitial pressure of O_2 kinetics parameters during contractions.*

	Healthy (*n*=8)	Healthy + BAY41 (*n*=8)	HFmrEF (*n*=7)	HFmrEF + BAY41 (*n*=10)
$PO_{2(BL)}$, mmHg	26.4 ± 4.2	31.6 ± 3.0 *****	22.5 ± 4.6	26.2 ± 2.9 *
Δ_1PO_2, mmHg	14.4 ± 2.8	15.1 ± 1.6	12.8 ± 4.3	12.7 ± 4.7
TD, s	10 ± 4	8 ± 6	5 ± 3	8 ± 4
T_{63}, s	25 ± 10	25 ± 5	25 ± 6	26 ± 10
$PO_{2(Nadir)}$, mmHg	12.0 ± 3.6	16.5 ± 3.7 *****	9.7 ± 3.1	13.4 ± 4.9
MRT, s	34 ± 12	35 ± 7	31 ± 9	34 ± 11
Δ_2PO_2, mmHg	1.5 ± 1.0	5.3 ± 3.9 *****	3.0 ± 2.2	3.2 ± 2.2
TD_2, s	76 ± 43	78 ± 8	77 ± 29	74 ± 26
$PO_{2(End\text{-}contract)}$, mmHg	14.2 ± 3.6	20.8 ± 6.2 *****	12.4 ± 1.7	16.6 ± 6.3 *****
AUC, mmHg·s	1333 ± 362	1826 ± 388 *****	1108 ± 239	1461 ± 427 *****

Data are means ± SD. *n*, number of rats, $PO_{2(BL)}$, PO_2 at baseline (-30-0 s); Δ_1PO_2, primary amplitude; TD, time delay; T_{63}, calculated time to reach 63% of the kinetic response; $PO_{2\ (Nadir)}$, lowest recorded PO_2 during contractions; MRT, mean response time; Δ_2PO_2, secondary amplitude; TD_2, secondary time delay; $PO_{2(End\text{-}Contract)}$, PO_2 at the end contractions (averaged 160-180 s); AUC, area under the curve during 0-180 s. ***** $P < 0.05$ vs vehicle within group; Analyzed via two-way ANOVA.

Table 2.3. *Interstitial pressure of O_2 kinetics parameters during SNP superfusion.*

	Healthy (*n*=8)	Healthy + BAY41 (*n*=6)	HFmrEF (*n*=7)	HFmrEF + BAY41 (*n*=10)
$PO_{2(BL)}$, mmHg	24.6 ± 1.5	31.1 ± 4.0 *	21.3 ± 3.7	23.8 ± 5.7
Δ_1PO_2, mmHg	15.3 ± 6.6	21.8 ± 5.3	18.6 ± 8.4	22.0 ± 9.1
TD, s	71 ± 57	61 ± 28	57 ± 39	45 ± 27
T_{63}, s	138 ± 74	184 ± 69	209 ± 38	136 ± 58 *
MRT, s	226 ± 102	245 ± 96	220 ± 50	150 ± 18 *
$PO_{2(End-SF)}$, mmHg	39.8 ± 6.9	52.8 ± 7.6 *	39.9 ± 9.7	45.8 ± 9.2
AUC (mmHg·s)	6332 ± 981	8025 ± 977 *	5789 ± 1283	7151 ± 1306 *

Data are means ± SD. *n*, number of rats, $PO_{2(BL)}$, PO_2 at baseline (-30-0 s); Δ_1PO_2, primary amplitude; TD, time delay; T_{63}, calculated time to reach 63% of the kinetic response; MRT, mean response time; $PO_{2(End-SF)}$, PO_2 at the end superfusion (averaged 160-180 s); AUC, area under the curve during superfusion and incubation (-30-360 s). * $P < 0.05$ vs vehicle within group. Analyzed via two-way ANOVA.

Table 2.4. *Interstitial pressure of O_2 kinetics parameters during SNP contractions.*

	Healthy (*n*=8)	Healthy + BAY41 (*n*=6)	HFmrEF (*n*=7)	HFmrEF + BAY41 (*n*=10)
$PO_{2(BL)}$, mmHg	39.8 ± 6.8	52.5 ± 7.6 *	39.6 ± 9.5	45.6 ± 9.1
Δ_1PO_2, mmHg	15.5 ± 3.5	16.7 ± 6.2	17.9 ± 6.1	16.3 ± 5.5
TD, s	4 ± 4	5 ± 5	4 ± 4	3 ± 4
T_{63}, s	30 ± 6	42 ± 8 *	51 ± 25	66 ± 36
$PO_{2(Nadir)}$, mmHg	21.6 ± 6.1	35.3 ± 8.9 *	20.8 ± 8.0	27.1 ± 9.8
MRT, s	42 ± 16	59 ± 23	54 ± 25	68 ± 38
$PO_{2(End\text{-}contract)}$, mmHg	24.3 ± 5.1	35.8 ± 8.5 *	21.6 ± 7.3	29.3 ± 7.2 *
AUC (mmHg·s)	2470 ± 580	3630 ± 731 *	2365 ± 682	3104 ± 703

Data are means ± SD. n, number of rats, $PO_{2(BL)}$, PO_2 at baseline (-30-0 s); Δ_1PO_2, primary amplitude; TD, time delay; T_{63}, calculated time to reach 63% of the kinetic response; $PO_{2(Nadir)}$, lowest recorded PO_2 during contractions; MRT, mean response time; $PO_{2(End\text{-}Contract)}$, PO_2 at the end contractions (averaged 160-180 s); AUC, area under the curve (0-180) s. * $P < 0.05$ vs vehicle within group. Analyzed via two-way ANOVA.

Figure 2.1. *Experimental protocol schematic.*

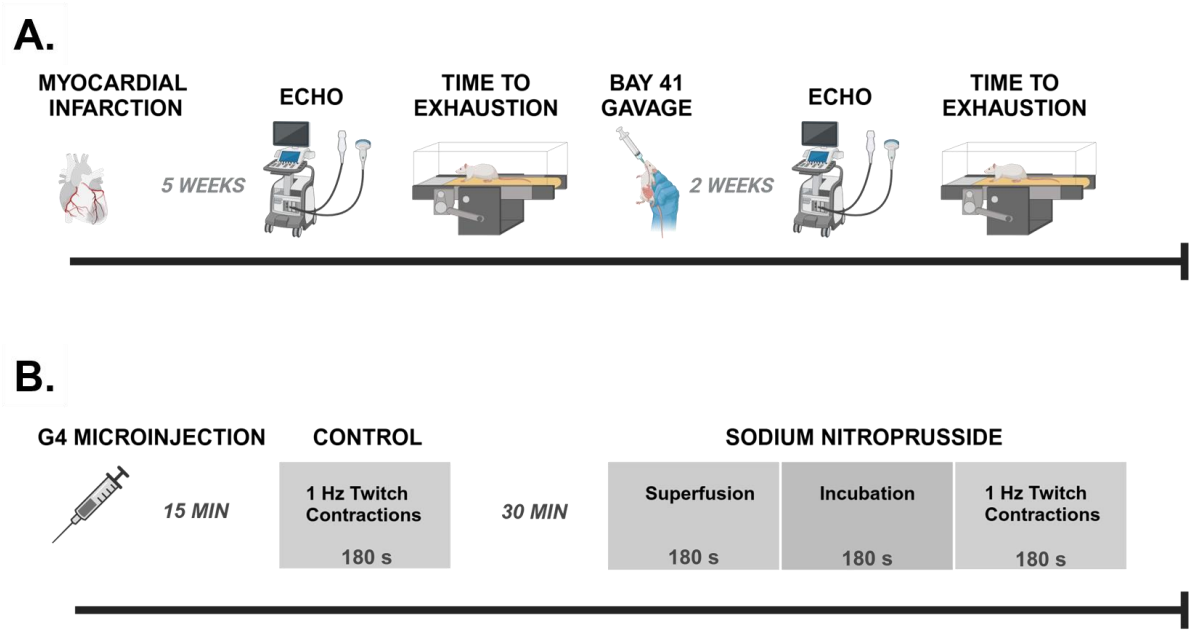

Figure 2.2. *Group mean and individually plotted time to exhaustion measurements.*

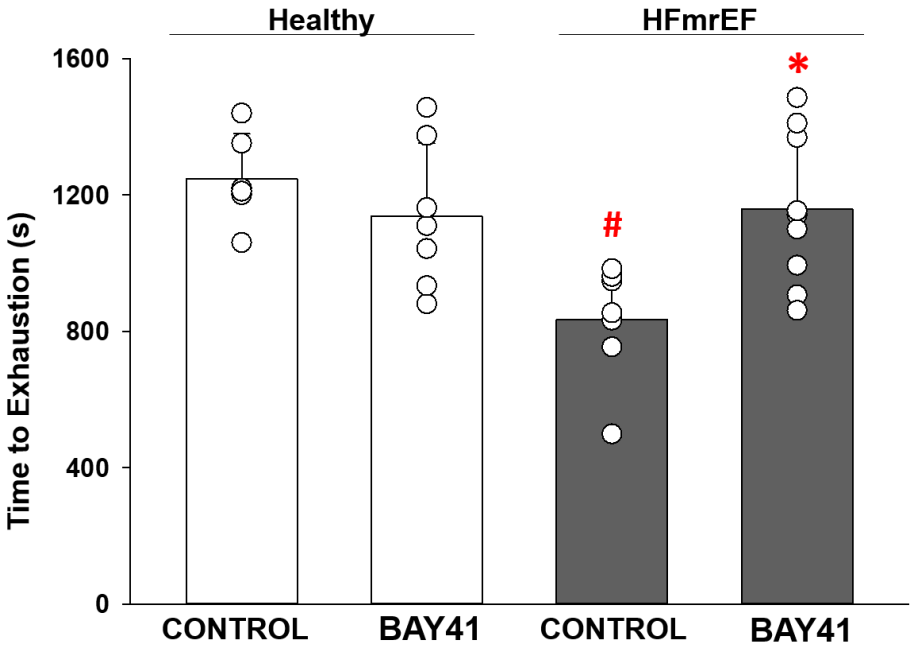

Data are mean ± SD. Healthy (*n*=6), Healthy + BAY41 (*n*=7), HFmrEF vehicle (*n*=7) and HFmrEF + BAY41 (*n*=9) rats. Data analyzed via two-way ANOVA with Tukey's post hoc analyses. #P<0.001 vs Healthy control; *P = 0.006 vs. vehicle within group.

Figure 2.3. *Interstitial pressure of O_2 during control contractions.*

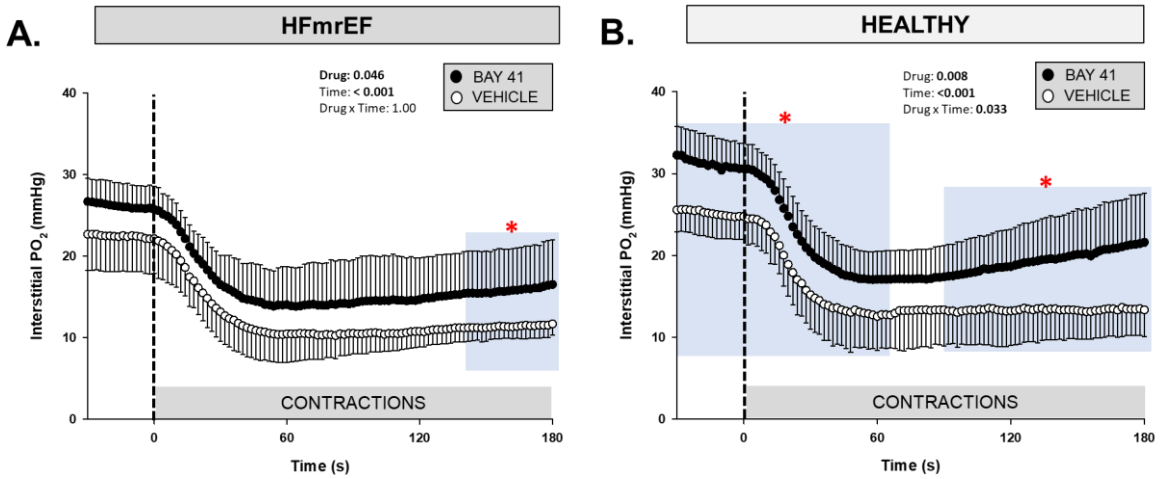

Data are mean ± SD. Healthy(*n*=8); Healthy + BAY41 (*n*=8); HFmrEF(*n*=7); HFmrEF + BAY41(*n*=10). The dashed line represents the onset of twitch contractions. A. HFmrEF + BAY41rats had a significantly higher $PO_2$is during steady-state contractions and from 140-180 s (blueinset) vs. HFmrEF control rats. B. Healthy + BAY41 rats had a significantly greater $PO_2$is at rest (-30-0) and during twitch contractions (30-60; 90-180 s) (blue inset). $PO_2$is was compared across time via two-way repeated measures ANOVA with Tukey's post hoc analyses. *P < 0.05 vs. vehicle within group.

Figure 2.4. *Interstitial pressure of O_2 during SNP superfusion.*

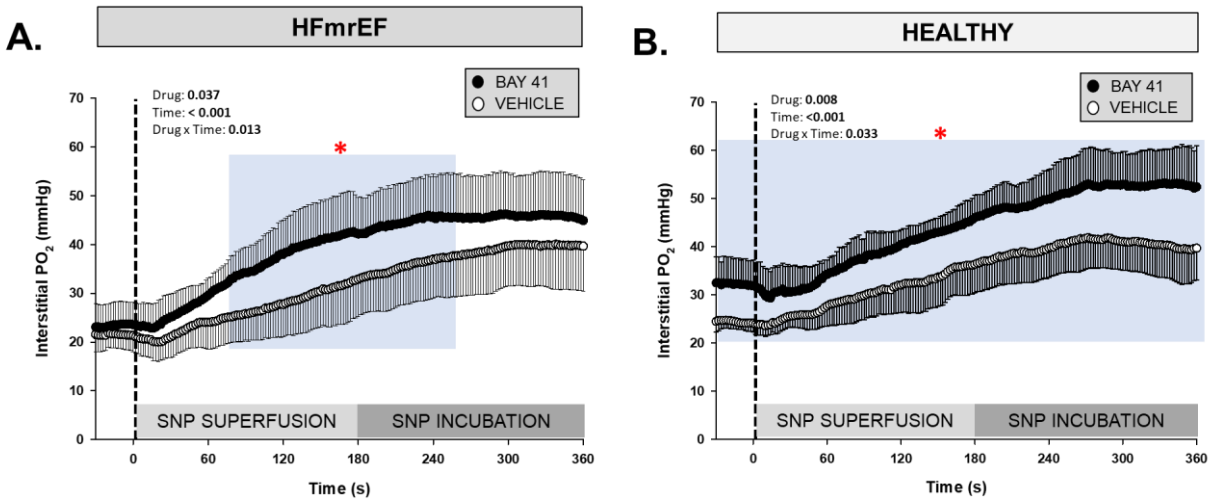

Data are mean ± SD. Healthy (*n*=8); Healthy + BAY41 (*n*=6); HFmrEF(*n*=7); HFmrEF + BAY41(*n*=10). At 0 s (dashed line) SNP was continuously superfused onto the muscle. The incubation period reflects a time for the $PO_2$is response to reach a steady state. **A.** HFmrEF + BAY41rats had a significantly higher $PO_2$is during 78-262 s (blue inset) vs. HFmrEF control rats. There was a significant Drug x Time interaction for the HFmrEF groups (P = 0.013). **B.** Healthy + BAY41 rats had a significantly greater $PO_2$is throughout the entire response. $PO_2$is was compared across time via two-way repeated measures ANOVA with Tukey's post hoc analyses. *P < 0.05 vs. vehicle within group.

Figure 2.5. *Interstitial pressure of O_2 during SNP contractions.*

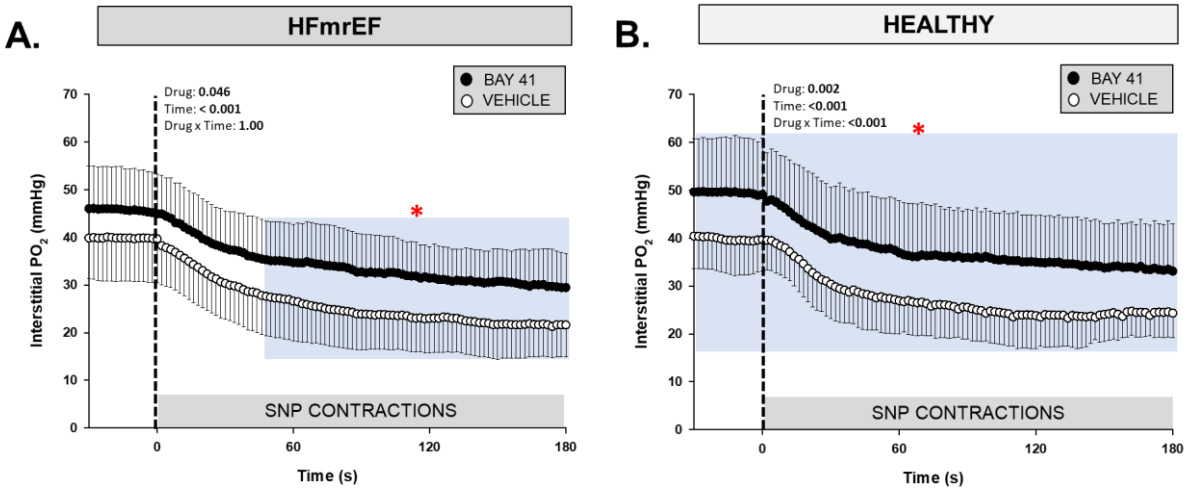

Data are mean ± SD. The dashed line represents the onset of twitch contractions. Healthy (*n*=8); Healthy + BAY41 (*n*=6); HFmrEF (*n*=7); HFmrEF + BAY41 (*n*=10). **A.** HFmrEF + BAY41 rats had a significantly higher $PO_2$is during 46-180 s (gray inset) vs. HFmrEF control rats. **B.** Healthy + BAY41 rats had a significantly greater $PO_2$is throughout the entire response. $PO_2$is was compared across time via two-way repeated measures ANOVA with Tukey's post hoc analyses. *P < 0.05 vs. vehicle within group.

Figure 2.6. *Normalized interstitial pressure of O_2 during control and SNP contractions.*

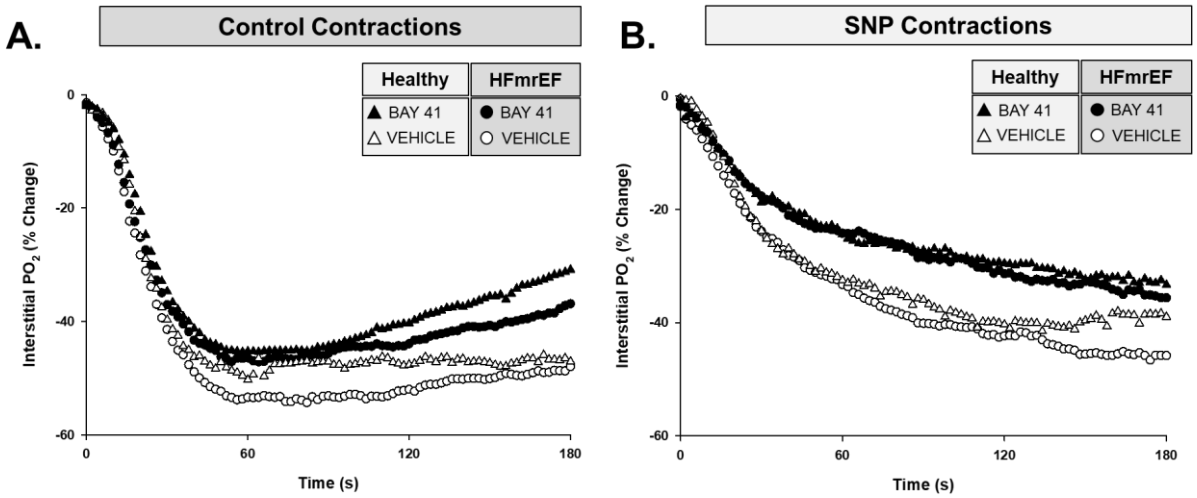

Data are averaged across animals Control: Healthy (*n*=8); Healthy + BAY41 (*n*=8); HFmrEF (*n*=7); HFmrEF + BAY41 (n=10); SNP: Healthy (*n*=8); Healthy + BAY41 (*n*=6); HFmrEF (*n*=7); HFmrEF + BAY41 (*n*=10). **A**. There was no significant difference in percent change within groups during control contractions. **B.** SNP slows the kinetic response to contractions in all groups versus control conditions, however to the greatest extent in the BAY41-treated rats. There was a statistically less $PO_2$is % change in HFmrEF + BAY41 rats during 60-180 s (blue inset) and in Healthy + BAY41 rats from 86-146 s. $PO_2$is was compared across time via two-way repeated measures ANOVA with Tukey's post hoc analyses. *P < 0.05 vs. vehicle within group.

Figure 2.7. *Spinotrapezius sGCβ1 and SOD1 expression.*

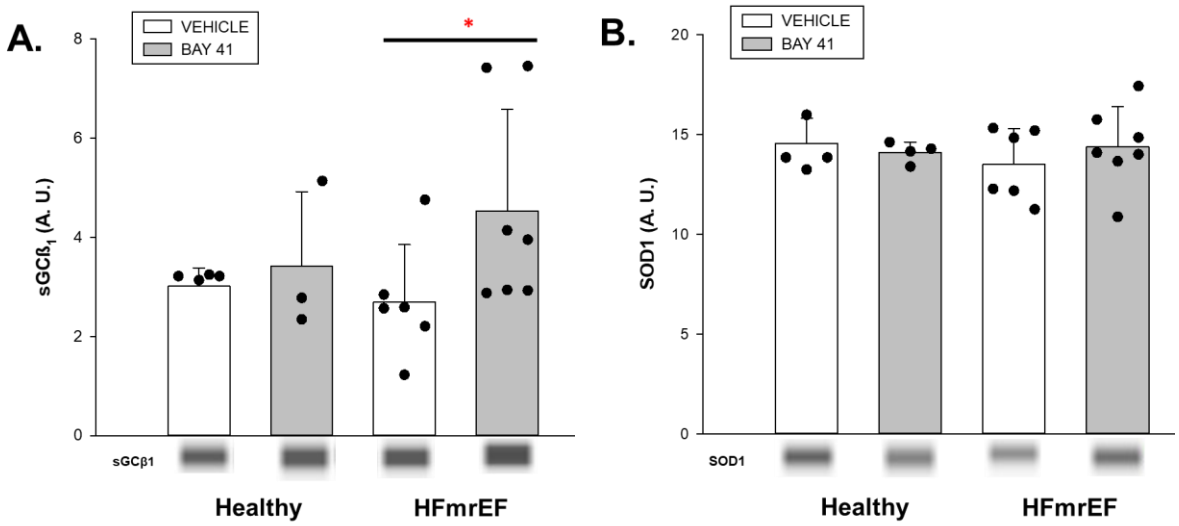

Data are mean ± SD. 21 samples of spinotrapezius muscle (Healthy, *n*=4; Healthy + BAY41, *n*=4; HFmrEF, *n*=6; HFmrEF + BAY41, *n*=7) were used to measure soluble guanylyl cyclase beta one ***(***sGCβ1) and superoxide dismutase 1 (SOD1) expression via western immunoblotting. Representative western blot images are presented below each graph. **A.** There was a significantly greater expression of sGCβ1 in the spinotrapezius muscle of HFmrEF + BAY41 rats. ($P < 0.05$) **B.** No statistical difference was detected between groups and within conditions in spinotrapezius SOD1 expression. Data analyzed via two-way ANOVA mixed effects. *$P < 0.05$ vs. vehicle within group.

Chapter 3 - Tumor bearing in untreated breast cancer decreases exercise tolerance without lowering maximal oxygen uptake in rats

Abstract

Breast cancer patients' maximal O_2 uptake ($\dot{V}O_2max$) values average 60-80% of age-predicted values which is often attributed to adjuvant therapy rather than risk factors, comorbidities, or the tumor and associated factors (e.g., pro-inflammatory cytokines). It is crucial to understand the physiological mechanisms behind exercise intolerance in breast cancer patients to enhance targeted interventions; however, the effect of breast cancer, as an isolated condition on $\dot{V}O_2max$, exercise tolerance, and resting cardiac function has not been investigated. We hypothesized that breast cancer, in the absence of underlying conditions or chemotherapy, would lower $\dot{V}O_2max$, exercise tolerance, and cardiac function in proportion to tumor mass. Female Fischer-344 rats (~6-8 months, *n*=8) were acclimatized to treadmill running for 5 days at 25 m/min for 5 min/day. To measure $\dot{V}O_2max$, rats were placed within a plexiglass metabolic chamber connected to CO_2 and O_2 analyzers. Tests began at 25 m/min and increased (5 m/min) until exhaustion. Echocardiography determined cardiac function before rats received a mammary intraductal injection of rat adenocarcinoma cells (MATBIII, 6 x 10^3 in 50 µl saline). Tumor growth was monitored daily and ~7 days following palpation (~24 days post-injection), $\dot{V}O_2max$ and echocardiography measurements were repeated. Tumor mass and volume were 2.1 ± 0.6 g and 1685 ± 428 (range 256-3749) mm^3, respectively. Body mass (217 ± 6 vs 218 ± 6 g), $\dot{V}O_2max$ (72.1 ± 2.7 vs 70.0±2.8 ml/kg·min; P > 0.05), and all measures of cardiac function were unchanged following tumor formation, with no significant correlation between tumor mass and $\dot{V}O_2max$ (P>0.05). However, time to exhaustion (376 ± 20 vs 297 ± 25 s), final treadmill speed (48 ± 1 vs 42 ± 2 m/s), distance run (209 ± 16 vs 152 ± 18 m), and total work (45 ± 3 vs 32 ±4

m·kg) were significantly reduced with tumor bearing. Contrary to our hypothesis, breast cancer did not affect $\dot{V}O_2max$ or cardiac function, but reduced exercise tolerance.

Introduction

Maximal oxygen uptake ($\dot{V}O_2max$), measured during maximal cycle ergometry or treadmill exercise assesses the coordinated capacity of the pulmonary, cardiovascular, and muscle systems to transport and utilize O_2. A high $\dot{V}O_2max$ and physical activity level are associated with greater exercise tolerance and lowered risk of breast cancer (Barlow et al., 2012; Bianchini et al., 2002; Figueira et al., 2018; Lamkin & Garland, 2020; Moore et al., 2016) which is the most diagnosed malignancy in U.S. women with 272,454 new cases in 2021 (CDC, 2024).

A cardinal phenotype of breast cancer patients is a low $\dot{V}O_2max$ (Jones et al., 2012; Lakoski et al., 2012; Scott et al., 2018) with values typically ranging from 60-80% of age-predicted values (Jones et al., 2012; Klassen et al., 2014; Scott et al., 2024). It is assumed that this low $\dot{V}O_2max$ results primarily from adjuvant anticancer therapies (Hurria et al., 2016; Jones et al., 2012; Klassen et al., 2014; Scott et al., 2018). Monoclonal antibodies and anthracyclines, such as trastuzumab and doxorubicin, are cardiotoxic and increase the risk and prevalence of cardiomyopathy, arrhythmia, heart failure, and skeletal muscle dysfunction (Singal & Iliskovic, 1998; Smuder, 2019; Varghese et al., 2021; Wadhwa et al., 2009). Chemotherapy-induced cardiomyocyte injury decreases left ventricular (LV) ejection fraction in breast cancer patients (Shan et al., 1996; Von Hoff et al., 1977) and contributes to a ~10% or more reduction in $\dot{V}O_2max$ (Courneya et al., 2007; Jones et al., 2012; Okwuosa et al., 2019; Wiestad et al., 2020). However, this is belied by the absence of requisite $\dot{V}O_2max$ validation tests (Poole & Jones, 2017) and reliance on relative rather than absolute $\dot{V}O_2$ values; especially where therapy results in altered body mass. An exemplar of this is seen in Peel et al. (Peel et al., 2014) where, despite no change in absolute $\dot{V}O_2max$ (1.6 L/min pre- and post-chemotherapy), the ~10% increase in body mass across treatment lowered the relative $\dot{V}O_2max$ proportionally and in the absence of

cardiovascular dysfunction. This observation raises the question: how much of the low $\dot{V}O_2$max post-therapy in individuals with breast cancer is 1) present pre-therapy, 2) pre-existed the cancer or 3) resulted from the pro-inflammatory impact of tumor-bearing?

Pre-treatment cancer patients have an extraordinarily low $\dot{V}O_2$max compared with the predicted $\dot{V}O_2$max for 50-59-year-old women (i.e., 30.4 ml/kg/min) (Edvardsen et al., 2013). Specifically, breast cancer patients pre-treatment may have a $\dot{V}O_2$max below 20 ml/kg·min with 32% falling below the 15.4 ml/kg·min (Jones et al., 2012) that is considered necessary for functional independence (Paterson et al., 1999). We propose that the reductions in $\dot{V}O_2$max before anticancer therapy are either characteristic of individuals at greater risk for cancer or due to the impact of the tumor itself, which is profoundly inflammatory (Brown et al., 2020; Furman et al., 2019). In the rat, 8 weeks of untreated prostate tumor-bearing significantly reduced LV and skeletal muscle(s) mass and running endurance compared to sham-operated animals (Esau et al., 2017). LV mass was negatively correlated to tumor mass in these prostate cancer rats (Esau et al., 2017), which suggests that tumor-bearing itself can decrease cardiovascular and skeletal muscle function even in the absence of decreased muscle oxidative enzymes. Similarly, in the transgenic polyoma middle T oncoprotein model of breast cancer in mice, breast cancer induces reductions in endurance capacity and concomitant increases in muscular weakness in the absence of changes in skeletal muscle mass or citrate synthase activity (Mader et al., 2022). Unfortunately, $\dot{V}O_2$max was not measured in those investigations.

$\dot{V}O_2$max measurements are a useful tool in exercise oncology to assess the feasibility or preliminary effectiveness of a pharmacological or exercise intervention. Higher $\dot{V}O_2$max and activity levels are associated with less solid tumor hypoxia and reduced growth rates (Lamkin & Garland, 2020; Thompson et al., 2017) as well as a lower incidence of treatment-related

toxicities, exercise intolerance, and cardiovascular risk (Haykowsky et al., 2022; Jones et al., 2012b; Scott et al., 2018). One imperative here is that a higher $\dot{V}O_2$max not only supports the effective implementation of exercise therapy but is also pivotal in further enhancements in $\dot{V}O_2$max which has been demonstrated to decrease immune suppression and tumor progression (Wennerberg et al., 2020), lessen fatigue (Wagner & Cella, 2004) and improve clinical outcomes for individuals with breast cancer. For example, a 3.5 ml/kg/min increase in $\dot{V}O_2$peak is associated with an 18% lower cardiovascular mortality risk in cancer patients (Barlow et al., 2012).

There is a pressing urgency to characterize the physiological mechanisms underpinning exercise intolerance in breast cancer patients to improve risk stratification and guide targeted interventions (Lyon et al., 2022; Scott et al., 2019). As such, preclinical animal cancer models are essential to investigate tumor pathophysiology and resolve the mechanisms by which exercise is protective and anti-tumorigenic (Lamkin & Garland, 2020). These models have significant advantages given that genetic, nutritional, and exercise backgrounds are invariant, and the type and duration of cancer are controlled with the presence/absence of treatment protocols dictated by the investigators.

Herein the 13572 MAT B-III orthotopic model of mammary intraductal breast cancer in the rat was utilized to test the hypothesis that breast cancer itself, in the absence of underlying conditions and chemotherapy, would lower $\dot{V}O_2$max and exercise tolerance in proportion to tumor mass.

Methods

Animals

Female retired breeder Fischer-344 rats (~6-8 months, *n*=10) were obtained from Charles River Laboratories (Boston, MA). Two rats were excluded from this study due to tumor ulceration. Upon arrival at Kansas State University, rats were housed in facilities approved by the Association for the Assessment and Accreditation of Laboratory Animal Care. Rats were maintained on a 12:12 hour light-dark cycle in a thermoneutral environment and food and water were provided ad libitum. All procedures were approved by the Institutional Animal Care and Use Committee at Kansas State University (Protocol #4684) and complied with the National Institutes of Health Guide for the Care and Use of Laboratory Animals. A subsample of healthy rats (*n*=5) were used for morphometric comparisons.

Orthotopic Breast Cancer Model

The 13762 MAT B III adenocarcinoma cell line (CRL-1666; ATCC, Manassas, VA) originated from rat mammary glands. The cells were cultured in McCoy's 5A (modified) medium, supplemented with 10% fetal bovine serum, and stored in a 5% CO_2 incubator until reaching confluency. Cell counts and viability were tested with Trypan blue staining prior to breast cancer cell injection procedures. While anesthetized under 2.5% isoflurane-O_2 and positioned on a heating pad to maintain core temperature at ~37°C (measured via rectal thermometer), using a 20-G needle, 6 x 10^3 cells in 50µL of saline were injected into a left abdominal mammary duct (Ferreira et al., 2023). Rats were monitored closely for ~2 hours for signs of distress.

Experimental Protocol

The experimental protocol is shown in Figure 3.1. All rats were acclimated to treadmill running on a custom-built motor treadmill for 5 min/day at 25 m/min up a 5% incline. Importantly, this acclimation protocol does not elicit training adaptations in skeletal muscle (Copp et al., 2009). Within 5 days of completing acclimation, $\dot{V}O_2max$ was measured using previously established methods from our laboratory (Poole et al., 2020). Following 24 hours of recovery, pre-breast cancer echocardiography determined baseline cardiac characteristics, and intraductal breast cancer cell injections were performed while under 2.5% isoflurane anesthesia (*see "Orthotopic Breast Cancer Model"*). Animals were monitored daily for signs of tumor growth. Upon tumor palpation, daily measurements of tumor volume were made using calipers. Tumor volume was measured in two orthogonal dimensions with the greatest dimension of the tumor being recorded as length, and the other as width. Tumor volume was calculated as $(l \times w^2)/2$, which is the standard formula for tumor mass estimation in breast cancer rats (Faustino-Rocha et al., 2013). We monitored the time course of tumor growth and based on this experience, the final (post) measurement protocols and experiments were conducted ~1 week following tumor palpation to avoid ulceration. Following tumor growth (~24 days post-injection) rats performed a post-$\dot{V}O_2max$ test and 24 hours afterwards post-echocardiographic measurements were made. Animals were anesthetized (~2.5% isoflurane anesthesia) and echocardiograms measured LV function and then the right carotid artery was isolated, cannulated, and a 2-French catheter-tip pressure transducer (Millar Instruments, Houston, TX, USA) was advanced into the LV for measurements of systolic and diastolic pressures and changes in LV pressure over time (LV $\Delta P/\Delta T$). Following the experimental protocol and while under isoflurane anesthesia (~2.5%), rats were euthanized with an overdose of pentobarbital sodium (>100mg/kg) and the tumor, heart and skeletal muscle samples were removed for morphometric evaluation.

Determination of $\dot{V}O_2$max and Exercise Tolerance

Following acclimation, $\dot{V}O_2$max was determined utilizing previously established methods that have been used extensively in our laboratory (Copp et al., 2009). Before each test, CO_2 and O_2 analyzers (models CD-3A and S-3A/I, respectively, AEI Technologies, Pittsburgh, PA) were calibrated with precision-mixed gases that span the expected range of gas concentrations. Each rat was weighed and placed within a plexiglass metabolic chamber designed to fit within one treadmill lane. Initiation of the maximal exercise test consisted of 1-minute intervals beginning at 25 m/min and progressively increasing by 5 m/min every minute until the rat was unable to keep pace with the treadmill belt. Time to exhaustion was recorded to the nearest second and the test was terminated to avoid injury. Exhaustion was confirmed by a slowing of the righting reflex. Each rat was reweighed following $\dot{V}O_2$max measurements, and the results reflect the post-exercise test weight (Table 3.1). This protocol has been demonstrated to yield reproducible measurements of $\dot{V}O_2$max and time to exhaustion in rats in our laboratory (Copp et al., 2009, 2010; Poole et al., 2020) and elsewhere (Bedford et al., 1979). To determine the O_2 cost of exercise, we calculated the $\Delta\dot{V}O_2$ for both pre- and post-measurements (Maximal O_2 value – baseline O_2 value, ml/kg·min) and divided this value by the final speed run (s). We then subtracted the post-breast cancer ΔO_2/final speed from the pre-breast cancer ΔO_2/final speed to assess the degree of change between pre- and post- breast cancer measurements.

Transthoracic Echocardiography

Before breast cancer cell injections, rats were initially anesthetized with a 5% isoflurane-O_2 mixture and subsequently maintained on 2.5% isoflurane-O_2 while positioned on a heating pad to maintain core temperature at ~37°C (measured via rectal thermometer). Transthoracic echocardiography was performed using a commercially available system (Logiq S8; GE Health

Care, Milwaukee, WI) with an 18 MHz linear transducer (L8-18i) as previously described (Craig et al., 2019). Standard 2-dimensional and M-mode images from the midpapillary level were obtained with frame rates of >50 frames/s. M-mode measurements over 4 consecutive cardiac cycles determined ventricular dimensions and wall thicknesses. The measurements presented are the average of the 4 cardiac cycles. LV internal dimensions (ID, cm) and posterior wall (PW, cm) thicknesses were measured at end systole (LVIDs; LVPWs) and end diastole (LVIDd; LVPWd). Fractional shortening (FS, %) was calculated from the measurements of LV chamber diameters: FS = [(LVIDd-LVIDs)/LVIDd] × 100. LV end-systolic (LVESv, ml) and end-diastolic (LVEDv, ml) volumes were calculated using the Teicholz formula: LV volume = (7.0/2.4 + LV dimension) × LV dimension^3. Stroke volume (SV, ml) was calculated as: SV = LVEDv-LVESv. Ejection fraction (EF, %) was calculated as EF = [LVEDv-LVESv/LVEDv] × 100. Post-breast cancer echocardiography was performed 24 hours following $\dot{V}O_2$max measurements and before euthanasia.

Statistical Analyses

Student's paired t-tests were performed to determine differences in pre- and post-breast cancer $\dot{V}O_2$max, speed, distance, time to max, work, echocardiography, and LV pressures. Pearson's product-moment correlation was used to determine relationships among variables. Data are presented as means ± SE. Significance was accepted at $P < 0.05$.

Results

Morphometry and tumor burden

Body mass did not change during the protocol and non-tumor mass (total minus tumor weight) was not significantly different compared to the pre-tumor body mass (Table 3.1). Moreover, soleus muscle mass was not correlated with tumor burden ($r = 0.385$, $P = 0.272$). The final tumor burden was 2.1 ± 0.6 g (Table 3.1) and tumor volume was 1685 ± 428 (range 256-3749) mm^3. The healthy animals used to compare invasive hemodynamic measurements weighed 224 ± 4 g.

Left ventricular cardiac function

All animals displayed normal resting LV function before and following tumor establishment (Table 3.1, Figure 3.2). There were no differences in heart rate or cardiac output. Millar catheter measurements suggest no change in LV $\Delta P/\Delta T$; however, breast cancer rats had a significantly higher LVEDP in comparison to a subsample of healthy control rats ($P < 0.05$, Table 3.2). Cardiac output was not different pre- vs. post-breast cancer. No significant correlations between LV measurements and tumor mass were present ($r = 0.094$, $P = 0.825$, Figure 3.3).

Maximal oxygen uptake during exercise

$\dot{V}O_2$max was not different pre- vs. post-tumor growth (Figure 3.4, Table 3.1, $P = 0.534$). The respiratory exchange ratio at the end of exercise was not different between pre- and post-$\dot{V}O_2$max tests, respectively (1.12 ± 0.03 vs 1.07 ± 0.03; $P = 0.261$). ΔO_2 uptake (maximal - baseline) was not different between pre- and post-tumor growth $\dot{V}O_2$max tests, (pre: 46.1 ± 2.3

vs post: 43.3 ± 4.6 ml/kg·min; P = 0.537). In addition, tumor burden was not significantly associated with post-$\dot{V}O_2$max (r = 0.6726; P = 0.073).

Exercise tolerance

Exercise tolerance, as measured during the $\dot{V}O_2$max test, demonstrated that endurance time was significantly reduced (~21%) following tumor growth (P < 0.05, Table 3.1). Thus, with the incremental protocol these rats reached $\dot{V}O_2$max at a slower speed (P < 0.05, Table 3.1, Figure 3.5). The total distance run was ~27% lower following tumor growth and there was a ~29% reduced work capacity (P < 0.05, Table 3.1). There was a strong positive correlation between tumor size and O_2 cost of exercise (r = 0.923, P = 0.003, Figure 3.6), which suggests that, as tumor size increases, economy decreases.

Discussion

To our knowledge, this is the first investigation specifically examining how breast cancer impacts $\dot{V}O_2max$ in the absence of anticancer treatment in an animal model where activity, diet and genetic makeup are homogeneous. Our results demonstrate that despite exercise performance being reduced, $\dot{V}O_2max$ during treadmill running remained unaffected after breast cancer tumor establishment. Importantly, no signs of cardiac dysfunction, except for the elevated LVEDP, were observed concomitant with tumor bearing. Thus, without cardiovascular dysfunction, the reduced exercise tolerance may have resulted from intrinsic skeletal muscle contractile dysfunction. These results support that, while $\dot{V}O_2max$ is extremely low in individuals with breast cancer, the tumor itself and the associated pro-inflammatory state do not ipso facto lower $\dot{V}O_2max$. Accordingly, a low $\dot{V}O_2max$ observed in individuals with breast cancer may primarily result from comorbid conditions and the adverse effects of cancer treatments on cardiac function and cardiopulmonary O_2 transport.

$\dot{V}O_2max$ reflects the integrated function of cardiopulmonary, vascular, and skeletal muscle O_2 transport and is an independent predictor of cardiovascular mortality and morbidity in the general population (Astrand et al., 1973; Blair et al., 1989; Ross et al., 2016) as well as in individuals with cancer (Schmid & Leitzmann, 2015). Higher $\dot{V}O_2max$ and activity levels are associated with reduced tumor hypoxia and tumor growth rates (Lamkin & Garland, 2020; Thompson et al., 2017) as well as a lower incidence of treatment-related toxicities, exercise intolerance and cardiovascular risk (Jones, Haykowsky, Pituskin, et al., 2007; Schmid & Leitzmann, 2015; Scott et al., 2018). However, $\dot{V}O_2max$ is not always a reliable predictor of exercise tolerance. For instance, while exercise training may increase $\dot{V}O_2max$, this does not always translate to significant improvements in exercise tolerance (Jacobs et al., 2011).

Functional measures of physical performance, such as critical speed, may provide greater evidence for: 1) how cancer treatment compromises lifestyle activities, and 2) the efficacy of therapeutic/exercise interventions (Whipp & Ward, 2009). In this context, for running, exercise tolerance refers to the total duration of exercise that can be sustained at a given speed or as speed increases, which provides valuable insights into intramuscular contractile function and metabolism. Indeed, the National Accreditation Program for Breast Cancer Standards (American College of Surgeons; 2023.) requires functional assessment through the Patient-Reported Outcomes Measurement Information System (for) Physical Fitness (PROMIS PF) survey which, "*measures the outcome of patients or clients with musculoskeletal disorders by assessing physical function through a grading scale of activities of daily living* (*Patient-Reported Outcomes Measurement Information System (PROMIS) Physical Function (PF), PROMIS PF*, 2024)". Flores et al. recently observed that physical fitness is impaired similarly across tumor types independent of treatment (Flores et al., 2024).

Tumor Model

In preclinical research there are several different methods to induce breast cancer including: transgenic, syngeneic allograft, human cell lines and patient-derived xenograft (PDX) or patient derived orthotopic xenograft (PDOX), chemical carcinogens (1-methyl-1-nitrosourea (MNU) and 7,12-dimethylbenzathracene (DMBA)), as well as orthotopic implantation. Each model presents varied factors that must be considered (presence of estrogen, rodent strain and age, immune function, location of implantation/tumor growth) and other features which may complicate data interpretation (Ashcraft et al., 2016; Giles & Wellberg, 2020). In this investigation, we cultured rat mammary adenocarcinoma cells and performed injections directly in the mammary duct to recapitulate the host tissue environment. Studies suggest that such

orthotopic models are greater predictors of translational success than ectopic models (Ashcraft et al., 2016; Behbod et al., 2009; Valdez et al., 2011). Blood flow distribution in tumors is dependent mostly on where the tumor is grown (Garcia et al., 2016), and overlooking this factor could significantly compromise the validity of preclinical exercise oncology research. The rats used in this study were ~6-8 months old and the time from injection to final testing was ~24 days. In humans, a tumor may grow within the breast tissue for 1-5 years without noticeable palpation and regarding human age, the rat model herein reflects young adult women (~30 years old) bearing a tumor for ~2-3 years (Sengupta, 2013).

Maximal O_2 Uptake in Breast Cancer

Using a standardized protocol that displays high reproducibility (Copp et al., 2009), we found that $\dot{V}O_2$max was unchanged from pre- to post-breast cancer tumor development. Whilst contrary to our hypothesis, this finding strengthens the proposition that pre-existing low cardiorespiratory fitness combined with comorbidities/chemotoxicities, especially in those with higher cardiovascular risk (Bianchini et al., 2002; Jones, Haykowsky, Swartz, et al., 2007; Okwuosa et al., 2019; Scott et al., 2024), may be responsible for the low $\dot{V}O_2$max in breast cancer patients rather than the cancer itself. These results highlight the urgency to define reliable, valid, and translatable exercise measurements in breast cancer models. Unlike other forms of cancer (i.e., lung, gastric, esophageal (Baracos et al., 2018)), individuals with breast cancer exhibit a low prevalence of cachexia (Fox et al., 2009) and are more likely to gain weight during chemotherapy (Vance et al., 2011). This is important, because while breast cancer patients exhibit a reduction in $\dot{V}O_2$max after adjuvant therapy (Peel et al., 2014), in some studies this reduction only appears when $\dot{V}O_2$max is calculated in relative terms (e.g., per kilogram of body weight) but not when measured in absolute terms (e.g., total oxygen uptake without considering

body weight). Like our findings, Kirkham et al. (Kirkham et al., 2022) found no differences in $\dot{V}O_2$peak between pre-chemotherapy breast cancer patients and body mass index (BMI)-matched non-cancer controls. As discussed above, $\dot{V}O_2$max does decrease with breast cancer treatment (Courneya et al., 2007) and remains lower than healthy sedentary controls (Jones et al., 2012a). Accordingly, targeted exercise and/or pharmaceutical approaches to improve $\dot{V}O_2$max can potentially offset the detrimental cardiovascular dysfunction incurred by chemotherapy as well as improving the efficacy of that treatment (Barlow et al., 2012; Jones, Haykowsky, Pituskin, et al., 2007; Scott et al., 2018) (*see below*).

Exercise training benefits cancer patients by increasing $\dot{V}O_2$max and is related to reduced solid tumor hypoxia and growth rates and a lower incidence of treatment-related toxicities, cardiovascular risk, and all-cause mortality (Barlow et al., 2012; Jones, Haykowsky, Pituskin, et al., 2007; Scott et al., 2018). This capacity for exercise training to reduce tumor hypoxia is important because hypoxia itself is associated with greater histological grade, increased risk of metastasis, reduced responses to anticancer therapy, and worse outcomes (Zhao et al., 2020). During exercise, in a rat model of prostate cancer, tumor blood flow increased by ~200% compared to basal conditions, inducing a ~50% reduction in tumor hypoxia (McCullough et al., 2014) and following exercise training, prostate cancer tumors had greater microvascular O_2 pressures than those in sedentary rats (McCullough et al., 2013). Collectively, this suggests a relationship between increases in $\dot{V}O_2$max and tumor blood flow.

Exercise Intolerance in Breast Cancer

~97% of breast cancer patients experience muscular weakness and fatigue before chemotherapy and independent of muscle wasting (Baracos et al., 2018), yet the mechanisms precipitating muscle dysfunction in cancer remain elusive (Reid & Moylan, 2011). Tumor-

derived inflammatory secretions are associated with diminished time to exhaustion (Mader et al., 2022) and reduced mitochondrial biogenesis (Wilson et al., 2019) in rodent breast cancer models. Likewise, we found that tumor-bearing breast cancer rats had a reduced time and speed at which they reached $\dot{V}O_2max$ (Table 1), which suggests intrinsic skeletal muscle dysfunction as a potential generative mechanism. Breast cancer mice have a reduced endurance capacity that is associated with 1) impaired muscular force development and 2) increased intramuscular and tumor-derived tumor necrosis factor alpha (TNF-α) (Mader et al., 2022). TNF-α has been demonstrated to compromise contractile function before cachexia (Reid & Moylan, 2011) and impairs peroxisome proliferator-activated receptor-gamma coactivator 1-alpha (PGC-1α)-mediated mitochondrial biogenesis (de Alvaro et al., 2004). Reduced PGC-1α is apparent in both human and rodent breast cancer skeletal muscle biopsies across all cancer subtypes and independent of treatment status (Wilson et al., 2020). These data warrant future studies addressing exercise and pharmaceutical approaches to reduce cancer-induced chronic inflammation and improving skeletal muscle function in breast cancer patients.

Cardiac measurements

Echocardiography identifies cardiovascular complications from chemotoxicity in breast cancer patients, which is a rapidly growing concern (Battisti et al., 2021; Shan et al., 1996; Wadhwa et al., 2009). Beaudry et al. (Esau et al., 2017) found that—before adjuvant treatment—breast cancer directly impairs heart function via reduced maximal cardiac output and potentially breast cancer-induced increases in LV stiffness are a potential culprit for the reduced aerobic capacity. Similarly, we found significantly increased LVEDP in breast cancer rats in comparison to healthy controls which is indicative of reduced ventricular compliance and LV stiffening (Zile et al., 2004) and is associated with exercise intolerance and skeletal muscle contractile

dysfunction (Bowen et al., 2017; Haykowsky et al., 2022). In the study herein, we measured cardiac morphology and function before and following tumor growth and saw no significant decline in key measures of cardiac function (EF, FS, SV, cardiac output; Figure 2, Table 2). This finding is important, because circulating tumor-secreted cytokines such as TNF-α (Esquivel-Velázquez et al., 2015), could potentially increase myocardial injury (Feldman et al., 2000) or induce cardiac cachexia (Levine et al., 1990). Also, there is evidence for cardiac cachexia in prostate cancer rats (Esau et al., 2017). We found no correlation between tumor burden and LV mass (Figure 3), which highlights that there may be distinct, pro-cachectic pathways in prostate cancer (Esau et al., 2017) and not in breast cancer. Variations in tumor phenotype, duration of tumor bearing, and/or the inoculation site may accelerate the development of cardiac and skeletal muscle cachexia (Matsuyama et al., 2015) which may explain differences between prostate (Esau et al., 2017) and breast cancer herein.

Clinical Insights

Our findings suggest that exercise intolerance in breast cancer patients is not solely a consequence of treatment or reduced $\dot{V}O_2$max but may originate from underlying physiological changes associated with the disease itself. Therefore, future studies must explore the specific molecular pathways that contribute to muscle dysfunction in this population, as identifying these pathways could lead to targeted exercise and/or pharmacological interventions. Promising results from Stanton et al. (Stanton et al., 2022) suggest that Pioglitazone, a treatment option for patients with diabetes mellitus, is effective in treating breast cancer-associated muscle fatigue by increasing upstream PGC-1α signaling and restoring skeletal muscle ATP content and ATPase activity.

Experimental Considerations

The preclinical model herein is considered the gold standard for modeling breast cancer tumor effects on systemic O_2 transport in rodents (Ashcraft et al., 2016). This allows for tight control over diet, physical activity, and genetic variability in the absence of comorbidities or treatment effects. Alternative models, such as the PDOX/PDX, which use human cancer cell lines, are more often studied, and most require immunocompromised recipient rodents. Immunodeficiencies are not typically present early in breast cancer diagnosis (Papatestas et al., 1976), therefore we argue that the model used herein better recapitulates changes in exercise capacity solely due to breast cancer. Nevertheless, as with any animal model, translation to humans with breast cancer should be made with caution. The animals used in this study were middle aged (~30-year-old woman equivalent) and therefore may not appropriately reflect the distinct cardiovascular and metabolic responses of breast cancer development that is seen in older women. It has been shown that older rodents develop more aggressive breast cancer than younger rodents (Sáez-Freire et al., 2018), therefore greater tumor growth and decrements in exercise tolerance may be seen in aged breast cancer rats. Lastly, we did not use a separate group of non-cancerous control animals to compare exercising measurements. However, the primary focus was to effectively demonstrate changes in $\dot{V}O_2max$ attributable to breast cancer and longitudinal measurements allowed us to analyze the extent of change within the same animals and minimize the number of animals consistent with best research practices.

Conclusion

This study provides evidence that 1) resting cardiac function and $\dot{V}O_2max$ during treadmill running remains unchanged between pre- and post-breast cancer assessments and 2) breast cancer contributes to exercise intolerance by reducing economy and elevating the O_2 cost of running. Collectively, these findings indicate that intrinsic muscle dysfunction may be present in breast cancer patients before the initiation of neoadjuvant or adjuvant therapies. Exercise can reduce mortality by ~40% in breast cancer (Lahart et al., 2015) and future research focused on understanding the mechanisms by which breast cancer affects muscle function could enhance the development of tailored exercise programs to improve physical fitness and overall health outcomes for individuals with breast cancer.

References

American College of Surgeons; 2023. National Accreditation Program for Breast Centers, American College of Surgeons. *Optimal Resources for Breast Care. 2024 Standards* (released February 2023).

Ashcraft, K. A., Peace, R. M., Betof, A. S., Dewhirst, M. W., & Jones, L. W. (2016). Efficacy and Mechanisms of Aerobic Exercise on Cancer Initiation, Progression, and Metastasis: A Critical Systematic Review of In Vivo Preclinical Data. *Cancer Research*, 76(14), 4032–4050.

Astrand, I., Astrand, P. O., Hallbäck, I., & Kilbom, A. (1973). Reduction in maximal oxygen uptake with age. *Journal of Applied Physiology*, 35(5), 649–654.

Baracos, V. E., Martin, L., Korc, M., Guttridge, D. C., & Fearon, K. C. H. (2018). Cancer-associated cachexia. *Nature Reviews. Disease Primers*, 4, 17105.

Barlow, C. E., Defina, L. F., Radford, N. B., Berry, J. D., Cooper, K. H., Haskell, W. L., Jones, L. W., & Lakoski, S. G. (2012). Cardiorespiratory fitness and long-term survival in "low-risk" adults. *Journal of the American Heart Association*, 1(4), e001354.

Battisti, N. M. L., Andres, M. S., Lee, K. A., Ramalingam, S., Nash, T., Mappouridou, S., Senthivel, N., Asavisanu, K., Obeid, M., Tripodaki, E.-S., Angelis, V., Fleming, E., Goode, E. F., John, S., Rosen, S. D., Allen, M., Stanway, S., Lyon, A. R., & Ring, A. (2021). Incidence of cardiotoxicity and validation of the Heart Failure Association-International Cardio-Oncology Society risk stratification tool in patients treated with trastuzumab for HER2-positive early breast cancer. *Breast Cancer Research and Treatment*, 188(1), 149–163.

Bedford, T. G., Tipton, C. M., Wilson, N. C., Oppliger, R. A., & Gisolfi, C. V. (1979). Maximum oxygen consumption of rats and its changes with various experimental procedures. *Journal of Applied Physiology: Respiratory, Environmental and Exercise Physiology*, 47(6), 1278–1283.

Behbod, F., Kittrell, F. S., LaMarca, H., Edwards, D., Kerbawy, S., Heestand, J. C., Young, E., Mukhopadhyay, P., Yeh, H.-W., Allred, D. C., Hu, M., Polyak, K., Rosen, J. M., & Medina, D. (2009). An intraductal human-in-mouse transplantation model mimics the subtypes of ductal carcinoma in situ. *Breast Cancer Research:* BCR, 11(5), R66.

Bianchini, F., Kaaks, R., & Vainio, H. (2002). Overweight, obesity, and cancer risk. *The Lancet. Oncology*, 3(9), 565–574.

Blair, S. N., Kohl, H. W., Paffenbarger, R. S., Clark, D. G., Cooper, K. H., & Gibbons, L. W. (1989). Physical fitness and all-cause mortality. A prospective study of healthy men and women. *Journal of the American Heart Association*, 262(17), 2395–2401.

Bowen, T. S., Brauer, D., Rolim, N. P. L., Bækkerud, F. H., Kricke, A., Ormbostad Berre, A.-M., Fischer, T., Linke, A., da Silva, G. J., Wisloff, U., & Adams, V. (2017). Exercise Training Reveals Inflexibility of the Diaphragm in an Animal Model of Patients With Obesity-Driven Heart Failure With a Preserved Ejection Fraction. *Journal of the American Heart Association*, 6(10), e006416.

Brown, J. C., Zhang, S., Ligibel, J. A., Irwin, M. L., Jones, L. W., Campbell, N., Pollak, M. N., Sorrentino, A., Cartmel, B., Harrigan, M., Tolaney, S. M., Winer, E. P., Ng, K., Abrams, T. A., Sanft, T., Douglas, P. S., Hu, F. B., Fuchs, C. S., & Meyerhardt, J. A. (2020). Effect of Exercise or Metformin on Biomarkers of Inflammation in Breast and Colorectal Cancer: A Randomized Trial. *Cancer Prevention Research* (Philadelphia, Pa.), 13(12), 1055–1062.

CDC. (2024, June 5). U.S. Cancer Statistics Breast Cancer Stat Bite. United States Cancer Statistics. https://www.cdc.gov/united-states-cancer-statistics/publications/breast-cancer-stat-bite.html

Copp, S. W., Davis, R. T., Poole, D. C., & Musch, T. I. (2009). Reproducibility of endurance capacity and VO2peak in male Sprague-Dawley rats. *Journal of Applied Physiology* (Bethesda, Md.: 1985), 106(4), 1072–1078.

Copp, S. W., Hirai, D. M., Musch, T. I., & Poole, D. C. (2010). Critical speed in the rat: Implications for hindlimb muscle blood flow distribution and fibre recruitment. *The Journal of Physiology*, 588(Pt 24), 5077–5087.

Courneya, K. S., Segal, R. J., Mackey, J. R., Gelmon, K., Reid, R. D., Friedenreich, C. M., Ladha, A. B., Proulx, C., Vallance, J. K. H., Lane, K., Yasui, Y., & McKenzie, D. C. (2007). Effects of aerobic and resistance exercise in breast cancer patients receiving adjuvant chemotherapy: A multicenter randomized controlled trial. *Journal of Clinical Oncology: Official Journal of the American Society of Clinical Oncology*, 25(28), 4396–4404.

Craig, J. C., Colburn, T. D., Caldwell, J. T., Hirai, D. M., Tabuchi, A., Baumfalk, D. R., Behnke, B. J., Ade, C. J., Musch, T. I., & Poole, D. C. (2019). Central and peripheral factors mechanistically linked to exercise intolerance in heart failure with reduced ejection fraction. *American Journal of Physiology. Heart and Circulatory Physiology*, 317(2), H434–H444.

de Alvaro, C., Teruel, T., Hernandez, R., & Lorenzo, M. (2004). Tumor necrosis factor alpha produces insulin resistance in skeletal muscle by activation of inhibitor kappaB kinase in a p38 MAPK-dependent manner. *The Journal of Biological Chemistry*, 279(17), 17070–17078.

Edvardsen, E., Hansen, B. H., Holme, I. M., Dyrstad, S. M., & Anderssen, S. A. (2013). Reference values for cardiorespiratory response and fitness on the treadmill in a 20- to 85-year-old population. *Chest*, 144(1), 241–248.

Esau, P. J., Gittemeier, E. M., Opoku-Acheampong, A. B., Korynne S. Rollins, Baumfalk, D. R., Poole, D. C., Musch, T. I., Behnke, B. J., & Copp, S. W. (2017). Prostate cancer reduces endurance exercise capacity in association with reductions in cardiac and skeletal muscle mass in the rat. *American Journal of Cancer Research*, 7(12), 2566–2576.

Esquivel-Velázquez, M., Ostoa-Saloma, P., Palacios-Arreola, M. I., Nava-Castro, K. E., Castro, J. I., & Morales-Montor, J. (2015). The role of cytokines in breast cancer development and progression. *Journal of Interferon & Cytokine Research: The Official Journal of the International Society for Interferon and Cytokine Research*, 35(1), 1–16.

Faustino-Rocha, A., Oliveira, P. A., Pinho-Oliveira, J., Teixeira-Guedes, C., Soares-Maia, R., da Costa, R. G., Colaço, B., Pires, M. J., Colaço, J., Ferreira, R., & Ginja, M. (2013). Estimation of rat mammary tumor volume using caliper and ultrasonography measurements. *Lab Animal*, 42(6), 217–224.

Feldman, A. M., Combes, A., Wagner, D., Kadakomi, T., Kubota, T., Li, Y. Y., & McTiernan, C. (2000). The role of tumor necrosis factor in the pathophysiology of heart failure. *Journal of the American College of Cardiology*, 35(3), 537–544.

Ferreira, T., Gama, A., Seixas, F., Faustino-Rocha, A. I., Lopes, C., Gaspar, V. M., Mano, J. F., Medeiros, R., & Oliveira, P. A. (2023). Mammary Glands of Women, Female Dogs and Female Rats: Similarities and Differences to Be Considered in Breast Cancer Research. *Veterinary Sciences*, 10(6), 379.

Figueira, A. C. C., Cortinhas, A., Soares, J. P., Leitão, J. C., Ferreira, R. P., & Duarte, J. A. (2018). Efficacy of Exercise on Breast Cancer Outcomes: A Systematic Review and Meta-analysis of Preclinical Data. *International Journal of Sports Medicine*, 39(5), 327–342.

Flores, A. M., Shah, M., Bedjeti, K., Franklin, P. D., Peipert, J. D., Garcia, S. F., Lancki, N., Webster, K. A., O'Connor, M., & Cella, D. (2024). Risk of significant functional impairment across cancer diagnosis and care continuum. *Cancer*.

Fox, K. M., Brooks, J. M., Gandra, S. R., Markus, R., & Chiou, C.-F. (2009). Estimation of Cachexia among Cancer Patients Based on Four Definitions. *Journal of Oncology*, 2009, 693458.

Furman, D., Campisi, J., Verdin, E., Carrera-Bastos, P., Targ, S., Franceschi, C., Ferrucci, L., Gilroy, D. W., Fasano, A., Miller, G. W., Miller, A. H., Mantovani, A., Weyand, C. M., Barzilai, N., Goronzy, J. J., Rando, T. A., Effros, R. B., Lucia, A., Kleinstreuer, N., & Slavich, G. M. (2019). Chronic inflammation in the etiology of disease across the life span. *Nature Medicine*, 25(12), 1822–1832.

Garcia, E., Becker, V. G. C., McCullough, D. J., Stabley, J. N., Gittemeier, E. M., Opoku-Acheampong, A. B., Sieman, D. W., & Behnke, B. J. (2016). Blood flow responses to

mild-intensity exercise in ectopic vs. Orthotopic prostate tumors; dependence upon host tissue hemodynamics and vascular reactivity. *Journal of Applied Physiology* (Bethesda, Md.: 1985), 121(1), 15–24.

Giles, E. D., & Wellberg, E. A. (2020). Preclinical Models to Study Obesity and Breast Cancer in Females: Considerations, Caveats, and Tools. *Journal of Mammary Gland Biology and Neoplasia*, 25(4), 237–253.

Haykowsky, M. J., Kirkham, A. A., Li, T., Pituskin, E., Thompson, R. B., Paterson, D. I., Foulkes, S. J., Halle, M., Sarma, S., Howden, E., Nelson, M. D., & La Gerche, A. (2022). Determinants of oxygen utilization in breast cancer: Similarities between heart failure with preserved ejection fraction. *Progress in Cardiovascular Diseases*, 74, 45–52.

Hurria, A., Jones, L., & Muss, H. B. (2016). Cancer Treatment as an Accelerated Aging Process: Assessment, Biomarkers, and Interventions. American Society of Clinical Oncology Educational Book. *American Society of Clinical Oncology.* Annual Meeting, 35, e516-522.

Jacobs, R. A., Rasmussen, P., Siebenmann, C., Díaz, V., Gassmann, M., Pesta, D., Gnaiger, E., Nordsborg, N. B., Robach, P., & Lundby, C. (2011). Determinants of time trial performance and maximal incremental exercise in highly trained endurance athletes. *Journal of Applied Physiology* (Bethesda, Md.: 1985), 111(5), 1422–1430.

Jones, L. W., Courneya, K. S., Mackey, J. R., Muss, H. B., Pituskin, E. N., Scott, J. M., Hornsby, W. E., Coan, A. D., Herndon, J. E., Douglas, P. S., & Haykowsky, M. (2012). Cardiopulmonary function and age-related decline across the breast cancer survivorship continuum. *Journal of Clinical Oncology: Official Journal of the American Society of Clinical Oncology*, 30(20), 2530–2537.

Jones, L. W., Haykowsky, M. J., Swartz, J. J., Douglas, P. S., & Mackey, J. R. (2007). Early breast cancer therapy and cardiovascular injury. *Journal of the American College of Cardiology*, 50(15), 1435–1441.

Jones, L. W., Haykowsky, M., Pituskin, E. N., Jendzjowsky, N. G., Tomczak, C. R., Haennel, R. G., & Mackey, J. R. (2007). Cardiovascular reserve and risk profile of postmenopausal women after chemoendocrine therapy for hormone receptor—Positive operable breast cancer. *The Oncologist*, 12(10), 1156–1164.

Kirkham, A. A., Pituskin, E., Mackey, J. R., Grenier, J. G., Ian Paterson, D., Haykowsky, M. J., & Thompson, R. B. (2022). Longitudinal Changes in Skeletal Muscle Metabolism, Oxygen Uptake, and Myosteatosis During Cardiotoxic Treatment for Early-Stage Breast Cancer. *The Oncologist*, 27(9), e748–e754.

Klassen, O., Schmidt, M. E., Scharhag-Rosenberger, F., Sorkin, M., Ulrich, C. M., Schneeweiss, A., Potthoff, K., Steindorf, K., & Wiskemann, J. (2014). Cardiorespiratory fitness in

breast cancer patients undergoing adjuvant therapy. *Acta Oncologica* (Stockholm, Sweden), 53(10), 1356–1365.

Lahart, I. M., Metsios, G. S., Nevill, A. M., & Carmichael, A. R. (2015). Physical activity, risk of death and recurrence in breast cancer survivors: A systematic review and meta-analysis of epidemiological studies. *Acta Oncologica* (Stockholm, Sweden), 54(5), 635–654.

Lakoski, S. G., Eves, N. D., Douglas, P. S., & Jones, L. W. (2012). Exercise rehabilitation in patients with cancer. *Nature Reviews. Clinical Oncology*, 9(5), 288–296.

Lamkin, D. M., & Garland, T. (2020). Translating Preclinical Research for Exercise Oncology: Take It to the VO2max. *Frontiers in Oncology*, 10, 575657.

Levine, B., Kalman, J., Mayer, L., Fillit, H. M., & Packer, M. (1990). Elevated circulating levels of tumor necrosis factor in severe chronic heart failure. *The New England Journal of Medicine*, 323(4), 236–241.

Lyon, A. R., López-Fernández, T., Couch, L. S., Asteggiano, R., Aznar, M. C., Bergler-Klein, J., Boriani, G., Cardinale, D., Cordoba, R., Cosyns, B., Cutter, D. J., de Azambuja, E., de Boer, R. A., Dent, S. F., Farmakis, D., Gevaert, S. A., Gorog, D. A., Herrmann, J., Lenihan, D., … ESC Scientific Document Group. (2022). 2022 ESC Guidelines on cardio-oncology developed in collaboration with the European Hematology Association (EHA), the European Society for Therapeutic Radiology and Oncology (ESTRO) and the International Cardio-Oncology Society (IC-OS). European Heart Journal. *Cardiovascular Imaging*, 23(10), e333–e465.

Mader, T., Chaillou, T., Alves, E. S., Jude, B., Cheng, A. J., Kenne, E., Mijwel, S., Kurzejamska, E., Vincent, C. T., Rundqvist, H., & Lanner, J. T. (2022). Exercise reduces intramuscular stress and counteracts muscle weakness in mice with breast cancer. *Journal of Cachexia, Sarcopenia and Muscle*, 13(2), 1151–1163.

Matsuyama, T., Ishikawa, T., Okayama, T., Oka, K., Adachi, S., Mizushima, K., Kimura, R., Okajima, M., Sakai, H., Sakamoto, N., Katada, K., Kamada, K., Uchiyama, K., Handa, O., Takagi, T., Kokura, S., Naito, Y., & Itoh, Y. (2015). Tumor inoculation site affects the development of cancer cachexia and muscle wasting. *International Journal of Cancer*, 137(11), 2558–2565.

McCullough, D. J., Nguyen, L. M.-D., Siemann, D. W., & Behnke, B. J. (2013). Effects of exercise training on tumor hypoxia and vascular function in the rodent preclinical orthotopic prostate cancer model. *Journal of Applied Physiology* (Bethesda, Md.: 1985), 115(12), 1846–1854.

McCullough, D. J., Stabley, J. N., Siemann, D. W., & Behnke, B. J. (2014). Modulation of blood flow, hypoxia, and vascular function in orthotopic prostate tumors during exercise. *Journal of the National Cancer Institute*, 106(4), dju036.

Moore, S. C., Lee, I.-M., Weiderpass, E., Campbell, P. T., Sampson, J. N., Kitahara, C. M., Keadle, S. K., Arem, H., Berrington de Gonzalez, A., Hartge, P., Adami, H.-O., Blair, C. K., Borch, K. B., Boyd, E., Check, D. P., Fournier, A., Freedman, N. D., Gunter, M., Johannson, M., … Patel, A. V. (2016). Association of Leisure-Time Physical Activity With Risk of 26 Types of Cancer in 1.44 Million Adults. *JAMA Internal Medicine*, 176(6), 816–825.

Okwuosa, T. M., Ray, R. M., Palomo, A., Foraker, R. E., Johnson, L., Paskett, E. D., Caan, B., & Jones, L. W. (2019). Pre-Diagnosis Exercise and Cardiovascular Events in Primary Breast Cancer: Women's Health Initiative. *JACC. CardioOncology*, 1(1), 41–50.

Papatestas, A. E., Lesnick, G. J., Genkins, G., & Aufses, A. H. (1976). The prognostic significance of peripheral lymphocyte counts in patients with breast carcinoma. *Cancer*, 37(1), 164–168.

Paterson, D. H., Cunningham, D. A., Koval, J. J., & St Croix, C. M. (1999). Aerobic fitness in a population of independently living men and women aged 55-86 years. *Medicine and Science in Sports and Exercise*, 31(12), 1813–1820.

Patient-Reported Outcomes Measurement Information System (PROMIS) Physical Function (PF), PROMIS PF. (2024, September). APTA. https://www.apta.org/patient-care/evidence-based-practice-resources/test-measures/patient-reported-outcomes-measurement-information-system-promis-physical-function-pf-promis-pf

Peel, A. B., Thomas, S. M., Dittus, K., Jones, L. W., & Lakoski, S. G. (2014). Cardiorespiratory fitness in breast cancer patients: A call for normative values. *Journal of the American Heart Association*, 3(1), e000432.

Poole, D. C., Copp, S. W., Colburn, T. D., Craig, J. C., Allen, D. L., Sturek, M., O'Leary, D. S., Zucker, I. H., & Musch, T. I. (2020). Guidelines for animal exercise and training protocols for cardiovascular studies. *American Journal of Physiology. Heart and Circulatory Physiology*, 318(5), H1100–H1138.

Poole, D. C., & Jones, A. M. (2017). Measurement of the maximum oxygen uptake $\dot{V}O_2$max: $\dot{V}O_2$peak is no longer acceptable. *Journal of Applied Physiology* (Bethesda, Md.: 1985), 122(4), 997–1002.

Reid, M. B., & Moylan, J. S. (2011). Beyond atrophy: Redox mechanisms of muscle dysfunction in chronic inflammatory disease. *The Journal of Physiology*, 589(Pt 9), 2171–2179.

Ross, R., Blair, S. N., Arena, R., Church, T. S., Després, J.-P., Franklin, B. A., Haskell, W. L., Kaminsky, L. A., Levine, B. D., Lavie, C. J., Myers, J., Niebauer, J., Sallis, R., Sawada, S. S., Sui, X., Wisløff, U., American Heart Association Physical Activity Committee of the Council on Lifestyle and Cardiometabolic Health, Council on Clinical Cardiology, Council on Epidemiology and Prevention, Stroke Council. (2016). Importance of

Assessing Cardiorespiratory Fitness in Clinical Practice: A Case for Fitness as a Clinical Vital Sign: A Scientific Statement From the American Heart Association. *Circulation*, 134(24), e653–e699.

Sáez-Freire, M. D. M., Blanco-Gómez, A., Castillo-Lluva, S., Gómez-Vecino, A., Galvis-Jiménez, J. M., Martín-Seisdedos, C., Isidoro-García, M., Hontecillas-Prieto, L., García-Cenador, M. B., García-Criado, F. J., Patino-Alonso, M. C., Galindo-Villardón, P., Mao, J.-H., Prieto, C., Castellanos-Martín, A., Kaderali, L., & Pérez-Losada, J. (2018). The biological age linked to oxidative stress modifies breast cancer aggressiveness. *Free Radical Biology & Medicine*, 120, 133–146.

Schmid, D., & Leitzmann, M. F. (2015). Cardiorespiratory fitness as predictor of cancer mortality: A systematic review and meta-analysis. *Annals of Oncology: Official Journal of the European Society for Medical Oncology*, 26(2), 272–278.

Scott, J. M., Dolan, L. B., Norton, L., Charles, J. B., & Jones, L. W. (2019). Multisystem Toxicity in Cancer: Lessons from NASA's Countermeasures Program. *Cell*, 179(5), 1003–1009.

Scott, J. M., Lee, J., Michalski, M. G., Batch, K., Simpson, A. L., Peoples, J., Lee, C. P., Harrison, J. N., Yu, A. F., Sasso, J. P., Dang, C., Moskowitz, C. S., Jones, L. W., & Eves, N. D. (2024). Mechanisms of Exercise Intolerance Across the Breast Cancer Continuum: A Pooled Analysis of Individual Patient Data. *Medicine and Science in Sports and Exercise*, 56(4), 590–599.

Scott, J. M., Zabor, E. C., Schwitzer, E., Koelwyn, G. J., Adams, S. C., Nilsen, T. S., Moskowitz, C. S., Matsoukas, K., Iyengar, N. M., Dang, C. T., & Jones, L. W. (2018). Efficacy of Exercise Therapy on Cardiorespiratory Fitness in Patients With Cancer: A Systematic Review and Meta-Analysis. *Journal of Clinical Oncology: Official Journal of the American Society of Clinical Oncology*, 36(22), 2297–2305.

Sengupta, P. (2013). The Laboratory Rat: Relating Its Age With Human's. *International Journal of Preventive Medicine*, 4(6), 624–630.

Shan, K., Lincoff, A. M., & Young, J. B. (1996). Anthracycline-induced cardiotoxicity. *Annals of Internal Medicine*, 125(1), 47–58.

Singal, P. K., & Iliskovic, N. (1998). Doxorubicin-induced cardiomyopathy. *The New England Journal of Medicine*, 339(13), 900–905.

Smuder, A. J. (2019). Exercise stimulates beneficial adaptations to diminish doxorubicin-induced cellular toxicity. *American Journal of Physiology. Regulatory, Integrative and Comparative Physiology*, 317(5), R662–R672.

Stanton, D. A., Wilson, H. E., Chapa, M. G., Link, J. N., Lupinacci, K., Geldenhuys, W. J., & Pistilli, E. E. (2022). Rescue of a peroxisome proliferator activated receptor gamma gene

network in muscle after growth of human breast tumour xenografts. *JCSM Rapid Communications*, 5(2), 239–253.

Thompson, H. J., Jones, L. W., Koch, L. G., Britton, S. L., Neil, E. S., & McGinley, J. N. (2017). Inherent aerobic capacity-dependent differences in breast carcinogenesis. *Carcinogenesis*, 38(9), 920–928.

Valdez, K. E., Fan, F., Smith, W., Allred, D. C., Medina, D., & Behbod, F. (2011). Human primary ductal carcinoma in situ (DCIS) subtype-specific pathology is preserved in a mouse intraductal (MIND) xenograft model. *The Journal of Pathology*, 225(4), 565–573.

Vance, V., Mourtzakis, M., McCargar, L., & Hanning, R. (2011). Weight gain in breast cancer survivors: Prevalence, pattern and health consequences. *Obesity Reviews: An Official Journal of the International Association for the Study of Obesity*, 12(4), 282–294.

Varghese, S. S., Johnston, W. J., Eekhoudt, C. R., Keats, M. R., Jassal, D. S., & Grandy, S. A. (2021). Exercise to Reduce Anthracycline-Mediated Cardiovascular Complications in Breast Cancer Survivors. *Current Oncology* (Toronto, Ont.), 28(5), 4139–4156.

Von Hoff, D. D., Rozencweig, M., Layard, M., Slavik, M., & Muggia, F. M. (1977). Daunomycin-induced cardiotoxicity in children and adults. A review of 110 cases. *The American Journal of Medicine*, 62(2), 200–208.

Wadhwa, D., Fallah-Rad, N., Grenier, D., Krahn, M., Fang, T., Ahmadie, R., Walker, J. R., Lister, D., Arora, R. C., Barac, I., Morris, A., & Jassal, D. S. (2009). Trastuzumab mediated cardiotoxicity in the setting of adjuvant chemotherapy for breast cancer: A retrospective study. *Breast Cancer Research and Treatment*, 117(2), 357–364.

Wagner, L. I., & Cella, D. (2004). Fatigue and cancer: Causes, prevalence and treatment approaches. *British Journal of Cancer*, 91(5), 822–828.

Wennerberg, E., Lhuillier, C., Rybstein, M. D., Dannenberg, K., Rudqvist, N.-P., Koelwyn, G. J., Jones, L. W., & Demaria, S. (2020). Exercise reduces immune suppression and breast cancer progression in a preclinical model. *Oncotarget*, 11(4), 452–461.

Whipp, B. J., & Ward, S. A. (2009). Quantifying intervention-related improvements in exercise tolerance. *The European Respiratory Journal*, 33(6), 1254–1260.

Wiestad, T. H., Raastad, T., Nordin, K., Igelström, H., Henriksson, A., Demmelmaier, I., & Berntsen, S. (2020). The Phys-Can observational study: Adjuvant chemotherapy is associated with a reduction whereas physical activity level before start of treatment is associated with maintenance of maximal oxygen uptake in patients with cancer. *BMC Sports Science, Medicine & Rehabilitation*, 12, 53.

Wilson, H. E., Rhodes, K. K., Rodriguez, D., Chahal, I., Stanton, D. A., Bohlen, J., Davis, M., Infante, A. M., Hazard-Jenkins, H., Klinke, D. J., Pugacheva, E. N., & Pistilli, E. E.

(2019). Human Breast Cancer Xenograft Model Implicates Peroxisome Proliferator-activated Receptor Signaling as Driver of Cancer-induced Muscle Fatigue. *Clinical Cancer Research: An Official Journal of the American Association for Cancer Research*, 25(7), 2336–2347.

Wilson, H. E., Stanton, D. A., Montgomery, C., Infante, A. M., Taylor, M., Hazard-Jenkins, H., Pugacheva, E. N., & Pistilli, E. E. (2020). Skeletal muscle reprogramming by breast cancer regardless of treatment history or tumor molecular subtype. *NPJ Breast Cancer*, 6, 18.

Zhao, Z., Mu, H., Li, Y., Liu, Y., Zou, J., & Zhu, Y. (2020). Clinicopathological and prognostic value of hypoxia-inducible factor-1α in breast cancer: A meta-analysis including 5177 patients. Clinical & Translational Oncology: *Official Publication of the Federation of Spanish Oncology Societies and of the National Cancer Institute of Mexico*, 22(10), 1892–1906.

Zile, M. R., Baicu, C. F., & Gaasch, W. H. (2004). Diastolic heart failure—Abnormalities in active relaxation and passive stiffness of the left ventricle. *The New England Journal of Medicine*, 350(19), 1953–1959.

Table 3.1. *Animal morphometry and maximal oxygen uptake measurements.*

	Pre-Breast Cancer (*n*=8)	Post-Breast Cancer (*n*=8)
Body weight (g)	217 ± 6	218 ± 6
Tumor weight (g)		2.1 ± 0.6
Non-tumor body weight (g)		215 ± 5
$\dot{V}O_2$ max (ml/kg·min)	72.0 ± 2.7	70.0 ± 2.8
Time to max (s)	376 ± 20	297 ± 25 *
Final speed (m/s)	48 ± 1	42 ± 2 *
Total distance (m)	209 ± 16	152 ± 18 *
Work (m·kg)	45 ± 3	32 ± 4 *

Data are means ± SE. *n*, number of rats; ***** $P < 0.05$ vs pre-breast cancer. Analyzed via student's paired t-test.

Table 3.2. *Echocardiography of left ventricular function.*

	Pre-Breast Cancer (n=8)	Post-Breast Cancer (n=8)
LVIDd, cm	0.67 ± 0.01	0.63 ± 0.03
LVIDs, cm	0.36 ± 0.01	0.33 ± 0.02
LVPWd, cm	0.18 ± 0.10	0.18 ± 0.02
LVPWs, cm	0.28 ± 0.01	0.31 ± 0.09
FS, %	46 ± 1	54 ± 4
LVEDV, ml	0.67 ± 0.05	0.60 ± 0.07
LVESV, ml	0.12 ± 0.01	0.10 ± 0.03
SV, ml	0.55 ± 0.04	0.52 ± 0.05
EF, %	82 ± 1	87 ± 3
Heart rate (bpm)	304 ± 6	314 ± 12
Cardiac output (mL/min)	167 ± 12	163 ± 17
LV Δ*P*/Δ*T* (mmHg/s)	8024 ± 191 ¥	8585 ± 717
LVEDP (mmHg)	2 ± 0 ¥	5 ± 1 *

Data are means ± SE. n, number of rats; LV, left ventricular, LVIDd, LV internal diameter in diastole; LVIDs, LV internal diameter in systole; LVPWd, LV posterior wall in diastole; LVPWs, LV posterior wall in systole; FS, fractional shortening; LVEDV, LV end diastolic volume; LVESV, LV end systolic volume; SV, stroke volume; EF, ejection fraction; bpm, beats per minute; LV ΔP/ΔT, LV change in pressure over change in time; LVEDP, LV end diastolic pressure; * $P < 0.05$ vs pre-breast cancer; ¥ measured from subsample of healthy control rats (*n*=5).

Figure 3.1. *Schematic representation of the experimental protocol.*

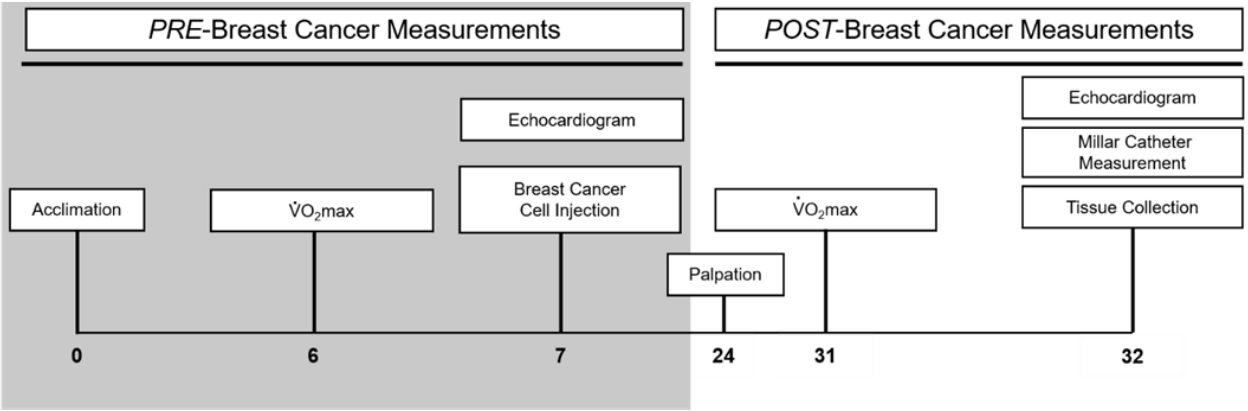

Day 0-5, acclimation; day 6, pre-$\dot{V}O_2$max; day 7, pre-echocardiography and breast cancer cell injection; day 24, first palpation; day 24-31 tumor growth; day 31, post-$\dot{V}O_2$max; day 32, post-echocardiography, Millar catheter measurements, and tissue collection.

Figure 3.2. *Representative images of pre-/post-breast cancer LV echocardiography.*

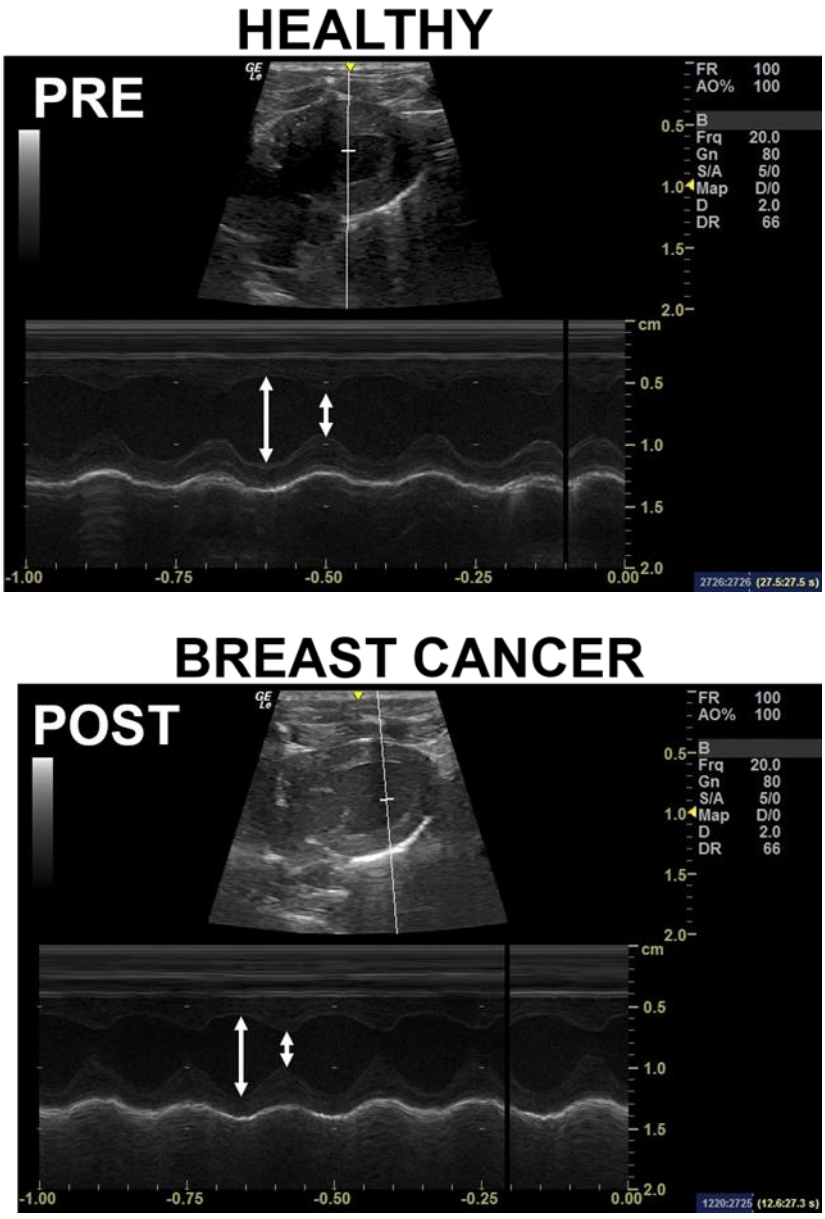

Left ventricle, LV. No changes were seen between cardiac function over time (~25 days between measurements). Arrows represent the LV during diastole (widened 1st arrow) and during systole (narrow 2nd arrow).

Figure 3.3. *Tumor burden versus left ventricular mass.*

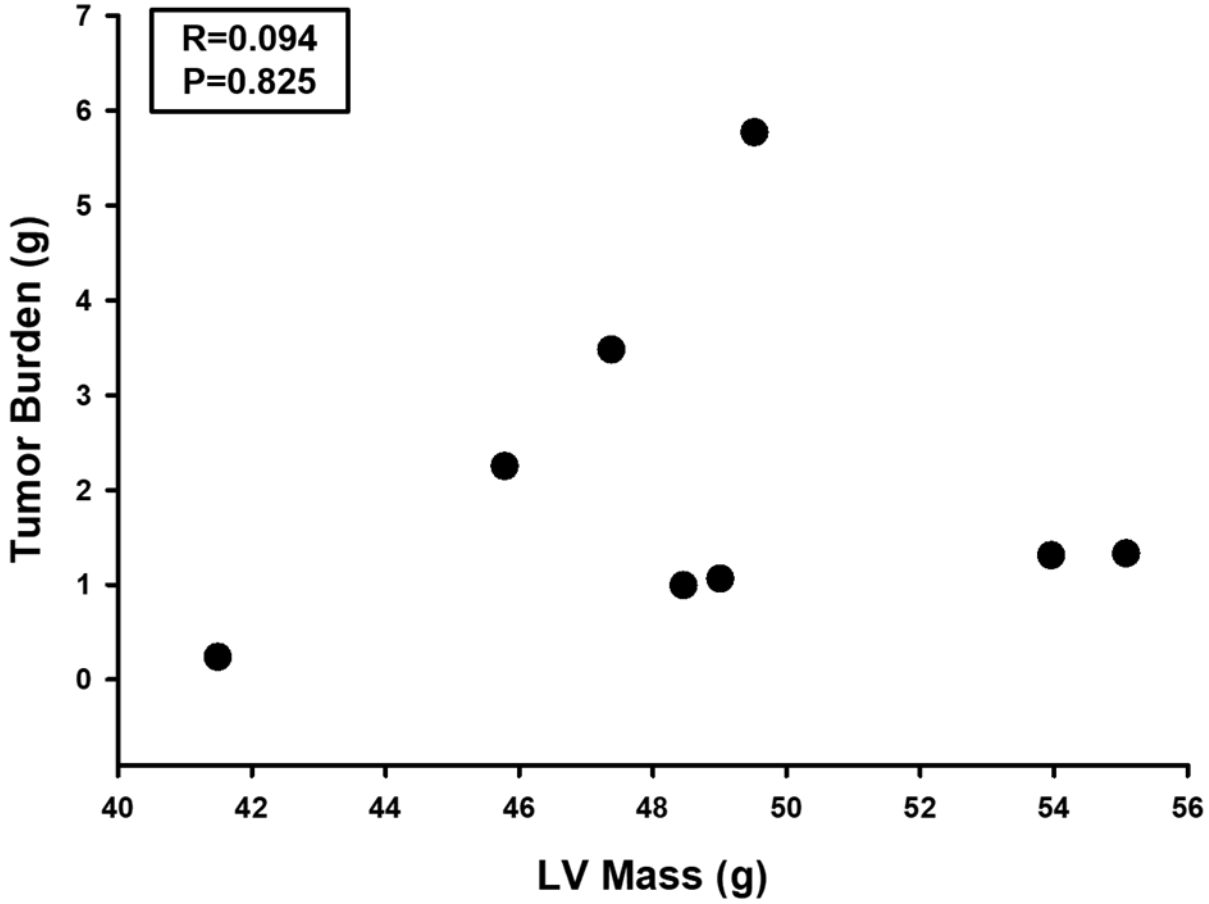

Breast cancer rats (*n*=8) display no significant correlation between tumor burden and left ventricular (LV) mass.

Figure 3.4. *Maximal oxygen uptake between pre-/post-breast cancer tumor development.*

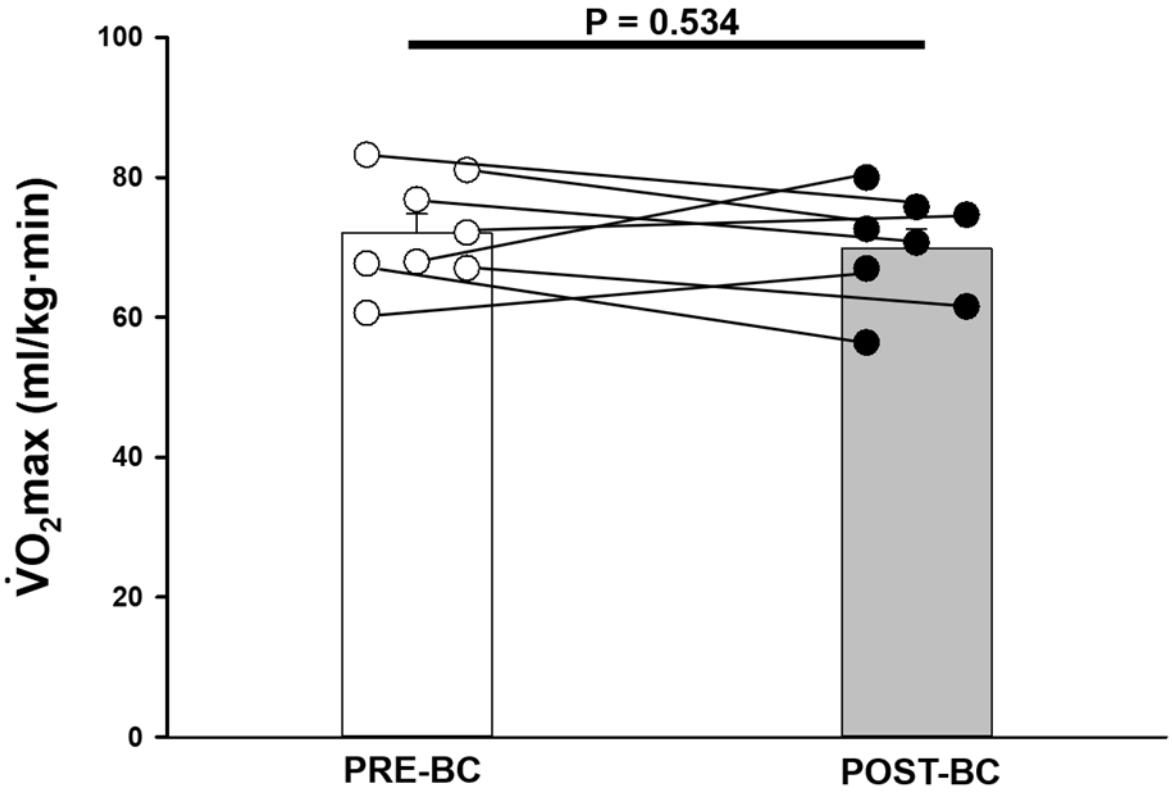

Pre-breast cancer (BC, *n*=8, left) vs post-breast cancer (*n*=8, right) relative $\dot{V}O_2$max. There was no difference in pre- vs post-$\dot{V}O_2$max measurements (P=0.534). Data are mean ± SE with individual data points plotted.

Figure 3.5. *Speed x body weight between pre-/post-breast cancer tumor development.*

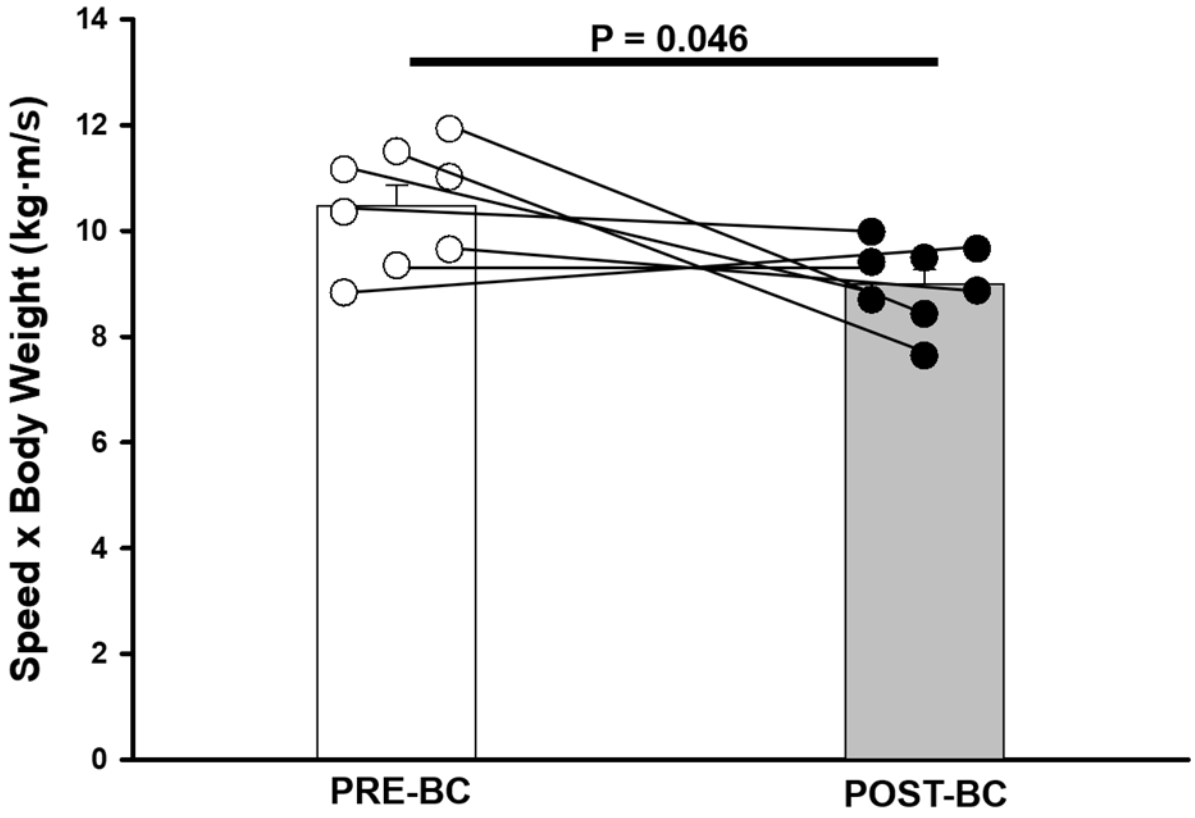

Pre-breast cancer (BC, *n*=8, left) vs post-breast cancer (*n*=8, right) final speed x body weight. There was a significant difference in pre- versus post-measurements. Data are mean ± SE and individual datum points.

Figure 3.6. *Oxygen cost of exercise and total breast cancer tumor burden.*

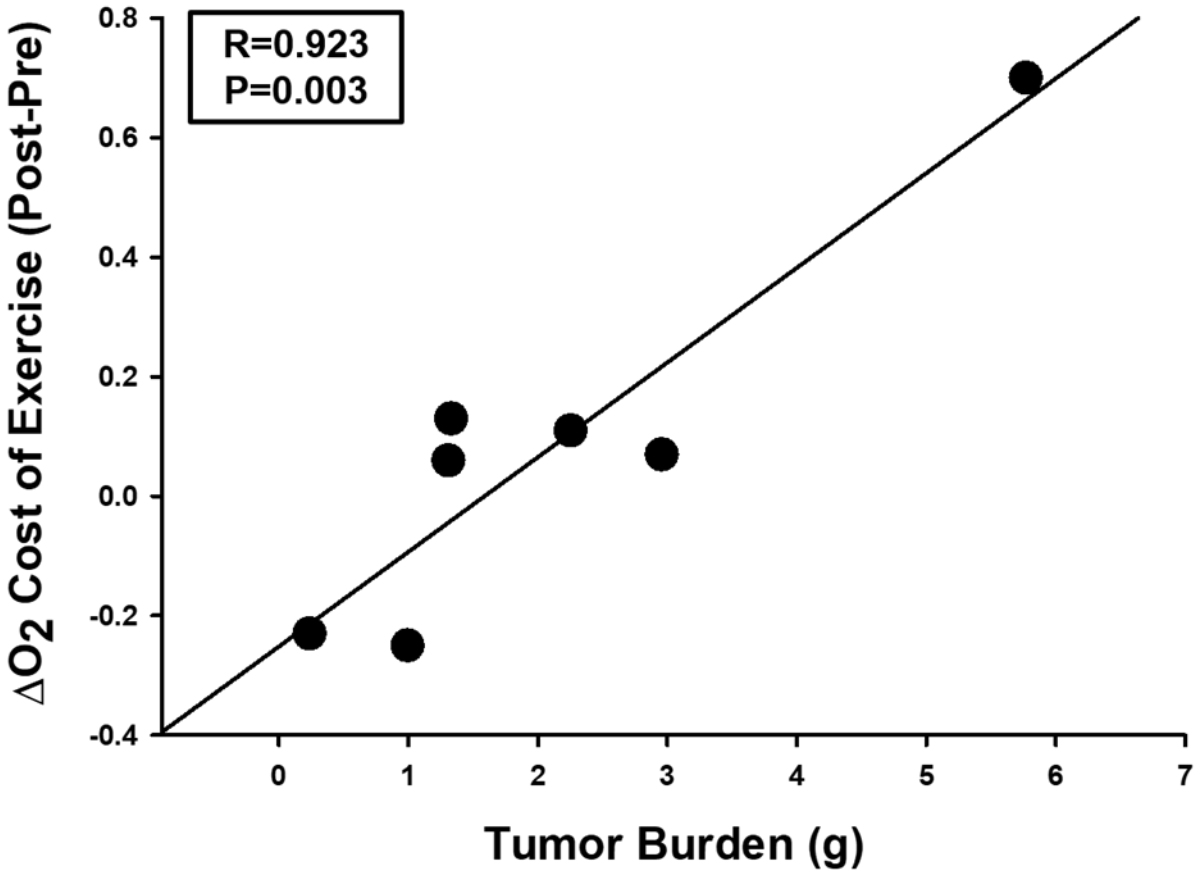

Change in O_2 cost of exercise ($\Delta\dot{V}O_2$(ml/kg·min)/final speed (m/s)) between post- and pre-breast cancer (*n=7*). This graph displays that an increase in O_2 cost of exercise is attributable, in part, to increases in tumor burden. One rat was not included due to error in collecting baseline O_2 uptake measurement.

Chapter 4 - Skeletal muscle microvascular oxygenation in breast cancer: Role of nitric oxide bioavailability

Abstract

Skeletal muscle dysfunction and exercise intolerance are present prior to chemotherapy in women diagnosed with breast cancer. Reduced nitric oxide (NO) bioavailability reduces the dynamic matching between skeletal muscle oxygen delivery ($\dot{Q}O_2$) and mitochondrial demand ($\dot{V}O_2$) during exercise; however, whether this occurs in breast cancer has not been investigated. We hypothesized that the interstitial pressure of O_2 ($PO_2$is), which is directly related to the matching between $\dot{Q}O_2$ and $\dot{V}O_2$, would be reduced at rest and during 1-Hz twitch contractions due, in part, to decreased NO bioavailability. Intraductal injections of MATBIII adenocarcinoma cells induced breast cancer in female Fischer-344 rats (*n*=9) or vehicle control (*n*=9). ~24 days post-injection, phosphorescence quenching determined the resting and contracting spinotrapezius muscle $PO_2$is during control, sodium nitroprusside (SNP, 300uM) and L-nitro arginine methyl ester (L-NAME, 1.5 mM) conditions. Breast cancer rats had a significantly elevated resting (31.9±1.6 vs. 27.8±1.6 mmHg; P=0.002) and contracting (19.5±2.4 vs. 15.8±1.8 mmHg; P=0.003) $PO_2$is and faster $PO_2$is kinetics (time delay 9±3 vs. 12±2 s; P=0.019) with comparison to healthy rats, respectively. Relative to control conditions, SNP improved the $PO_2$is kinetics response to contractions (time constant, 30 ± 9 vs. 48 ± 17 s; P=0.016; mean response time: 38±11 vs. 55±19 s; P=0.047), whereas LNAME abolished these effects (MRT: 21±4 s, P=0.008 vs. control; P=0.003 vs. SNP). These findings indicate that there is significant microvascular dysfunction present in breast cancer that can be attenuated with increased NO bioavailability.

Introduction

Breast cancer (BC) is the most diagnosed cancer in women worldwide (Sung et al., 2021) and is associated with exercise intolerance and skeletal muscle dysfunction (Klassen et al., 2017). Within oncology, skeletal muscle dysfunction is traditionally attributed to muscle atrophy (e.g., cancer-associated cachexia) (Kilgour et al., 2010). While this assumption is true for cancers in males, females with BC typically remain weight stable (Stephens et al., 2012) despite exercise intolerance in the early stages of tumor development (Klassen et al., 2017) that is associated with treatment failure, chemotoxicity (Prado et al., 2009), and shorter survival (Villaseñor et al., 2012). Exercise training is a valuable therapeutic option for BC patients (Courneya et al., 2003) however, exercise intolerance limits the ability to perform exercise and reduces adherence to exercise programs (Jones et al., 2012). Thus, understanding the physiological mechanisms underlying BC-induced exercise intolerance is key to improving their quality and quantity of life.

A low maximal oxygen uptake ($\dot{V}O_2max$) during exercise is associated with higher mortality among BC patients (Jones et al., 2012). Primarily, attention has focused on the central mediators of exercise intolerance and reduced $\dot{V}O_2max$ second to impaired cardiac function (i.e., cardiotoxicity) following anti-cancer therapy (anthracyclines; doxorubicin/epirubicin) (Cardinale et al., 2020). Although $\dot{V}O_2max$ is not necessarily reduced as a consequence of BC tumor bearing alone (Weber et al., 2025), a limited body of clinical and pre-clinical evidence in BC suggests that the reduced exercise capacity (Beaudry et al., 2019; Mader et al., 2022) and impaired exercise economy (Weber et al., 2025) likely stem from peripheral dysfunction in the O_2 transport cascade (Haykowsky et al., 2022; Koivula et al., 2024). Increased sympathetic activity (Jones et al., 2012), endothelial dysfunction (Jones et al., 2013), aberrant calcium handling (Wilson et al., 2019), and mitochondrial dysfunction (Wilson et al., 2019) have been

implicated in reducing exercise capacity in BC. This dysfunction may be due to impaired coupling of peripheral vascular responses to skeletal muscle metabolic demand, resulting from vascular endothelial damage and loss of effective nitric oxide (NO) signaling.

NO-mediated increases in O_2 delivery to skeletal muscle ($\dot{Q}O_2$) at the onset of exercise are important to meet the rapidly rising mitochondrial demand ($\dot{V}O_2$), establish a pressure gradient (PO_2) necessary for O_2 diffusion, and support the O_2 cost of exercise (Colburn et al., 2020; McAllister et al., 2008). Reduced vascular NO bioavailability, coupled with augmented production of reactive oxygen species (ROS) contributes to systemic endothelial dysfunction early in BC tumor growth (Buczek et al., 2018; Smeda et al., 2018) a time when reductions in exercise tolerance begin to emerge (Mader et al., 2022). Such changes may diminish the ability of skeletal muscle to augment $\dot{Q}O_2$ at exercise onset and therefore elevate glycolysis (Hogan et al., 1992), slow $\dot{V}O_2$ kinetics (Poole & Musch, 2023), and accelerate fatigue.

Whether $\dot{Q}O_2$-to-$\dot{V}O_2$ matching and the muscle oxygenation kinetics are impaired in BC remain unknown. The partial pressure of O_2 in the interstitial space ($PO_2$is) reflects the instantaneous dynamic relationship between $\dot{Q}O_2$ and $\dot{V}O_2$ at the level of the skeletal muscle. Altered $PO_2$is from healthy values indicates dysfunctional metabolic control within the skeletal muscle microvasculature (Hogan et al., 1992). A higher $PO_2$is would suggest aberrant heterogeneity of $\dot{Q}O_2$ to the muscle and a lower $PO_2$is may be consequent to diminishing O_2 availability. At exercise onset, the inability to match $\dot{Q}O_2$ and $\dot{V}O_2$ generates a precipitous fall in $PO_2$is, subsequently reducing total skeletal muscle oxygenation. Altogether, these insights would enhance our knowledge behind how BC alters intramyocyte PO_2, metabolic control, and exercise capacity.

Thus, in an orthotopic rat model of BC compared to healthy controls, we hypothesized that there would be 1) impaired matching between skeletal muscle $\dot{Q}O_2$-to-$\dot{V}O_2$ at rest and during twitch contractions (faster $PO_2$is kinetics), 2) restoration of the $PO_2$is profiles to that of healthy controls rats following administration of exogenous NO donor sodium nitroprusside (SNP) via the NO-mediated vasodilatory response, and 3) inhibition of NO production L-nitro arginine methyl ester (L-NAME) would augment the impaired $\dot{Q}O_2$-to-$\dot{V}O_2$ matching from control conditions. This investigation was designed to provide potential mechanistic insights into BC-induced exercise intolerance which may be indicated by the $\dot{Q}O_2$-to-$\dot{V}O_2$ relationship. In addition, the results of this study may determine whether perturbations in $\dot{Q}O_2$-to-$\dot{V}O_2$ matching, if present in BC, could be normalized by increasing NO bioavailability.

Methods

Ethical approval

All procedures were approved by the Institutional Animal Care and Use Committee of Kansas State University (Protocol # 4684), conformed to the Guide for the Care and Use of Laboratory Animals published by the US National Institutes of Health (NIH Publication No. 85-23, revised 1985), and conducted according to the National Research Council Guide for the Care and Use of Laboratory Animals. Experiments were performed on female Fischer-344 retired-breeder rats (~6-8 months, *n*=26; Hilltop Lab, Scottdale, PA). Upon arrival, animals were maintained in accredited (Association for the Assessment and Accreditation of Laboratory and Animal Care) animal facilities under a 12:12 h light: dark cycle with food and water provided *ad libitum*.

Orthotopic breast cancer model

The 13762 MAT B III adenocarcinoma cell line (CRL-1666; ATCC, Manassas, VA) originates from rat mammary glands. The cells were cultured in McCoy's 5A (modified) medium, supplemented with 10% fetal bovine serum, and stored in a 5% CO_2 incubator until reaching confluency. Cell counts and viability were tested with Trypan blue staining prior to BC cell injection procedures. While anesthetized under 2.5% isoflurane-O_2 and positioned on a heating pad to maintain core temperature at ~37°C (measured via rectal thermometer), using a 20-G needle, 6 x 10^3 cells in 50 µL of saline (breast cancer, BC, *n*=16) or 50 µL of saline (healthy control, HC, *n*=10) was injected into the left abdominal mammary duct. Rats were monitored closely for ~2 hours for signs of distress. Five days following tumor palpation (~24 days post injection) skeletal muscle $PO_2$is measurements were performed.

Surgical preparations and experimental protocol

Rats were anesthetized with a 5% isoflurane-O_2 mixture and maintained with 2.5% isoflurane-O_2 while core temperature was kept at ~37°C (measured via rectal thermometer). The left carotid artery was isolated and cannulated with PE-10 connected to PE-50 (Intra-Medic polyethylene tubing; Clay Adams Brand, Benton, Dickson and Company, Sparks, MD) to measure mean arterial pressure (MAP) and heart rate (HR) (Digi-Med BPA; Model 400). A second catheter was placed in the caudal artery for administration of pentobarbital sodium anesthesia (50 mg ml^{-1}) and arterial blood sampling. Rats were then transitioned to pentobarbital sodium anesthesia (20 mg kg^{-1} body weight i.a.) while the concentration of isoflurane decreased and subsequently discontinued. The depth of anesthesia was regularly monitored via toe pinch and palpebral reflex with pentobarbital anesthesia supplemented (3.5-7.0 mg kg^{-1}) as necessary during experimentation.

To exteriorize the spinotrapezius muscle, the overlying skin and fascia were carefully removed from the mid-dorsal-caudal region and the spinotrapezius muscle was exposed. This exteriorization does not alter vascular or nervous supply to the muscle (Bailey et al., 2000; Gray, 1973; Kindig et al., 1999). Silver wire electrodes were sutured (6-0 silk) to the rostral (cathode) and caudal (anode) regions of the muscle to induce twitch contractions. The muscle was continuously superfused with Krebs-Henseleit bicarbonate-buffered solution (4.7 mM KCl, 2.0 mM $CaCl_2$, 2.4 mM $MgSO_4$, 131 mM NaCl, and 22 mM $NaHCO_3$; pH = 7.40; equilibrated with 5% CO_2-95% N_2 at 38°C) and the adjacent tissue was covered with Saran wrap (S.C. Johnson & Son, Racine, WI) to minimize dehydration.

All the following measurements were completed in a dark room to minimize interference with the phosphorescent signal. Oxyphor G4 (Pd-meso-tetra-(3,5-dicarboxyphenyl)-tetrabenzo-

porphyrin), a phosphorescent probe that permits the dynamic visualization of tissue PO_2(Esipova et al., 2011), was injected locally into the muscle (3-4 injections 10 μL at 10 μM concentration) using a 29 G needle. Care was taken to avoid damaging any visible vasculature. A bifurcated light guide was positioned ~3-4 mm above the surface of the exposed muscle in a field absent of large vessels. The spinotrapezius muscle was covered with Saran wrap (S.C. Johnson & Son, Racine, WI) to minimize dehydration during a 15 min period that allows for diffusion of Oxyphor G4 throughout the muscle and into the interstitial space.

A frequency domain phosphorimeter (PMOD 500; Oxygen Enterprises, Philadelphia, PA) determined resting and contracting $PO_2$is during three separate protocols: control (CON, no superfusion), sodium nitroprusside superfusion (SNP, 3 ml of a 300 μM solution), and L-nitro arginine methyl ester (L-NAME, 3.5 ml of a 1.5mM solution) as previously described (Hirai et al., 2012). Twitch contractions were electrically evoked (1-Hz, 6 V, 2 ms pulse duration) with a Grass S88 Stimulator (Quincy, MA) for 180 s and $PO_2$is was measured and recorded at 2 s intervals throughout the duration of the protocol. This stimulation protocol elicits ~4-5-fold increase in $\dot{Q}O_2$ and a ~7-fold increase in $\dot{V}O_2$ that is consistent with moderate intensity exercise (Behnke et al., 2001; Hirai et al., 2013). Between each protocol 30 minutes of recovery allowed for the $PO_2$is to return to baseline values. Following CON measurements, the spinotrapezius was superfused with SNP for 180 s and $PO_2$is was continuously recorded (Ferreira et al., 2006). Afterwards, the same protocol was repeated with L-NAME superfusion. Immediately following $PO_2$is measurements, 0.3 ml of blood was sampled from the caudal artery catheter for arterial blood gases analyses. Following the last contraction protocol, rats were euthanized via pentobarbital sodium (>100 mg kg^{-1}) overdose and tissues were harvested for weight measurements.

Analysis of interstitial PO_2 kinetics

The principles of the phosphorescence quenching method have been described previously (Behnke et al., 2001). This method applies the Stern-Volmer relationship (Esipova et al., 2011) which describes the quantitative O_2 dependence of the phosphorescent probe (G4) via the following equation:

$$\mathrm{PO_2} = \left(\frac{\tau^{\circ}}{\tau - 1}\right) \Big/ (\mathrm{k_Q} \times \tau^{\circ})$$

where k_Q is the quenching constant and τ and τ° are the phosphorescence lifetimes at the ambient O_2 concentration and in the absence of O_2, respectively. In tissues at 32.3°C (muscle surface temperature ~32.5°C) the parameters for G4 were as follows: k_Q of 258 mmHg s^{-1} and τ^0 of 226 μs. Muscle temperature does not change appreciably during the contraction protocol herein, therefore the phosphorescence lifetime is affected exclusively by the PO_2. The kinetics analyses of the $PO_2$is response during contractions was modeled with $PO_2$is measurements collected during 30 s of rest and 180 s of contractions:

$$\mathrm{PO_2(t)} = \mathrm{PO_{2(BL)}} - \Delta PO_2 \left[1 - \mathrm{e}^{-\frac{(-t-TD)}{\tau}}\right]$$

The SNP response was fit with $PO_2$is during superfusion:

$$\mathrm{PO_2(t)} = \mathrm{PO_{2(BL)}} + \Delta \mathrm{PO_2} \left[1 - \mathrm{e}^{-\frac{(-\mathrm{t}-TD)}{\tau}}\right]$$

where PO_2(t) represents the $PO_2$is at any given timepoint, $PO_{2(BL)}$ corresponds to the 30 s of resting $PO_2$is before contractions, ΔPO_2 is the amplitude for the initial decay of $PO_2$is, TD is time delay preceding the decay in $PO_2$is, and τ is the constant (i.e., the time required to reach 63% of the amplitude). Model fits were determined by: 1) the coefficient of determination, 2)

sum of the squared residuals, and 3) visual inspection and analysis of the model fit to the data and residuals.

Mean response time (MRT) is the overall kinetics of the primary and secondary responses during contractions or SNP superfusion (Macdonald et al., 1997):

$$\mathrm{MRT} = \mathrm{TD} + \tau$$

where TD and τ are defined above. The time taken to reach 63% of the response was determined independent of modeling procedures (T_{63}). Area under the curves (AUC, mmHg·s) were integrated by summing each 2 s measurement across the 360 s of superfusion and incubation or 180 s of contractions and recovery protocols.

Statistical analysis

Statistical analyses and curve fitting were performed using a commercially available software package (SigmaPlot 12.5, Systat Software, San Jose, CA). Unpaired Student's t-tests were performed to determine differences in morphological characteristics and to detect differences present in $PO_2$is kinetic parameters. A two-way repeated measures ANOVA was used to evaluate temporal interactions (Group x Time) during $PO_2$is measurements. Normality was assessed using the Shapiro-Wilk test. If either the normality or equal variance assumptions were violated, a Mann-Whitney rank-sum test was used to compare the above variables. Tukey *post hoc* tests were used for multiple comparisons when significant differences were detected. Data are presented as the group mean ± SD. Significance was accepted at $P < 0.05$ unless otherwise stated.

Results

Body mass was not different between groups (HC: 219 ± 9 g; BC: 212 ± 14 g, P=0.202) and the average tumor weight was 2.04 ± 1.80 g (range: 0.24 – 5.77 g). There was no relationship between tumor burden and soleus or left ventricle mass (Figure 4.1) demonstrating that this model does not induce muscle wasting. No differences were observed in resting or contracting heart rate (HR) or mean arterial pressure (MAP) between groups during CON, SNP, or L-NAME protocols (P>0.05); however, SNP superfusion resulted in a decrease in MAP from resting conditions in both HC (from 100 ± 8 to 82 ± 10 mmHg, P=0.004) and BC (from 94 ± 10 to 79 ± 9 mmHg, P=0.001) animals. There were no differences in arterial O_2 saturation (HC: 94 ± 5%; BC: 95 ± 4%; P=0.453), systemic hematocrit (HC: 31.2 ± 2.7%; 25.0 ± 6.7%; P=0.067), or arterial pH (HC 7.44 ± 0.06; BC: 7.44 ± 0.05; P=0.747).

Eighteen rats (HC, *n*=9; BC, *n*=9) were analyzed for CON PO_2*is* kinetics. Group mean spinotrapezius muscle $PO_2$is profiles at rest and during contractions are presented in Figure 4.2 and the model derived kinetics parameters in Table 4.1. $PO_2$is was higher in BC rats in all instances at rest (0-30 s; $P < 0.05$), during steady-state contractions (0-180 s) ($P < 0.05$), and when reaching the $PO_{2(NADIR)}$ (P=0.003). BC rats evinced a speedier fall in $PO_2$is at the onset of contractions (reduced TD; P=0.019).

Sixteen rats (HC, *n*=7; BC, *n*=9) were analyzed for SNP PO_2*is* kinetics. Group mean spinotrapezius muscle $PO_2$is responses during the SNP condition are presented in Figure 4.3 and the model derived kinetics parameters in Table 4.2. During superfusion, BC rats had a lower magnitude increase in $PO_2$is in comparison to HC animals (Figure 4.3, inset; P=0.039). SNP superfusion slowed $PO_2$is kinetics at the onset of contractions in both groups (i.e., greater T, MRT vs. control conditions; P<0.05); but, BC rats maintained a faster TD versus HC rats

(P=0.007) (Table 4.2). There was a substantially greater magnitude change in $PO_2$is ($\Delta PO_{2(CONTRACT)}$) in BC rats versus HC rats (P=0.047). Specifically, BC rats had a significantly lower $PO_2$is from 400-540 s (P<0.05).

Twelve rats (HC, *n*=7; BC, *n*=5) were used for L-NAME $PO_2$is kinetics analyses. Group mean spinotrapezius muscle $PO_2$is responses during the L-NAME condition are presented in Figure 4.4 and the model derived kinetics parameters in Table 4.3. At the onset of contractions, BC rats had a significantly longer TD versus HC rats (TD, P=0.028). Despite this, there was no statistical difference in the temporal $PO_2$is profile during L-NAME superfusion, incubation, or contractions (P>0.05). $\Delta PO_{2(NADIR)}$ was not different between groups (P=0.214). Figure 4.5 highlights the differences seen within HC and BC groups across CON, SNP, and L-NAME conditions.

Discussion

The primary original findings of this study support that skeletal muscle $\dot{Q}O_2$-to-$\dot{V}O_2$ matching is impaired at rest and during contractions in BC compared to HC rats. Increasing NO bioavailability via the exogenous NO-donor SNP improved skeletal muscle $PO_2$is in BC rats, but was unable to restore the contracting $PO_2$is profile to that of HC rats. Decreasing NO bioavailability with NOS inhibition by L-NAME lowered $PO_2$is levels substantially, which has direct implications on muscular metabolic control. Altogether, our data suggest that in BC, NO is essential to maintaining $\dot{Q}O_2/\dot{V}O_2$ and perturbations that affect NO bioavailability likely play a crucial role in limiting exercise tolerance in BC.

Interstitial PO_2 in breast cancer

At rest, BC rats had a substantially higher $PO_2$is (Figure 4.2). Elevated resting $PO_2$is could be interpreted as a higher $\dot{Q}O_2$, potentially facilitated through 1) intramuscular pro-inflammatory cytokines (TNF-α, IL-6) that increase local $\dot{Q}O_2$ despite unchanged metabolic demand (Argilés et al., 2023; Habanjar et al., 2023; Mader et al., 2022) or 2) greater reliance on glycolytic metabolism where adenosine bi-products increase vascular smooth muscle relaxation (Nayeem et al., 2009).

The increased $PO_2$is in BC rats persisted throughout contractions and one potential explanation for this result is that aberrant $\dot{Q}O_2$ heterogeneity and a lower ability to increase fractional O_2 extraction, possibly due to increased intramuscular ROS (Habanjar et al., 2023; Mader et al., 2022), reduces the diffusive capacity of O_2 (DO_2) in BC. Hirai et al demonstrated, in healthy spinotrapezius muscle, acute increases of hydrogen peroxide, a ubiquitous ROS, elevates resting and contracting microvascular PO_2 relative to control conditions through disproportionate increases in $\dot{Q}O_2$ and $\dot{V}O_2$ (Hirai et al., 2011). ROS-induced microvascular

dysfunction disrupts capillary blood flow regulation which results in an uneven distribution of RBCs and reduced O_2 extraction (Ellis et al., 2002; Heinonen et al., 2015; Walley, 1996). This is exemplified in our dataset by the higher $PO_2$is coupled with a speedier fall (↓TD) during contractions. Importantly, such perturbations are expected to slow $\dot{V}O_2$ kinetics during exercise, requiring greater substrate-level phosphorylation to meet ATP demands, accelerate glycogen depletion, and culminate in exercise intolerance (Poole et al., 2018).

Effect of altered nitric oxide bioavailability on interstitial PO_2 in breast cancer

NO signaling has an important role in modulating $PO_2$is both as a powerful vasodilatory agent (increases $\dot{Q}O_2$ via smooth muscle relaxation (Stamler & Meissner, 2001)) and by competitive inhibition of mitochondrial enzymes (reduces $\dot{V}O_2$) (Jones et al., 2021; Larsen et al., 2011). Increased NO bioavailability (SNP) should then increase $\dot{Q}$ and/or decrease $\dot{V}O_2$, while decreased NO bioavailability (L-NAME) would induce the opposite effects. The expected outcome of SNP superfusion would be an increased $PO_2$is while L-NAME superfusion would decrease $PO_2$is (as demonstrated in microvascular PO_2 measurements (Hirai et al., 2013)).

Augmented $\dot{Q}O_2$ induced by SNP evoked large increases in $PO_2$is in both HC and BC rats. Despite this, BC rats had a lower sensitivity to SNP (↓$\Delta PO_2$is), which suggests that there may be downstream dysfunction in NO signaling (oxidized soluble guanylyl cyclase (Gerassimou et al., 2007)) or greater ROS-mediated scavenging of NO (Smeda et al., 2018). During contractions, SNP slowed the time constant relative to control conditions in both BC and HC rats, thereby improving the dynamic matching of $\dot{Q}O_2$ and $\dot{V}O_2$ (Figure 4.4). It is noteworthy that while the TD was increased in HC rats, it was unchanged between CON and SNP conditions in BC rats. As $PO_2$is is represented by $\dot{Q}O_2/\dot{V}O_2$, the TD at the onset of contractions is incredibly sensitive to the hyperemic $\dot{Q}O_2$ response and to the mitochondrial O_2 demand for ATP

production. Any such perturbations from HC animal values would be expected to contribute to slowed $\dot{V}O_2$ kinetics (Poole & Musch, 2023). Therefore, it is possible that while SNP provoked greater total $\dot{Q}O_2$ to the muscle, it was unable to improve RBC flux through capillaries not supporting flow, thereby reflecting a reduced DO_2.

Inhibition of NOS reveals that NO plays a crucial role in the control of skeletal muscle $\dot{Q}O_2$, especially for females (Majmudar et al., 2000). As demonstrated previously in healthy female rats (Craig et al., 2018), L-NAME superfusion did not alter resting $PO_2$is, which suggests that eNOS-mediated production does not play a role in maintaining $\dot{Q}O_2/\dot{V}O_2$ within the spinotrapezius interstitial space at rest in HC or BC rats. The spinotrapezius muscle is mixed-fiber type (Delp & Duan, 1996) and previous findings in our lab have highlighted that L-NAME reduces skeletal muscle blood flow to a greater degree in muscles with a higher proportion of type I and type IIa muscle fibers (Copp et al., 2010), therefore, L-NAME may induce greater changes in predominantly oxidative muscles, like the soleus. As $\dot{V}O_2$ increased during contractions, BC rats evinced a greater relative rate of change for $PO_2$is (represented by $\Delta PO_2/T$) versus HC rats, which may mark the presence of low capillary-to-fiber surface area for O_2 flux (Poole & Musch, 2023) and suggests rapid desaturation during contractions was necessary to support mitochondrial O_2 requirements and intramyocyte DO_2. It cannot be ignored, though, that reduced mitochondrial oxidative capacity within skeletal muscle is observed early in BC in the clinical (Wilson et al., 2021) and preclinical (Mader et al., 2022) populations, which, if present, would likely contribute to these findings.

Mechanisms of skeletal muscle dysfunction in breast cancer: hypotheses and future directions

A conceptual framework based on these findings suggests that within the skeletal muscle microvasculature in BC there may be pathologically heterogeneous O_2 delivery at rest that

persists through contractions to disrupt the kinetic coupling between $\dot{Q}O_2$ and $\dot{V}O_2$. Inadequate O_2 delivery does not necessarily impair mitochondrial O_2 uptake during whole body exercise (Weber et al., 2025), but promotes the accumulation of fatigue-associated metabolites, impairs contractile function (Mader et al., 2022; Wilson et al., 2021), and increases the O_2 cost of exercise. When NO bioavailability increases within the muscle, the spatial and temporal distribution of RBCs becomes more homogeneous, enhancing DO_2 by increasing the number of RBCs adjacent to contracting myocytes (Federspiel & Popel, 1986). However, inhibiting NO-mediated vasodilation with L-NAME exacerbates $\dot{Q}O_2$ heterogeneity, causing stopped capillaries to remain occluded and sluggish ones to persist.

Clinical Implications

Substantial evidence indicates that enhanced NO function plays a crucial role in the beneficial adaptations of skeletal muscle hemodynamic and metabolic control with exercise training (Green et al., 2004; McAllister et al., 2008). Mader et al. recently demonstrated that in weight-stable BC mice, 4 weeks of voluntary wheel running counteracted exercise intolerance and BC-induced muscle weakness partially owed to reduced intramuscular cytokine production (Mader et al., 2022). Previous findings from our lab have indicated that exercise training improves the rate of adjustment in $\dot{Q}O_2$ during contractions (Hirai et al., 2012) likely due, in part, to enhanced NO-mediated regulation of RBC flux and reduced spatial heterogeneities of contracting muscle microvascular oxygenation (Koga et al., 2007). By ameliorating NO dysfunction, exercise training not only supports metabolic and vascular adaptations in the context of cancer, but may also modify the tumor microenvironment. Despite equivocal evidence in the capacity for exercise training to reduce tumor growth (Jones et al., 2010; Westerlind et al., 2003), exercise has been demonstrated to increase (Jones et al., 2010) and improve (McCullough

et al., 2013) tumor vascularization, alter the molecular profile (Mader et al., 2022), augment tumor perfusion (McCullough et al., 2013, 2014), and increase tumor PO_2 (McCullough et al., 2014), all of which are expected to slow tumor growth and potentially increase the delivery of anti-cancer treatment.

Experimental considerations

Prior investigations regarding the systemic effects of cancer have largely used rodent models that induce cachexia, which limits the clinical application and therapeutic insight in predominantly female cancers, specifically breast cancer(Rentz et al., 2023). Importantly, only a small percentage of women with BC experience body weight loss (Fox et al., 2009), despite a significant proportion reporting severe exercise intolerance early in diagnosis (Neefjes et al., 2017) that typically worsens during radiation and chemotherapy and persist for years post-treatment (Bower et al., 2000). In this investigation we utilized an intraductal, orthotopic and syngeneic model of BC in rats, which is considered to be the gold standard approach to model BC in immunocompetent animals (Ashcraft et al., 2016), to resolve the effects of BC on skeletal muscle oxygenation. It must be noted that a single animal model of BC may not fully capture the complexities of skeletal muscle responses in human subjects. Retired-breeder rats were used in this study and it cannot be ignored that multiparity may reduce vascular compliance due to altered endothelial function (Dhawan et al., 2004; Reckelhoff, 1997), which may contribute to our findings. Evidence suggests that tumor-bearing mice with distinct molecular subtypes of BC display a reduced rate of force development and twitch relaxation (Bohlen et al., 2018; Wilson et al., 2021). The primary focus of this study was to assess the relationship between skeletal muscle $\dot{Q}O_2$ and $\dot{V}O_2$ at a given absolute intensity (1-Hz), which provides insight into metabolic impairments regardless of force output. Moreover, investigations emphasizing microcirculatory

capillary hemodynamics in BC at rest and during contractions would allow us to parse the degree of muscular dysfunction present alongside systemic mechanisms (metabolic and sex hormones, inflammatory markers, immune dysfunction), molecular mechanisms (e.g. cell signaling pathways), and how these relate to tumor biology (apoptosis, proliferation) and, ultimately, patient prognosis.

Conclusions

This study highlights that BC rats exhibit marked impairments in $\dot{Q}O_2$-to-$\dot{V}O_2$ matching compared to healthy rats and that NO plays a crucial role in regulating $PO_2$is during small muscle mass exercise, with BC rats showing reduced sensitivity to NO modulation. While SNP improved $\dot{Q}O_2/\dot{V}O_2$ matching in both groups, BC rats did not exhibit the same improvements, indicating potential microvascular dysfunction. These findings underscore the importance of NO signaling in muscle oxygenation and suggest that therapeutic strategies targeting NO pathways could help improve exercise tolerance in BC along the continuum of disease and survivorship.

References

Argilés, J. M., López-Soriano, F. J., Stemmler, B., & Busquets, S. (2023). Cancer-associated cachexia—Understanding the tumour macroenvironment and microenvironment to improve management. *Nature Reviews. Clinical Oncology*, *20*(4), 250–264. https://doi.org/10.1038/s41571-023-00734-5

Ashcraft, K. A., Peace, R. M., Betof, A. S., Dewhirst, M. W., & Jones, L. W. (2016). Efficacy and Mechanisms of Aerobic Exercise on Cancer Initiation, Progression, and Metastasis: A Critical Systematic Review of In Vivo Preclinical Data. *Cancer Research*, *76*(14), 4032–4050. https://doi.org/10.1158/0008-5472.CAN-16-0887

Bailey, J. K., Kindig, C. A., Behnke, B. J., Musch, T. I., Schmid-Schoenbein, G. W., & Poole, D. C. (2000). Spinotrapezius muscle microcirculatory function: Effects of surgical exteriorization. *American Journal of Physiology. Heart and Circulatory Physiology*, *279*(6), H3131-3137. https://doi.org/10.1152/ajpheart.2000.279.6.H3131

Beaudry, R. I., Howden, E. J., Foulkes, S., Bigaran, A., Claus, P., Haykowsky, M. J., & Gerche, A. L. (2019). Determinants of exercise intolerance in breast cancer patients prior to anthracycline chemotherapy. *Physiological Reports*, *7*(1), e13971. https://doi.org/10.14814/phy2.13971

Behnke, B. J., Kindig, C. A., Musch, T. I., Koga, S., & Poole, D. C. (2001). Dynamics of microvascular oxygen pressure across the rest-exercise transition in rat skeletal muscle. *Respiration Physiology*, *126*(1), 53–63. https://doi.org/10.1016/s0034-5687(01)00195-5

Bohlen, J., McLaughlin, S. L., Hazard-Jenkins, H., Infante, A. M., Montgomery, C., Davis, M., & Pistilli, E. E. (2018). Dysregulation of metabolic-associated pathways in muscle of breast cancer patients: Preclinical evaluation of interleukin-15 targeting fatigue. *Journal of Cachexia, Sarcopenia and Muscle*, *9*(4), 701–714. https://doi.org/10.1002/jcsm.12294

Bower, J. E., Ganz, P. A., Desmond, K. A., Rowland, J. H., Meyerowitz, B. E., & Belin, T. R. (2000). Fatigue in breast cancer survivors: Occurrence, correlates, and impact on quality of life. *Journal of Clinical Oncology: Official Journal of the American Society of Clinical Oncology*, *18*(4), 743–753. https://doi.org/10.1200/JCO.2000.18.4.743

Buczek, E., Denslow, A., Mateuszuk, L., Proniewski, B., Wojcik, T., Sitek, B., Fedorowicz, A., Jasztal, A., Kus, E., Chmura-Skirlinska, A., Gurbiel, R., Wietrzyk, J., & Chlopicki, S. (2018). Alterations in NO- and PGI2- dependent function in aorta in the orthotopic murine model of metastatic 4T1 breast cancer: Relationship with pulmonary endothelial dysfunction and systemic inflammation. *BMC Cancer*, *18*(1), 582. https://doi.org/10.1186/s12885-018-4445-z

Cardinale, D., Iacopo, F., & Cipolla, C. M. (2020). Cardiotoxicity of Anthracyclines. *Frontiers in Cardiovascular Medicine*, *7*, 26. https://doi.org/10.3389/fcvm.2020.00026

Colburn, T. D., Hirai, D. M., Craig, J. C., Ferguson, S. K., Weber, R. E., Schulze, K. M., Behnke, B. J., Musch, T. I., & Poole, D. C. (2020). Transcapillary PO2 gradients in contracting muscles across the fibre type and oxidative continuum. *The Journal of Physiology*, *598*(15), 3187–3202. https://doi.org/10.1113/JP279608

Copp, S. W., Hirai, D. M., Hageman, K. S., Poole, D. C., & Musch, T. I. (2010). Nitric oxide synthase inhibition during treadmill exercise reveals fiber-type specific vascular control in the rat hindlimb. *American Journal of Physiology. Regulatory, Integrative and Comparative Physiology*, *298*(2), R478-485. https://doi.org/10.1152/ajpregu.00631.2009

Courneya, K. S., Mackey, J. R., Bell, G. J., Jones, L. W., Field, C. J., & Fairey, A. S. (2003). Randomized controlled trial of exercise training in postmenopausal breast cancer survivors: Cardiopulmonary and quality of life outcomes. *Journal of Clinical Oncology: Official Journal of the American Society of Clinical Oncology*, *21*(9), 1660–1668. https://doi.org/10.1200/JCO.2003.04.093

Craig, J. C., Colburn, T. D., Hirai, D. M., Schettler, M. J., Musch, T. I., & Poole, D. C. (2018). Sex and nitric oxide bioavailability interact to modulate interstitial Po2 in healthy rat skeletal muscle. *Journal of Applied Physiology (Bethesda, Md.: 1985)*, *124*(6), 1558–1566. https://doi.org/10.1152/japplphysiol.01022.2017

Delp, M. D., & Duan, C. (1996). Composition and size of type I, IIA, IID/X, and IIB fibers and citrate synthase activity of rat muscle. *Journal of Applied Physiology (Bethesda, Md.: 1985)*, *80*(1), 261–270. https://doi.org/10.1152/jappl.1996.80.1.261

Dhawan, V., Brookes, Z. L. S., & Kaufman, S. (2004). Long-term effects of repeated pregnancies (multiparity) on blood pressure regulation. *Cardiovascular Research*, *64*(1), 179–186. https://doi.org/10.1016/j.cardiores.2004.06.018

Ellis, C. G., Bateman, R. M., Sharpe, M. D., Sibbald, W. J., & Gill, R. (2002). Effect of a maldistribution of microvascular blood flow on capillary O(2) extraction in sepsis. *American Journal of Physiology. Heart and Circulatory Physiology*, *282*(1), H156-164. https://doi.org/10.1152/ajpheart.2002.282.1.H156

Esipova, T. V., Karagodov, A., Miller, J., Wilson, D. F., Busch, T. M., & Vinogradov, S. A. (2011). Two new "protected" oxyphors for biological oximetry: Properties and application in tumor imaging. *Analytical Chemistry*, *83*(22), 8756–8765. https://doi.org/10.1021/ac2022234

Federspiel, W. J., & Popel, A. S. (1986). A theoretical analysis of the effect of the particulate nature of blood on oxygen release in capillaries. *Microvascular Research*, *32*(2), 164–189. https://doi.org/10.1016/0026-2862(86)90052-x

Ferreira, L. F., Hageman, K. S., Hahn, S. A., Williams, J., Padilla, D. J., Poole, D. C., & Musch, T. I. (2006). Muscle microvascular oxygenation in chronic heart failure: Role of nitric oxide availability. *Acta Physiologica (Oxford, England)*, *188*(1), 3–13. https://doi.org/10.1111/j.1748-1716.2006.01598.x

Fox, K. M., Brooks, J. M., Gandra, S. R., Markus, R., & Chiou, C.-F. (2009). Estimation of Cachexia among Cancer Patients Based on Four Definitions. *Journal of Oncology*, *2009*, 693458. https://doi.org/10.1155/2009/693458

Gerassimou, C., Kotanidou, A., Zhou, Z., Simoes, D. C. M., Roussos, C., & Papapetropoulos, A. (2007). Regulation of the expression of soluble guanylyl cyclase by reactive oxygen species. *British Journal of Pharmacology*, *150*(8), 1084–1091. https://doi.org/10.1038/sj.bjp.0707179

Gray, S. D. (1973). Rat spinotrapezius muscle preparation for microscopic observation of the terminal vascular bed. *Microvascular Research*, *5*(3), 395–400. https://doi.org/10.1016/0026-2862(73)90055-1

Green, D. J., Maiorana, A., O'Driscoll, G., & Taylor, R. (2004). Effect of exercise training on endothelium-derived nitric oxide function in humans. *The Journal of Physiology*, *561*(Pt 1), 1–25. https://doi.org/10.1113/jphysiol.2004.068197

Habanjar, O., Bingula, R., Decombat, C., Diab-Assaf, M., Caldefie-Chezet, F., & Delort, L. (2023). Crosstalk of Inflammatory Cytokines within the Breast Tumor Microenvironment. *International Journal of Molecular Sciences*, *24*(4), 4002. https://doi.org/10.3390/ijms24044002

Haykowsky, M. J., Kirkham, A. A., Li, T., Pituskin, E., Thompson, R. B., Paterson, D. I., Foulkes, S. J., Halle, M., Sarma, S., Howden, E., Nelson, M. D., & La Gerche, A. (2022). Determinants of oxygen utilization in breast cancer: Similarities between heart failure with preserved ejection fraction. *Progress in Cardiovascular Diseases*, *74*, 45–52. https://doi.org/10.1016/j.pcad.2022.10.005

Heinonen, I., Koga, S., Kalliokoski, K. K., Musch, T. I., & Poole, D. C. (2015). Heterogeneity of Muscle Blood Flow and Metabolism: Influence of Exercise, Aging, and Disease States. *Exercise and Sport Sciences Reviews*, *43*(3), 117–124. https://doi.org/10.1249/JES.0000000000000044

Hirai, D. M., Copp, S. W., Ferguson, S. K., Holdsworth, C. T., McCullough, D. J., Behnke, B. J., Musch, T. I., & Poole, D. C. (2012). Exercise training and muscle microvascular oxygenation: Functional role of nitric oxide. *Journal of Applied Physiology (Bethesda, Md.: 1985)*, *113*(4), 557–565. https://doi.org/10.1152/japplphysiol.00151.2012

Hirai, D. M., Copp, S. W., Ferguson, S. K., Holdsworth, C. T., Musch, T. I., & Poole, D. C. (2013). The NO donor sodium nitroprusside: Evaluation of skeletal muscle vascular and metabolic dysfunction. *Microvascular Research*, *85*, 104–111. https://doi.org/10.1016/j.mvr.2012.11.006

Hirai, D. M., Copp, S. W., Schwagerl, P. J., Musch, T. I., & Poole, D. C. (2011). Acute effects of hydrogen peroxide on skeletal muscle microvascular oxygenation from rest to contractions. *Journal of Applied Physiology (Bethesda, Md.: 1985)*, *110*(5), 1290–1298. https://doi.org/10.1152/japplphysiol.01489.2010

Hogan, M. C., Arthur, P. G., Bebout, D. E., Hochachka, P. W., & Wagner, P. D. (1992). Role of O2 in regulating tissue respiration in dog muscle working in situ. *Journal of Applied Physiology (Bethesda, Md.: 1985)*, *73*(2), 728–736. https://doi.org/10.1152/jappl.1992.73.2.728

Holloszy, J. O., & Coyle, E. F. (1984). Adaptations of skeletal muscle to endurance exercise and their metabolic consequences. *Journal of Applied Physiology: Respiratory, Environmental and Exercise Physiology*, *56*(4), 831–838. https://doi.org/10.1152/jappl.1984.56.4.831

Jones, A. M., Vanhatalo, A., Seals, D. R., Rossman, M. J., Piknova, B., & Jonvik, K. L. (2021). Dietary Nitrate and Nitric Oxide Metabolism: Mouth, Circulation, Skeletal Muscle, and Exercise Performance. *Medicine and Science in Sports and Exercise*, *53*(2), 280–294. https://doi.org/10.1249/MSS.0000000000002470

Jones, L. W., Courneya, K. S., Mackey, J. R., Muss, H. B., Pituskin, E. N., Scott, J. M., Hornsby, W. E., Coan, A. D., Herndon, J. E., Douglas, P. S., & Haykowsky, M. (2012). Cardiopulmonary function and age-related decline across the breast cancer survivorship continuum. *Journal of Clinical Oncology: Official Journal of the American Society of Clinical Oncology*, *30*(20), 2530–2537. https://doi.org/10.1200/JCO.2011.39.9014

Jones, L. W., Fels, D. R., West, M., Allen, J. D., Broadwater, G., Barry, W. T., Wilke, L. G., Masko, E., Douglas, P. S., Dash, R. C., Povsic, T. J., Peppercorn, J., Marcom, P. K., Blackwell, K. L., Kimmick, G., Turkington, T. G., & Dewhirst, M. W. (2013). Modulation of circulating angiogenic factors and tumor biology by aerobic training in breast cancer patients receiving neoadjuvant chemotherapy. *Cancer Prevention Research (Philadelphia, Pa.)*, *6*(9), 925–937. https://doi.org/10.1158/1940-6207.CAPR-12-0416

Jones, L. W., Viglianti, B. L., Tashjian, J. A., Kothadia, S. M., Keir, S. T., Freedland, S. J., Potter, M. Q., Moon, E. J., Schroeder, T., Herndon, J. E., & Dewhirst, M. W. (2010). Effect of aerobic exercise on tumor physiology in an animal model of human breast cancer. *Journal of Applied Physiology (Bethesda, Md.: 1985)*, *108*(2), 343–348. https://doi.org/10.1152/japplphysiol.00424.2009

Kilgour, R. D., Vigano, A., Trutschnigg, B., Hornby, L., Lucar, E., Bacon, S. L., & Morais, J. A. (2010). Cancer-related fatigue: The impact of skeletal muscle mass and strength in patients with advanced cancer. *Journal of Cachexia, Sarcopenia and Muscle*, *1*(2), 177–185. https://doi.org/10.1007/s13539-010-0016-0

Kindig, C. A., Musch, T. I., Basaraba, R. J., & Poole, D. C. (1999). Impaired capillary hemodynamics in skeletal muscle of rats in chronic heart failure. *Journal of Applied Physiology (Bethesda, Md.: 1985)*, *87*(2), 652–660. https://doi.org/10.1152/jappl.1999.87.2.652

Kindig, C. A., Walsh, B., Howlett, R. A., Stary, C. M., & Hogan, M. C. (2005). Relationship between intracellular PO2 recovery kinetics and fatigability in isolated single frog myocytes. *Journal of Applied Physiology (Bethesda, Md.: 1985)*, *98*(6), 2316–2319. https://doi.org/10.1152/japplphysiol.00355.2004

Klassen, O., Schmidt, M. E., Ulrich, C. M., Schneeweiss, A., Potthoff, K., Steindorf, K., & Wiskemann, J. (2017). Muscle strength in breast cancer patients receiving different treatment regimes. *Journal of Cachexia, Sarcopenia and Muscle*, *8*(2), 305–316. https://doi.org/10.1002/jcsm.12165

Koga, S., Poole, D. C., Ferreira, L. F., Whipp, B. J., Kondo, N., Saitoh, T., Ohmae, E., & Barstow, T. J. (2007). Spatial heterogeneity of quadriceps muscle deoxygenation kinetics during cycle exercise. *Journal of Applied Physiology (Bethesda, Md.: 1985)*, *103*(6), 2049–2056. https://doi.org/10.1152/japplphysiol.00627.2007

Koivula, T., Uurasmaa, T.-M., Han, C., Maaniitty, T., Latifi, S., Lempiäinen, S., Kalliokoski, K., Sundberg, C. J., Rundqvist, H., Anttila, K., Minn, H., Knuuti, J., & Heinonen, I. (2024). Myocardial blood flow in newly diagnosed breast cancer patients at rest and during exercise. *iScience*, *27*(11), 111081. https://doi.org/10.1016/j.isci.2024.111081

Larsen, F. J., Schiffer, T. A., Borniquel, S., Sahlin, K., Ekblom, B., Lundberg, J. O., & Weitzberg, E. (2011). Dietary inorganic nitrate improves mitochondrial efficiency in humans. *Cell Metabolism*, *13*(2), 149–159. https://doi.org/10.1016/j.cmet.2011.01.004

Macdonald, M., Pedersen, P. K., & Hughson, R. L. (1997). Acceleration of VO2 kinetics in heavy submaximal exercise by hyperoxia and prior high-intensity exercise. *Journal of Applied Physiology (Bethesda, Md.: 1985)*, *83*(4), 1318–1325. https://doi.org/10.1152/jappl.1997.83.4.1318

Mader, T., Chaillou, T., Alves, E. S., Jude, B., Cheng, A. J., Kenne, E., Mijwel, S., Kurzejamska, E., Vincent, C. T., Rundqvist, H., & Lanner, J. T. (2022). Exercise reduces intramuscular stress and counteracts muscle weakness in mice with breast cancer. *Journal of Cachexia, Sarcopenia and Muscle*, *13*(2), 1151–1163. https://doi.org/10.1002/jcsm.12944

Majmudar, N. G., Robson, S. C., & Ford, G. A. (2000). Effects of the menopause, gender, and estrogen replacement therapy on vascular nitric oxide activity. *The Journal of Clinical Endocrinology and Metabolism*, *85*(4), 1577–1583. https://doi.org/10.1210/jcem.85.4.6530

McAllister, R. M., Newcomer, S. C., & Laughlin, M. H. (2008). Vascular nitric oxide: Effects of exercise training in animals. *Applied Physiology, Nutrition, and Metabolism = Physiologie Appliquee, Nutrition Et Metabolisme*, *33*(1), 173–178. https://doi.org/10.1139/H07-146

McCullough, D. J., Nguyen, L. M.-D., Siemann, D. W., & Behnke, B. J. (2013). Effects of exercise training on tumor hypoxia and vascular function in the rodent preclinical orthotopic prostate cancer model. *Journal of Applied Physiology (Bethesda, Md.: 1985)*, *115*(12), 1846–1854. https://doi.org/10.1152/japplphysiol.00949.2013

McCullough, D. J., Stabley, J. N., Siemann, D. W., & Behnke, B. J. (2014). Modulation of blood flow, hypoxia, and vascular function in orthotopic prostate tumors during exercise. *Journal of the National Cancer Institute*, *106*(4), dju036. https://doi.org/10.1093/jnci/dju036

Nayeem, M. A., Ponnoth, D. S., Boegehold, M. A., Zeldin, D. C., Falck, J. R., & Mustafa, S. J. (2009). High-salt diet enhances mouse aortic relaxation through adenosine A2A receptor via CYP epoxygenases. *American Journal of Physiology. Regulatory, Integrative and Comparative Physiology*, *296*(3), R567-574. https://doi.org/10.1152/ajpregu.90798.2008

Neefjes, E. C. W., van den Hurk, R. M., Blauwhoff-Buskermolen, S., van der Vorst, M. J. D. L., Becker-Commissaris, A., de van der Schueren, M. A. E., Buffart, L. M., & Verheul, H. M. W. (2017). Muscle mass as a target to reduce fatigue in patients with advanced cancer. *Journal of Cachexia, Sarcopenia and Muscle*, *8*(4), 623–629. https://doi.org/10.1002/jcsm.12199

Poole, D. C., & Musch, T. I. (2023). Capillary-Mitochondrial Oxygen Transport in Muscle: Paradigm Shifts. *Function (Oxford, England)*, *4*(3), zqad013. https://doi.org/10.1093/function/zqad013

Poole, D. C., Richardson, R. S., Haykowsky, M. J., Hirai, D. M., & Musch, T. I. (2018). Exercise limitations in heart failure with reduced and preserved ejection fraction. *Journal of Applied Physiology (Bethesda, Md.: 1985)*, *124*(1), 208–224. https://doi.org/10.1152/japplphysiol.00747.2017

Prado, C. M. M., Baracos, V. E., McCargar, L. J., Reiman, T., Mourtzakis, M., Tonkin, K., Mackey, J. R., Koski, S., Pituskin, E., & Sawyer, M. B. (2009). Sarcopenia as a determinant of chemotherapy toxicity and time to tumor progression in metastatic breast cancer patients receiving capecitabine treatment. *Clinical Cancer Research: An Official Journal of the American Association for Cancer Research*, *15*(8), 2920–2926. https://doi.org/10.1158/1078-0432.CCR-08-2242

Reckelhoff, J. F. (1997). Age-related changes in renal hemodynamics in female rats: Role of multiple pregnancy and NO. *The American Journal of Physiology*, *272*(6 Pt 2), R1985-1989. https://doi.org/10.1152/ajpregu.1997.272.6.R1985

Rentz, L. E., Whetsell, M., Clayton, S. A., Mizener, A. D., Holásková, I., Chapa, M. G., Hoblitzell, E. H., Eubank, T. D., & Pistilli, E. E. (2023). Sexual Dimorphism of Skeletal Muscle in a Mouse Model of Breast Cancer: A Functional and Molecular Analysis. *bioRxiv: The Preprint Server for Biology*, 2023.06.07.544049. https://doi.org/10.1101/2023.06.07.544049

Smeda, M., Kieronska, A., Adamski, M. G., Proniewski, B., Sternak, M., Mohaissen, T., Przyborowski, K., Derszniak, K., Kaczor, D., Stojak, M., Buczek, E., Jasztal, A., Wietrzyk, J., & Chlopicki, S. (2018). Nitric oxide deficiency and endothelial-mesenchymal transition of pulmonary endothelium in the progression of 4T1 metastatic breast cancer in mice. *Breast Cancer Research: BCR*, *20*(1), 86. https://doi.org/10.1186/s13058-018-1013-z

Stamler, J. S., & Meissner, G. (2001). Physiology of nitric oxide in skeletal muscle. *Physiological Reviews*, *81*(1), 209–237. https://doi.org/10.1152/physrev.2001.81.1.209

Stephens, N. A., Gray, C., MacDonald, A. J., Tan, B. H., Gallagher, I. J., Skipworth, R. J. E., Ross, J. A., Fearon, K. C. H., & Greig, C. A. (2012). Sexual dimorphism modulates the impact of cancer cachexia on lower limb muscle mass and function. *Clinical Nutrition (Edinburgh, Scotland)*, *31*(4), 499–505. https://doi.org/10.1016/j.clnu.2011.12.008

Sung, H., Ferlay, J., Siegel, R. L., Laversanne, M., Soerjomataram, I., Jemal, A., & Bray, F. (2021). Global Cancer Statistics 2020: GLOBOCAN Estimates of Incidence and Mortality Worldwide for 36 Cancers in 185 Countries. *CA: A Cancer Journal for Clinicians*, *71*(3), 209–249. https://doi.org/10.3322/caac.21660

Villaseñor, A., Ballard-Barbash, R., Baumgartner, K., Baumgartner, R., Bernstein, L., McTiernan, A., & Neuhouser, M. L. (2012). Prevalence and prognostic effect of sarcopenia in breast cancer survivors: The HEAL Study. *Journal of Cancer Survivorship: Research and Practice*, *6*(4), 398–406. https://doi.org/10.1007/s11764-012-0234-x

Walley, K. R. (1996). Heterogeneity of oxygen delivery impairs oxygen extraction by peripheral tissues: Theory. *Journal of Applied Physiology (Bethesda, Md.: 1985)*, *81*(2), 885–894. https://doi.org/10.1152/jappl.1996.81.2.885

Weber, R. E., Schulze, K. M., Kenney, N. J., Scheuermann, B. C., Kunkel, O. N., Ade, C. J., Musch, T. I., Behnke, B. J., & Poole, D. C. (2025). Tumor bearing in untreated breast cancer decreases exercise tolerance without lowering maximal oxygen uptake in rats. *American Journal of Cancer Research*, *15*(2), 487–500. https://doi.org/10.62347/QCCZ2316

Westerlind, K. C., McCarty, H. L., Schultheiss, P. C., Story, R., Reed, A. H., Baier, M. L., & Strange, R. (2003). Moderate exercise training slows mammary tumour growth in adolescent rats. *European Journal of Cancer Prevention: The Official Journal of the European Cancer Prevention Organisation (ECP)*, *12*(4), 281–287. https://doi.org/10.1097/00008469-200308000-00007

Wilson, H. E., Rhodes, K. K., Rodriguez, D., Chahal, I., Stanton, D. A., Bohlen, J., Davis, M., Infante, A. M., Hazard-Jenkins, H., Klinke, D. J., Pugacheva, E. N., & Pistilli, E. E. (2019). Human Breast Cancer Xenograft Model Implicates Peroxisome Proliferator-activated Receptor Signaling as Driver of Cancer-induced Muscle Fatigue. *Clinical Cancer Research: An Official Journal of the American Association for Cancer Research*, *25*(7), 2336–2347. https://doi.org/10.1158/1078-0432.CCR-18-1565

Wilson, H. E., Stanton, D. A., Rellick, S., Geldenhuys, W., & Pistilli, E. E. (2021). Breast cancer-associated skeletal muscle mitochondrial dysfunction and lipid accumulation is reversed by PPARG. *American Journal of Physiology. Cell Physiology*, *320*(4), C577–C590. https://doi.org/10.1152/ajpcell.00264.2020

Table 4.1. *Interstitial pressure of O_2 kinetics parameters during contractions.*

	Healthy (*n* = 9)	**Breast Cancer** (*n* = 9)	***P***
$PO_{2(BL)}$, mmHg	27.8 ± 2.5	31.9 ± 1.6 *****	**0.002**
$\Delta PO_{2(CONTRACT)}$, mmHg	12.0 ± 2.4	12.3 ± 2.1	0.758
TD, s	12 ± 2	9 ± 3 *****	**0.019**
T, s	36 ± 12	30 ± 9	0.268
$PO_{2(NADIR)}$, mmHg	15.8 ± 1.8	19.5 ± 2.4 *****	**0.003**
MRT, s	48 ± 13	38 ± 11	0.118
$PO_{2(END-CONTRACT)}$, mmHg	15.8 ± 1.8	19.5 ± 2.4 *****	**0.003**
$\Delta PO_2/T$, mmHg·s	0.4 ± 0.2	0.5 ± 0.2	0.370

Data are means ± SD. *n*, number of rats, $PO_{2(BL)}$, PO_2 at baseline (averaged -30-0 s); $\Delta PO_{2(CONTRACT)}$, amplitude during contractions; TD, time delay; T, time to reach 63% of the kinetic response; $PO_{2(NADIR)}$, lowest recorded $PO_2$is during contractions; MRT, mean response time; $PO_{2(END-CONTRACT)}$, $PO_2$is at the end contractions (averaged 170-180 s). *****$P < 0.05$ vs. Healthy; Analyzed via unpaired Student's t-test.

Table 4.2. *Interstitial pressure of O_2 kinetics parameters during SNP contractions.*

	Healthy (*n* = 7)	**Breast Cancer (*n* = 9)**	***P***
$PO_{2(BL)}$, mmHg	48.8 ± 4.1 **¥**	44.4 ± 5.3 **¥**	0.113
$\Delta PO_{2(CONTRACT)}$, mmHg	14.9 ± 4.6	21.1 ± 5.8 ***¥**	**0.047**
TD, s	18 ± 9	7 ± 4 *	**0.007**
T, s	68 ± 23 **¥**	48 ± 17 **¥**	0.084
$PO_{2(NADIR)}$, mmHg	33.9 ± 6.4 **¥**	23.3 ± 6.7 *	**0.010**
MRT, s	86 ± 26 **¥**	55 ± 19 ***¥**	**0.022**
$PO_{2(END\text{-}CONTRACT)}$, mmHg	33.9 ± 6.4 **¥**	23.3 ± 6.7 *	**0.010**
ΔPO_2/T, mmHg·s	0.3 ± 0.2	0.5 ± 0.3 *	**0.054**

Data are means ± SD. *n*, number of rats; SNP, sodium nitroprusside; $PO_{2(BL)}$, $PO_2$is at baseline (averaged 330-360 s); $\Delta PO_{2(CONTRACT)}$, amplitude during contractions; TD, time delay; T, time to reach 63% of the kinetic response; $PO_{2(NADIR)}$, lowest recorded $PO_2$is during contractions; MRT, mean response time; $PO_{2(END\text{-}CONTRACT)}$, $PO_2$is at the end contractions (averaged 170-180 s). *P ≤ 0.05 vs. Healthy; ¥ P < 0.05 vs. control contractions within group. Analyzed via unpaired Student's t-test.

Table 4.3. *Interstitial pressure of O_2 kinetics parameters during L-NAME contractions.*

	Healthy (n = 7)	**Breast Cancer** (n = 5)	***P***
$PO_{2(BL)}$, mmHg	28.6 ± 6.7 #	30.9 ± 4.8 #	0.556
$\Delta PO_{2(CONTRACT)}$, mmHg	15.8 ± 6.4	20.4 ± 3.0 **¥**	0.214
TD, s	2 ± 2 **#¥**	6 ± 3 *****	**0.028**
T, s	22 ± 12 #	26 ± 15	0.644
$PO_{2(NADIR)}$, mmHg	12.8 ± 4.5 #	10.6 ± 4.1 **#¥**	0.465
MRT, s	23 ± 4 **#¥**	21 ± 4 **#¥**	0.417
$PO_{2(END\text{-}CONTRACT)}$, mmHg	16.2 ± 2.3 #	15.1 ± 4.5 **#¥**	0.523
ΔPO_2/T, mmHg·s	1.3 ± 0.9	1.0 ± 0.5	0.859

Data are means ± SD. *n*, number of rats, N^{ω}-nitro-L-arginine methyl ester (L-NAME); $PO_{2(BL)}$, $PO_2$is at baseline (averaged 330-360 s); $\Delta PO_{2(CONTRACT)}$, amplitude during contractions; TD, time delay; T, time to reach 63% of the kinetic response; $PO_{2(NADIR)}$, lowest recorded $PO_2$is during contractions; MRT, mean response time; $PO_{2(END\text{-}CONTRACT)}$, $PO_2$is at the end contractions (averaged 170-180 s). #P < 0.05 vs. SNP contractions within group; ¥P < 0.05 vs. control contractions within group. Analyzed via unpaired Student's t-test.

Figure 4.1. *Cardiac and muscle mass relative to tumor load.*

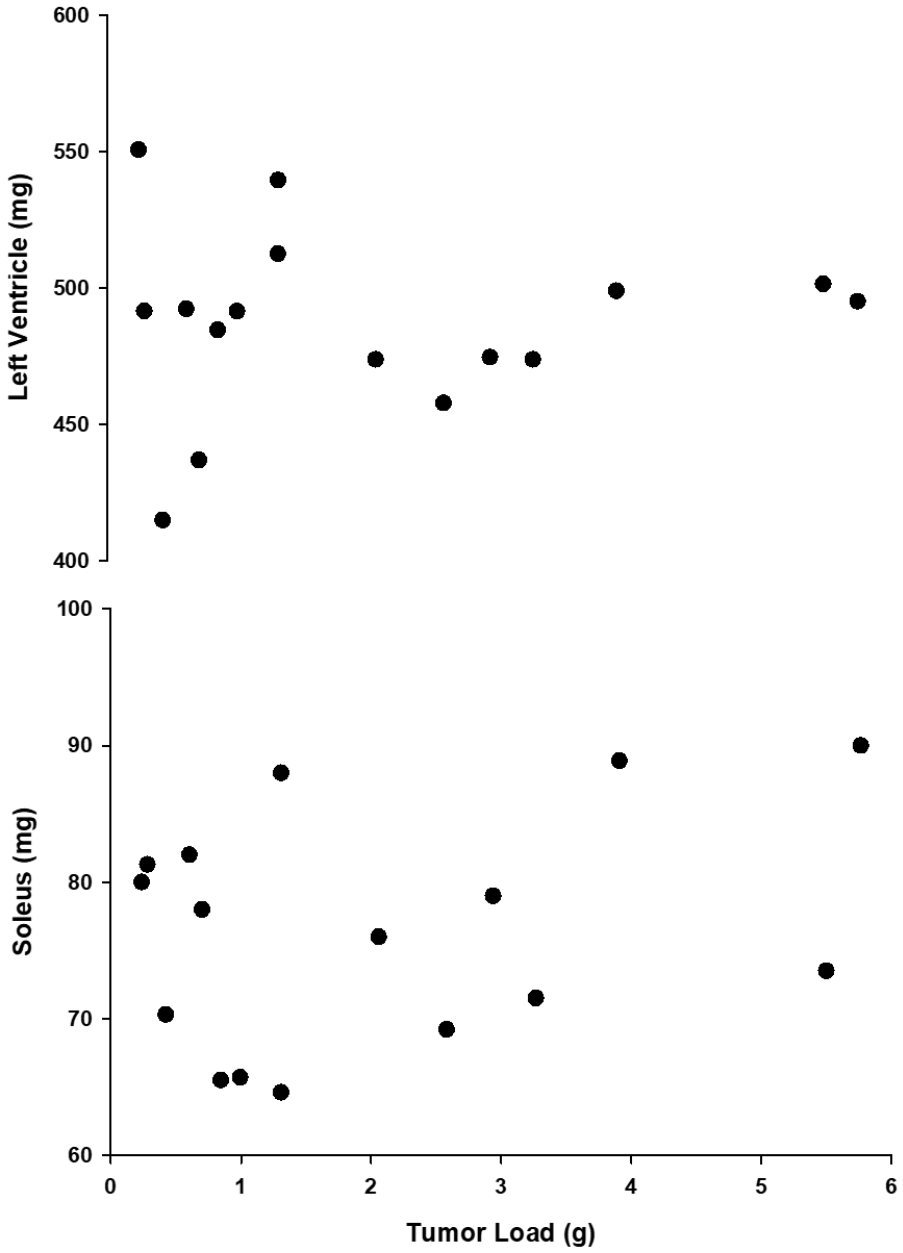

There were no significant correlations between left ventricle (r = 0.059, P = 0.829) or soleus weight (r = 0.220, P = 0.413) and total tumor load in breast cancer rats (*n*=16).

Figure 4.2. *Interstitial pressure of O_2 during control contractions.*

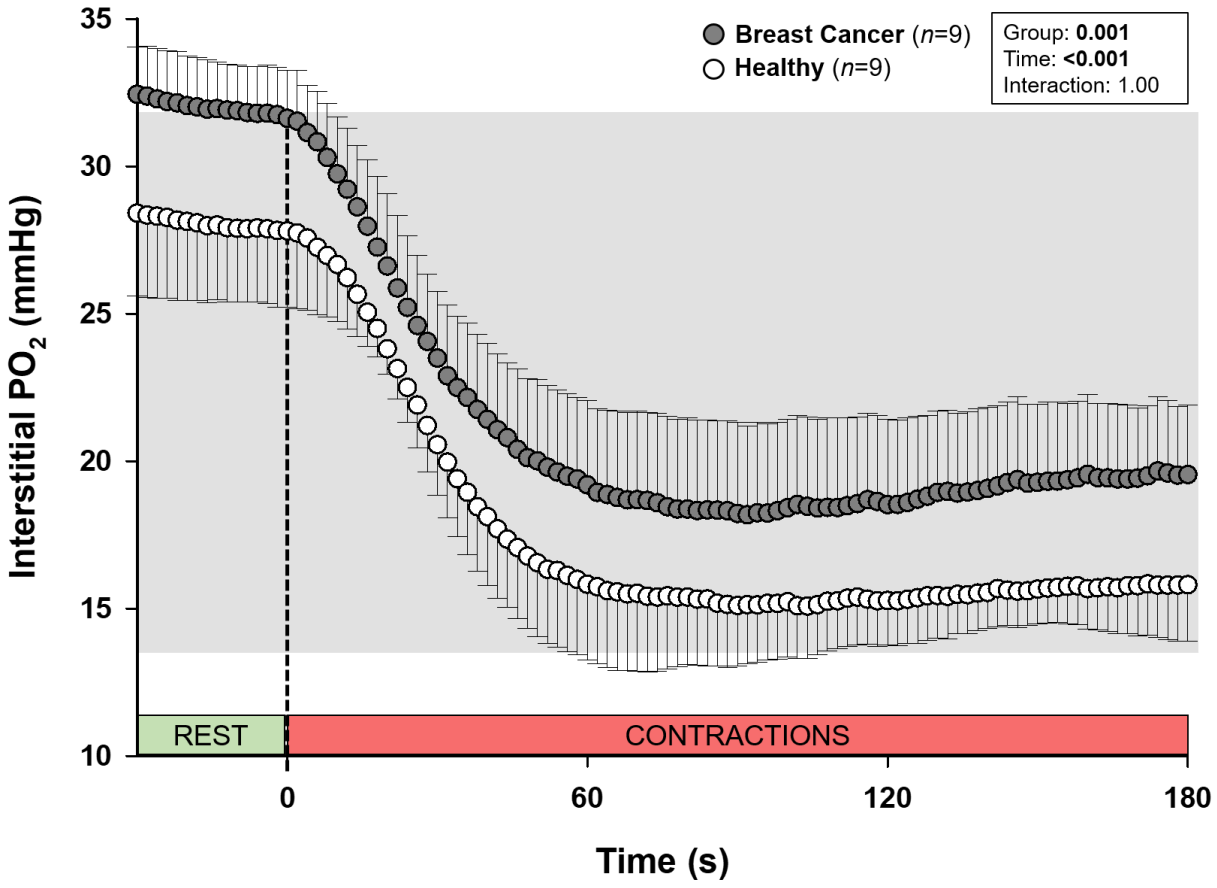

Breast cancer rats, *n*=9; healthy, *n*=9. Data are means ± SD. Analyzed via two-way repeated-measures ANOVA. The dashed line represents the onset of contractions. The gray shaded area represents a statistically significant (P<0.05) increase in resting and contracting PO2is in breast cancer versus healthy rats.

Figure 4.3. *Interstitial pressure of O_2 during SNP conditions.*

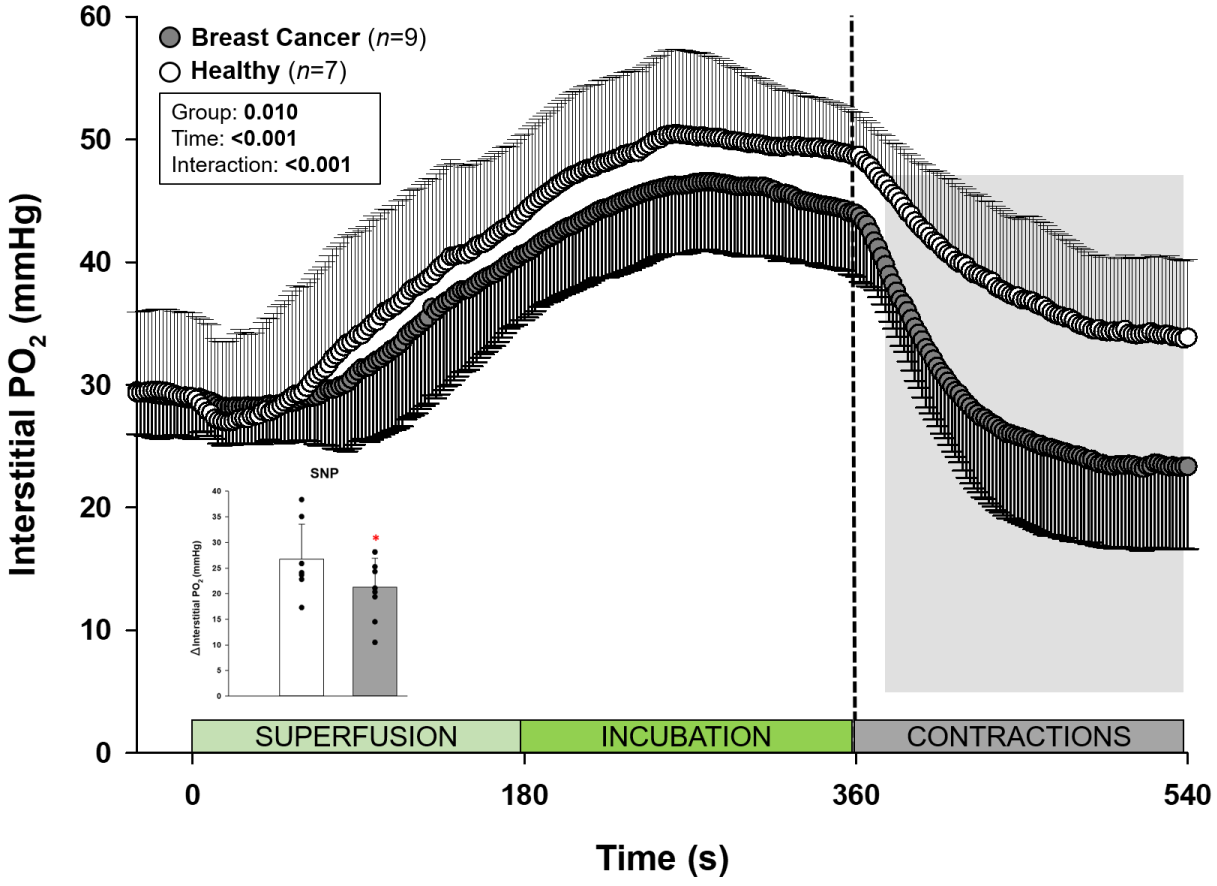

Breast cancer rats, *n*=9; healthy, *n*=7. Sodium nitroprusside (SNP) was superfused during 0-180s (3 ml; 300 μM) and incubation 180-360s was allowed for the stabilization of $PO_2$is. The dashed line represents the onset of contractions. The gray shaded area represents a statistically significant ($P<0.05$) increase in contracting $PO_2$is in breast cancer versus healthy rats (400-540 s). **Inset:** amplitude increase during SNP superfusion. BC rats had a lower amplitude increase (ΔInterstitial PO_2) during SNP superfusion versus HC rat ($P=0.039$). Data are means ± SD. Analyzed via two-way repeated-measures ANOVA.

Figure 4.4. *Interstitial pressure of O_2 during L-NAME conditions.*

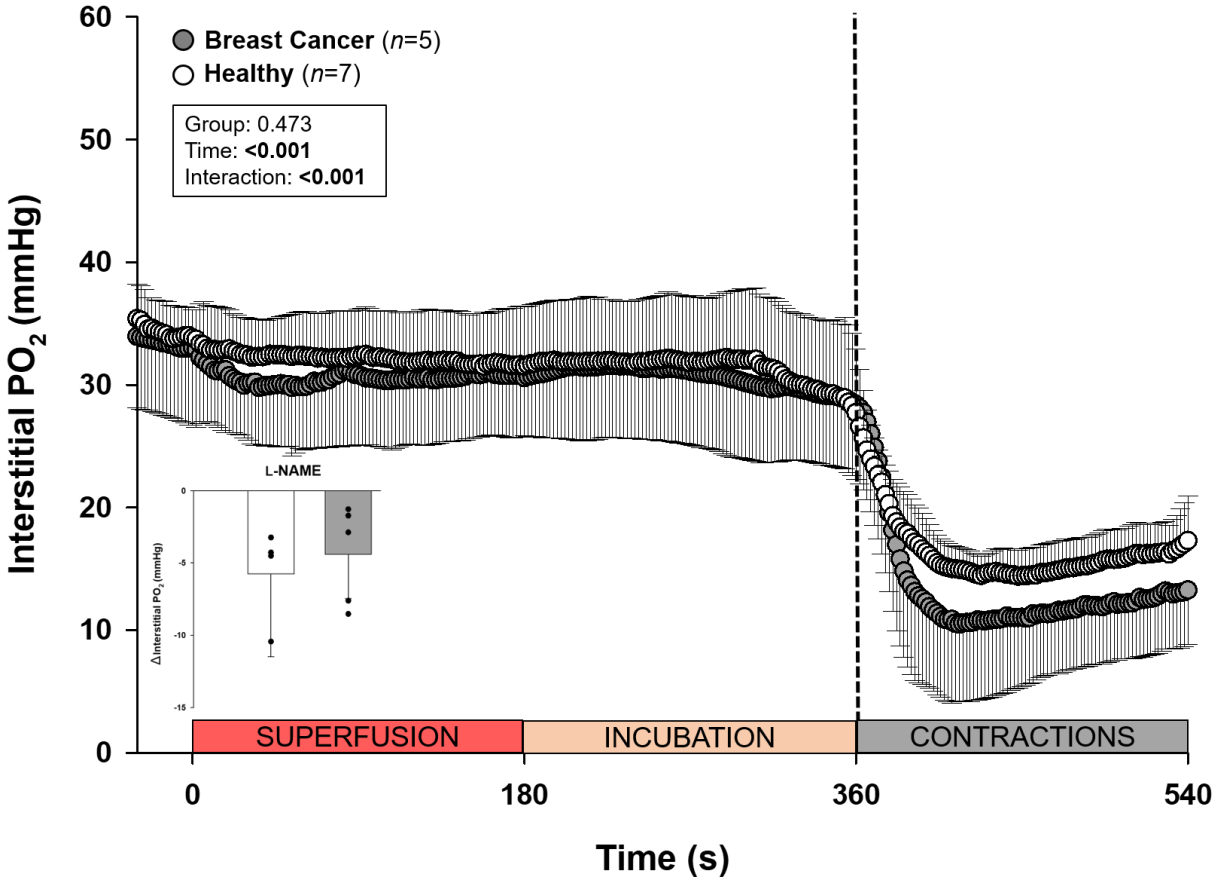

Breast cancer rats, *n*=9; healthy control, *n*=7. L-nitro arginine methyl ester (L-NAME) was superfused during 0-180s (3.5 ml; 1.5mm) and incubation 180-360s was allowed for the stabilization of $PO_2$is**.** The dashed line represents the onset of contractions. **Inset:** amplitude decrease during L-NAME superfusion. There was no significant difference in ΔInterstitial PO_2 during L-NAME superfusion between groups ($P > 0.05$). Data are means ± SD. Analyzed via two-way repeated-measures ANOVA.

Figure 4.5. *Interstitial pressure of O_2 during contractions in all conditions.*

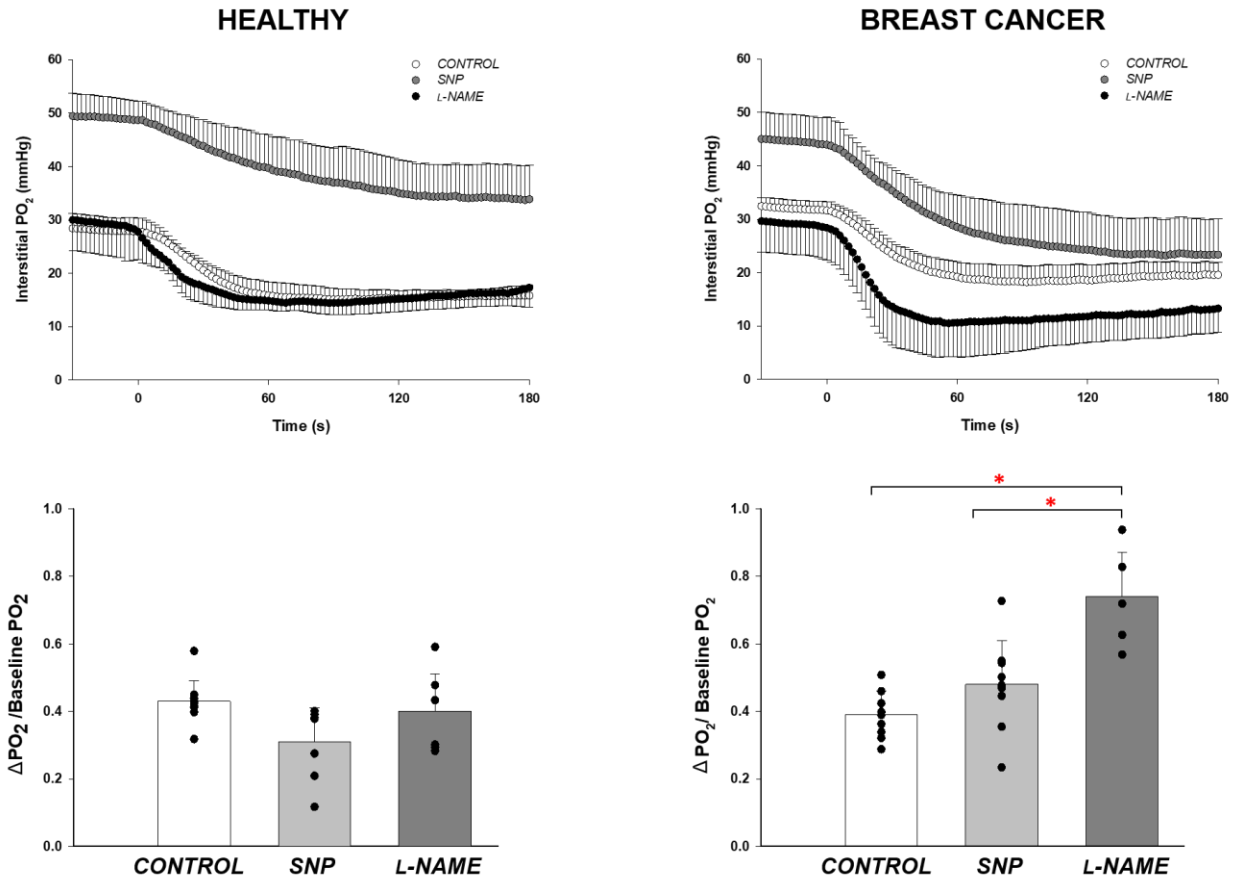

Top: (left) healthy $PO_2$is profiles during control (n=9), SNP (n=7), and L-NAME (n=7) conditions; (right) breast cancer $PO_2$is profiles during control (n=9), SNP (n=9), and L-NAME (n=5) conditions. Bottom: normalized $PO_2$is amplitude during contractions to baseline $PO_2$is in healthy (left) and breast cancer (right) rats. Control, open bar; sodium nitroprusside (SNP, 300 µM), light grey bar; N^{ω}-nitro-L-arginine methyl ester (L-NAME, 1.5 mM), dark grey bar. Data are means ± SD with individual data points. Analyzed via unpaired Student's t-test. *P < 0.01 versus control within condition.

Chapter 5 - Conclusions

The overall aim of the studies presented in this dissertation was to investigate the role that nitric oxide (NO)-soluble guanylyl cyclase (sGC) signaling has in regulating skeletal muscle O_2 blood flow ($\dot{Q}O_2$)-to-mitochondrial O_2 demand ($\dot{V}O_2$) matching and control of interstitial pressure of O_2 ($PO_2$is) kinetics in both heart failure (HF) and breast cancer (BC). In Chapter 2 we used a model of heart failure with moderately reduced ejection fraction (HFmrEF), a previously understudied phenotype of cardiovascular disease, to investigate the impact of increased soluble guanylyl cyclase (sGC) sensitivity (via sGC stimulators) on exercise capacity and skeletal muscle $PO_2$is. We found that sGC stimulators improve exercise capacity due, in part, to increased sensitivity to NO donation within the skeletal muscle vasculature and improved $PO_2$is kinetics. In Chapter 3 we established that BC, as an isolated condition, does not limit resting cardiac function or maximal O_2 uptake during exercise ($\dot{V}O_2$max), but does reduce exercise economy. In Chapter 4, we identified impaired skeletal muscle $\dot{Q}O_2$-to-$\dot{V}O_2$ matching and reduced NO sensitivity as potential mediators of exercise intolerance in therapy-naïve breast cancer. These findings provide evidence that within the skeletal muscle microvasculature dysfunctional NO signaling may play an important role in shaping the bi-directional relationship between heart failure and breast cancer.

Appendix A - Curriculum Vitae

EDUCATION

2025 Ph.D.* Kansas State University Concentration*:* Kinesiology
Dissertation: *Skeletal Muscle Oxygenation in Both Heart Failure and Breast Cancer: Mechanisms and Therapeutic Insights*

2020 M.S.* Kansas State University Concentration: Kinesiology
Thesis: *Effects of soluble guanylyl cyclase activation on skeletal muscle microcirculatory oxygen exchange in rats with heart failure with reduced ejection fraction*

2019 B.S.* Kansas State University Major: Life Sciences
McNair Scholar's Program Thesis: *Role of adenosine triphosphate-sensitive potassium channel function in exercise tolerance*
***First generation student**

PROFESSIONAL EXPERIENCE

2023 – 2025 **Johnson Cancer Research Center Fellow**
Manhattan, KS Cardiorespiratory Exercise Physiology Laboratory
Cardiovascular and Tumor Physiology Laboratory
Department of Kinesiology, Anatomy & Physiology
Kansas State University

2019 – 2024 **Graduate Teaching & Research Assistant**
Manhattan, KS Anatomy & Physiology, Exercise Physiology, Biobehavioral Basis of Physical Activity, Research Methods, Exercise Testing and Prescription, Advanced Cardiovascular Physiology
Department of Kinesiology, Anatomy and Physiology
Kansas State University

2016 – 2019 **McNair Scholar & Undergraduate Research Assistant**
Manhattan, KS Cardiopulmonary Exercise Physiology Laboratory
College of Veterinary Medicine
Department of Kinesiology, Anatomy & Physiology
Kansas State University

RESEARCH INTERESTS

An overarching theme of my research interests centers on investigating mechanisms responsible for altered blood flow and oxygen delivery under pathophysiological conditions. Specifically, I am interested in:

- The mechanistic bases for muscle vascular and contractile dysfunction in heart failure and breast cancer, as isolated and comorbid conditions.
- The role that nitric oxide-soluble guanylyl cyclase plays in oxygen transport to skeletal muscle in heart failure and breast cancer.
- Pharmaceutical and exercise strategies to improve exercise tolerance early in a disease continuum and prior to severe cardiovascular decline.

This research involves numerous *in vivo* and *in vitro* methodologies, such as:

- Establishing rodent models of pathophysiology:
    - Cell culture techniques and intraductal breast cancer cell injections to model intraductal carcinoma *in situ*
    - Left coronary artery ligation for the myocardial infarction model of heart failure, confirmed with left ventricular echocardiography

- Exercise measurements:
    - Maximal oxygen uptake during exercise, critical speed, time to exhaustion.

- Fluorescent microsphere technique
    - Infusion of fluorescent labeled microspheres into the arterial circulation and subsequent fluorometric assays to determine skeletal muscle blood flow at rest and during exercise.

- Phosphorescence quenching
    - Microinjection of oxyphor G4 to measure of O_2 flux at the capillary-myocyte interface to investigate the consequences of structural and functional perturbations on the relationships between capillary hemodynamics and muscle O_2 consumption.

- Intravital Microscopy
    - Gated phased-light technique for high resolution light microscopy that enables simultaneous measurement of all major structural (capillary volume density, diameter, surface area) and functional (proportion of capillaries flowing, RBC flux, RBC velocity, hematocrit) variables in muscle at rest.

PROFESSIONAL SOCIETIES

2019 – Present	American Physiological Society, Member
2020 – Present	American College of Sports Medicine, Member
2023 – Present	American Heart Association, Member
2024 – Present	International Cardio-Oncology Society, Member

HONORS & AWARDS

2019 Kansas State University First Learning Award *($2,000)*

2020 American Physiological Society, Integrative Physiology of Exercise Conference, Oral Presentation Award *($500)*

2020 Kansas State Graduate Research Forum, Oral Presentation Award, 2nd Place *($250)*

2021 Kansas State Graduate Research Forum, Oral Presentation Award *($250)*

2022 Kansas State Graduate Research Consortium, Oral Presentation Award, 1st Place *($500)*

2022 Outstanding Teaching Award, Department of Kinesiology, Kansas State

2023 Research in the State Poster Competition, Kansas State University, 1st Place *($500)*

2023 Sigma Xi Research Honor Society, Research Award *($100)*

2023 Johnson Cancer Research Center Summer Research Award, Kansas State University *($7,500)*

2024 Kansas State Health and Human Sciences Forum, 1st Place Poster Award (*$250*)

2024 Capitol Graduate Research Summit, Topeka, Kansas, 1st Place Poster Presentation *($750)*

EXTRAMURAL FUNDING

2025-2026 Johnson Cancer Research Center Fellowship*, PI: **Weber**
$35,000
Investigating the Bi-Directional Relationship Between Heart Failure and Breast Cancer: Mechanisms and Pharmaceutical Targets of O_2 Transport Dysfunction
Did not accept.

2024-2026 College of Veterinary Medicine SMILE Award, PI: **Weber**/Poole
$20,000
Elucidating the Intersection Between Cardiovascular Disease, Cancer, and Oxygen Transport: Mechanisms and Therapeutic Approaches

2024-2025 Johnson Cancer Research Center Fellowship, PI: **Weber**
$35,000
Investigating the Bi-Directional Relationship Between Heart Failure and Breast Cancer: Mechanisms and Pharmaceutical Targets of O_2 Transport Dysfunction

2021-2023 College of Veterinary Medicine SMILE Award, PI: Poole/**Weber**

$36,000
Soluble Guanylyl Cyclase Activator and Stimulator Effect on Skeletal Muscle Oxygenation in Male and Female Rats with Heart Failure.

Not Funded

2024 NIH NRSA Individual Predoctoral Fellowship to Promote Diversity in Health-Related Research (Parent F31-Diversity)
$45,873
Elucidating Mechanisms of Exercise Intolerance and Skeletal Muscle Dysfunction in Breast Cancer and Heart Failure

2021 Partnership for Clean Competition Predoctoral Fellowship
$200,000
Novel Approaches to Enhance Skeletal Muscle Oxygenation and Performance

2021 LabFront PhysioQ Summer Research Grant
$5,000
Effect of COVID-19 Mask on the Cardiorespiratory Response to Exercise

EDITORIAL & REVIEWING ACTIVITY

Microcirculation, Reviewer
Journal of Experimental and Laboratory Medicine, Reviewer

PRESENTATIONS & SEMINARS

Oral Presentations

Master's Thesis, Effects of soluble guanylyl cyclase activation on skeletal muscle microcirculatory oxygen exchange in rats with heart failure with reduced ejection fraction. November 11, 2020.

Integrative Physiology of Exercise Conference, Effects of soluble guanylyl cyclase activator on skeletal muscle capillary hemodynamics in heart failure rats with reduced ejection fraction, November 13, 2020. (Oral presentation award, $500)

Kansas State University College of Veterinary Medicine Seminar Series, Oxygen Transport Pathway in Health & Disease. December 5, 2023.

*TRIO McNair Scholars Program Panelist***,** Applying for Graduate Programs: What's Next? October 16, 2024.

Kansas State University College of Veterinary Medicine Seminar Series, Oxygen Transport Dysfunction in Pulmonary Hypertension and Breast Cancer. October 22, 2024.

Integrative Physiology of Exercise Conference, Effect of breast cancer on maximal oxygen uptake and exercise tolerance in female rats, November 22, 2024.

Centre for Heart Lung Innovation, St. Paul's Hospital, Vancouver, BC, Skeletal Muscle Oxygen Delivery in Breast Cancer, January 8, 2024.

University of Michigan, School of Kinesiology, Nitric Oxide-Mediated Skeletal Muscle Oxygen Delivery in Breast Cancer, January 16, 2024.

Poster Presentations

Experimental Biology: Contracting Skeletal Muscle Oxygen Pressures in Rats with Heart Failure: Impact of Soluble Guanylyl Cyclase Activator. April 4, 2022.

*Experimental Biology***:** ATP-sensitive K+ Channel Inhibition Diminishes Critical Speed in Male and Female Rats but $\dot{V}O_2$max in Females Only. April 12, 2021.

American Physiology Summit: Increased nitric oxide-soluble guanylyl cyclase signaling improves endurance capacity and contracting skeletal muscle oxygenation in healthy female rats. April 21, 2023.

American College of Sports Medicine: Nitric Oxide-soluble guanylyl cyclase activator increases endurance capacity and skeletal muscle oxygenation in male rats. May 31, 2023.

American Physiology Summit: Tumor Oxygenation in an Orthotopic Model of Breast Cancer: Impact of Dietary Nitrate Supplementation. April 5, 2024.

University Events

Kansas State University Graduate School Research, Arts, and Discovery Forum: Effects of Soluble Guanylyl Cyclase Activator on Microcirculatory Hemodynamics in Rat Skeletal Muscle. March 31, 2021. (Oral Presentation Award)

3 Minute Thesis Competition: Soluble guanylyl cyclase signaling in health and disease: Impact on oxygen transport. February 12, 2022.

Research, Scholarly and Creative Activities, and Research, Scholarly and Creative Activities, and Design Forum: Oxygen transport and downstream nitric oxide signaling. April 14, 2022. (Poster Award)

Kansas State University Graduate School Research, Arts, and Discovery Forum: Novel pharmaceuticals to improve exercise capacity in heart failure. March 8, 2023.

Kansas State University Graduate School Research, Arts, and Discovery Forum: Tumor oxygenation in an orthotopic model of intraductal breast cancer. April 12, 2023. (Poster Award)

Research and the State: Breast Cancer: Can it be beet? October 24, 2023. (Poster Award)

Kansas State University Graduate School Research, Arts, and Discovery Forum: Tumor pressure of oxygen in breast cancer rats: potential treatment avenues. April 11, 2024. (Poster Award)

BIBLIOGRAPHY (18 total; 2 first author, 1 in review, 2 in preparation; H-index: 8)

1. **Weber RE,** Schulze KM, Kenney NJ, Scheuermann BC, Kunkel ON, Ade CJ, Musch TI, Behnke BJ, Poole DC. Tumor bearing in untreated breast cancer decreases exercise tolerance without lowering maximal oxygen uptake in rats. Am J Cancer Res. 2025. PMID: 40084375.

2. **Weber RE,** Schulze KM, McCoach TE, Hageman KS, Horn AG, White ZJ, Sandner P, Hall SE, Behnke BJ, Musch TI, Poole DC. "Effects of soluble guanylyl cyclase stimulator on skeletal muscle oxygenation and exercise capacity in heart failure with mildly reduced ejection fraction" Exp Physiol, In review, 2025.

3. **Weber RE,** Schulze KM, Kenney NJ, Scheuermann BC, Kunkel ON, Ade CJ, Musch TI, Behnke BJ, Poole DC. Skeletal muscle oxygen pressure in breast cancer rats: role of nitric oxide signaling. In preparation, 2025.

4. **Weber RE,** Schulze KM, Musch TI, Poole DC. Soluble guanylyl cyclase stimulator effect on skeletal muscle oxygen pressures and capillary hemodynamics in healthy rats. In preparation, 2025.

5. Schulze KM, Horn AG, **Weber RE**, Hageman KS, Scheuermann BC, Ade CJ, Behnke BJ, Poole DC, Musch TI. Bulk and regional diaphragm blood flow during chemical hyperpnea in pulmonary hypertensive rats. Respir Physiol Neurobiol. 2025. PMID: 39971146.

6. Schulze KM, **Weber RE**, Horn AG, Hageman KS, Kenney NJ, Behnke BJ, Poole DC, Musch TI. Skeletal and respiratory muscle blood flow redistribution during submaximal exercise in pulmonary hypertensive rats. J Physiol. 2025. PMID: 39625445.

7. Schulze KM, Horn AG, Muller-Delp JM, White ZJ, Hall SE, Medarev SL, **Weber RE**, Poole DC, Musch TI, Behnke BJ. Pulmonary hypertension impairs vasomotor function in rat diaphragm arterioles. Microvasc Res. 2024. PMID: 38614154.

8. Schulze KM, Horn AG, **Weber RE**, Behnke BJ, Poole DC, Musch TI. Pulmonary hypertension alters blood flow distribution and impairs the hyperemic response in the rat diaphragm. Front Physiol. 2023. PMID: 38187132.

9. Horn AG, Schulze KM, **Weber RE**, Barstow TJ, Musch TI, Poole DC, Behnke BJ. Post-occlusive reactive hyperemia and skeletal muscle capillary hemodynamics. Microvasc Res. 2022. PMID: 34822837.

10. Horn AG, Kunkel ON, Schulze KM, Baumfalk DR, **Weber RE**, Poole DC, Behnke BJ. Supplemental oxygen administration during mechanical ventilation reduces diaphragm blood flow and oxygen delivery. J Appl Physiol. 2022. PMID: 35323060.

11. **Weber RE,** Schulze KM, Colburn TD, Horn AG, Hageman KS, Ade CJ, Hall SE, Sandner P, Musch TI, Poole DC. Capillary hemodynamics and contracting skeletal muscle oxygen

pressures in male rats with heart failure: Impact of soluble guanylyl cyclase activator. Nitric Oxide. 2022. PMID: 34871799.

12. Schulze KM, **Weber RE**, Colburn TD, Horn AG, Ade CJ, Hsu WW, Poole DC, Musch TI. The effects of pulmonary hypertension on skeletal muscle oxygen pressures in contracting rat spinotrapezius muscle. Exp Physiol. 2021. PMID: 34469618.

13. Schulze KM, Weber RE, Horn AG, Colburn TD, Ade CJ, Much TI, Poole DC. Effects of Pulmonary Hypertension on Microcirculatory Hemodynamics in Rat Skeletal Muscle. Microvascular Research. 2022. PMID: 35104507.

14. Ade CJ, Turpin VG, Parr SK, Hammond ST, White Z, **Weber RE**, Schulze KM, Colburn TD, Poole DC. Does wearing a facemask decrease arterial blood oxygenation and impair exercise tolerance? Respir Physiol Neurobiol. 2021. PMID: 34352384.

15. Colburn TD, **Weber RE**, Schulze KM, Hageman KS, Horn AG, Behnke BJ, Poole DC, Musch TI. Sexual dimorphism in vascular ATP-sensitive K+ channel function supporting interstitial PO_2 via convective and/or diffusive O2 transport. J Physiol. 2021. PMID: 34101850.

16. Horn AG, Baumfalk DR, Schulze KM, Kunkel ON, Colburn TD, **Weber RE**, Bruells CS, Musch TI, Poole DC, Behnke BJ. Effects of elevated positive end-expiratory pressure on diaphragmatic blood flow and vascular resistance during mechanical ventilation. J Appl Physiol. PMID: 32730173.

17. Colburn TD, **Weber RE**, Hageman KS, Caldwell JT, Schulze KM, Ade CJ, Behnke BJ, Poole DC, Musch TI. Vascular ATP-sensitive K+ channels support maximal aerobic capacity and critical speed via convective and diffusive O2 transport. J Physiol. 2020. PMID: 32798233.

18. Colburn TD, Hirai DM, Craig JC, Ferguson SK, **Weber RE**, Schulze KM, Behnke BJ, Musch TI, Poole DC. Transcapillary PO_2 gradients in contracting muscles across the fibre type and oxidative continuum. J Physiol. 2020. PMID: 32445225.

ACADEMIC & PROFESSIONAL SERVICE

2016 – 2025	Kansas Association for the Advancement of Women in Science, Member and Volunteer
2020 – 2022	Science Communication Fellowship, Sunset Zoo, Manhattan, Kansas
2020 – 2021	College of Veterinary Medicine Graduate Student Association Executive Team, Social Chair
2019 – 2020	Kansas State University Graduate Student Council Leadership Team, Governmental Relations Chair

MENTORING & TRAINING

Alaina DeVolder, B.S. (2019-2020) –Registered Nurse

Marissa Peaslee, B.S. (2020-2021) – Graduate Student at the University of Minnesota

Tyler McCoach, M.S. (2022-2023) – Medical Student at the University of Kansas

Hannah Wall (2022) – Medical Student at Kansas Osteopathic Medicine

Nathan Kenney (2022-2025) – Graduate Student at Kansas State University

McKinley Reagor (2024) – K-INBRE Summer Scholar

Alauna Parker (Summer 2024) – K-INBRE Summer Scholar

Daniel McVay (2024-2025) –Undergraduate Research Assistant (Pre-Medicine)

TEACHING EXPERIENCE

Kansas State University

- KIN 101: 5K to Half Marathon (1 semester)
- KIN 220: Biobehavioral Basis of Physical Activity Laboratory (2 semesters)
- KIN 310: Research Methods in Kinesiology (2 semesters)
- KIN 336: Exercise Physiology (9 semesters)
- KIN 360: Anatomy and Physiology Laboratory (7 semesters)
- KIN 615: Exercise Testing and Prescription (1 semester)
- KIN 625: Advanced Cardiovascular Physiology (1 semester)
- *Guest lectures* for Anatomy and Physiology (KIN 360), Advanced Cardiopulmonary Physiology (KIN 796)

TEVAL scores for overall effectiveness as an instructor (*adjusted average on a 5.0 scale*): 5K to Half Marathon (5.0), Biobehavioral Basis of Physical Activity (4.4), Exercise Physiology (4.8), Anatomy and Physiology (4.9), Exercise Testing and Prescription (4.4), Advanced Cardiovascular Physiology (4.3).

SCIENTIFIC ABSTRACTS (7 first-author; 16 co-authored; 23 total)

1. White ZJ, Sudasinghe K, **Weber RE,** Hall SE. Influence of in vivo HSP90α inhibition on irisin signaling to the brain. *Alzheimer's & Dementia*, 2025.

2. **Weber RE,** Kunkel ON, Kenney NJ, Schulze KM, Horn AG, Hageman KS, Musch TI, Behnke BJ, Poole DC. Tumor Oxygenation in an Orthotopic Model of Breast Cancer: Impact of Dietary Nitrate Supplementation. *Physiology,* 2024.

3. Schulze KM, Horn AG, **Weber RE,** Kenney NJ, Muller-Delp JM, Behnke BJ, Poole DC, Musch TI. Sulforaphane improves vasodilatory reactivity in diaphragm arterioles from rats with pulmonary hypertension. *Physiology,* 2024.
4. Kenney NJ, Horn AG, Schulze KM, **Weber RE**, Poole DC, Behnke BJ, Musch TI. Effects of aging on vasoconstrictor responses of diaphragm arterioles. *Physiology*, 2024.

5. Horn AG, Schulze KM, **Weber RE**, Kunkel ON, Poole DC, Behnke BJ. The impact of aging and biological sex on diaphragm hyperemia and blood flow distribution. *Physiology,* 2024.

6. **Weber RE,** Schulze KM, Hageman KS, Musch TI, Poole DC. Nitric Oxide-soluble guanylyl cyclase activator increases endurance capacity and skeletal muscle oxygenation in male rats. *Medicine & Sports Science*, 2023.

7. Schulze KM, **Weber RE**, Horn AG, Colburn TD, Ade CJ, Behnke BJ, Poole DC, Musch TI. Effect of Pulmonary Hypertension on Blood Flow in the Contracting Spinotrapezius Muscle*. Medicine & Science in Sports & Exercise*, 2023.

8. **Weber RE,** Schulze KM, Colburn TD, Horn AG, Hageman KS, Ade CJ, Hall SE, Sandner P, Musch TI, Poole DC. Increased nitric oxide-soluble guanylyl cyclase signaling improves endurance capacity and contracting skeletal muscle oxygenation in healthy female rats. *Physiology*, 2023.

9. Schulze KM, Horn AG, **Weber RE**, Ade CJ, Behnke BJ, Poole DC, Musch TI. Effects of pulmonary hypertension on diaphragm blood flow. *Physiology*, 2023.

10. Horn AG, Kunkel ON, Schulze KM, **Weber RE**, Ade CJ, Poole DC, Behnke BJ. The impact of aging and sex on diaphragm vasomotor function. *Physiology*, 2023.

11. **Weber RE**, Schulze KM, Hageman KS, Sandner P, Musch TI, Poole DC. Soluble guanylyl cyclase stimulator improves contracting oxygen pressures in heart failure rats. *The FASEB Journal, 2022.*

12. Schulze KM, **Weber RE**, Horn AG, Colburn TD, Ade CJ, Poole DC, Musch TI. Pulmonary Hypertension Induces Sex Differences in Control of Contracting Rat Skeletal Muscle Oxygen. *The FASEB Journal*, 2022.

13. Horn AG, Schulze KM, Baumfalk DR, **Weber RE,** Kunkel ON, Musch TI, Poole DC, Behnke BJ. Monocrotaline-induced Pulmonary Hypertension Impairs Diaphragm Vasomotor Function. *Physiology*, 2022.

14. Schulze KM, **Weber RE**, Colburn TD, Horn AG, Behnke BJ, Poole DC, Musch TI. Effects of Pulmonary Hypertension on Microcirculatory Hemodynamics in Rat Skeletal Muscle. *The FASEB Journal*, 2020.

15. **Weber RE**, Schulze KM, Colburn TD, Horn AG, Hageman KS, Ade CJ, Sandner P, Musch TI, Poole DC. Contracting Skeletal Muscle Oxygen Pressures in Rats with Heart Failure: Impact of Soluble Guanylyl Cyclase Activator. *The FASEB Journal*, 2022.

16. Baumfalk DR, Colburn TD, Horn AG, Kunkel ON, **Weber RE,** Musch TI, Behnke BJ. Effect of Prostate Cancer and Endurance Exercise Training on Aerobic Capacity. *The FASEB Journal*, 2020.

17. Schulze KM, Colburn TD, **Weber RE**, Hageman KS, Behnke BJ, Poole DC, Musch TI. Fiber-Type Effects of KATP Channel Inhibition via Glibenclamide on the Recovery of Interstitial PO_2 Following Muscle Contractions in Rats. *The FASEB Journal,* 2020.

18. Colburn TD, **Weber RE**, Schulze KM, Hageman KS, Behnke BJ, Poole DC, Musch TI. Vascular ATP-sensitive K+ (K_{ATP}) Channels: Sex and Fiber-type Differences in the Support of Contracting Muscle Blood Flow and Interstitial PO_2. *The FASEB Journal,* 2020.

19. **Weber RE**, Colburn TD, Schulze KM, Hageman KS, Behnke BJ, Musch TI, Poole DC. ATP-sensitive K+ Channel Inhibition Diminishes Critical Speed in Male and Female Rats but $\dot{V}O_2$max in Females Only. *The FASEB Journal*, 2020.

20. Colburn TD, **Weber RE**, Schulze KM, Hageman KS, Poole DC, Musch TI. Sex And Fiber-type Differences: Vascular ATP-sensitive K+ (KATP) Channels Support Critical Speed And Interstitial PO_2. *Medicine & Science in Sports & Exercise,* 2019.

21. Horn AG, Baumfalk DR, Schulze KM, Colburn TD, **Weber RE,** Kunkel ON, Bruells CS, Musch TI, Poole DC, Behnke BJ. Effects of Intrathoracic Pressure changes on Diaphragmatic Blood Flow during Mechanical Ventilation. *The FASEB Journal,* 2019.

22. **Weber RE**, Colburn TD, Schulze KM, Hageman KS, Musch TI, Poole DC. ATP-sensitive K+ Channel Inhibition via Glibenclamide Impairs Maximal Aerobic Capacity and Critical Speed of Healthy Rats without Compromising Cardiac Function. *The FASEB Journal,* 2019.

23. Colburn TD, **Weber RE,** Hageman KS, Musch TI, Poole DC. ATP-sensitive K+ channel inhibition impairs maximal aerobic capacity and critical speed of healthy rats without compromising cardiac function. *The FASEB Journal,* 2019.